Mon. Not. R. Astron. Soc. **265**, 553–580 (1993) and Microfiche MN265/1

Metallicity gradients in early-type galaxies

C. M. Carollo,[1] I. J. Danziger[1] and L. Buson[2]

[1] *European Southern Observatory, Karl-Schwarzschildstrasse 2, D-85748, Garching bei München, Germany*
[2] *Osservatorio Astronomico di Padova, Vicolo dell'Osservatorio 5, I-35100 Padova, Italy*

Accepted 1993 May 22. Received 1993 May 21; in original form 1993 January 16

ABSTRACT

Long-slit spectra in the range 4500–6500 Å have been obtained for a sample of 42 galaxies. Rotation velocities and velocity dispersions, together with radial line strength gradients of Mg_2, Mg_1, Hβ, Na D, TiO_1, TiO_2 and Fe_{5270}, have been measured to, on average, half an effective radius. To a high level of significance, Mg_2 gradients positively correlate with those of Mg_1 and Na D, but no correlation is observed with the other indices. In addition, correlations of Mg_2 gradients with various physical parameters are studied. For galaxies smaller than about 10^{11} $M_{\odot}$, the Mg_2 gradient increases with increasing mass, but more massive objects show no correlation. In low-mass galaxies, the correlation of Mg_2 gradients with mass suggests dissipative collapse as the mechanism acting during the initial star formation episode. Different formation mechanisms, such as, for example, a less dissipative collapse and/or merging of smaller systems, are discussed as a means of explaining the lack of correlation at higher masses. Even at low masses, the galactic mass seems not to influence either the position or the slope on the Fe_{5270}–Mg_2 plane, abundance ratios within galaxies depending on still-unidentified parameters.

Key words: galaxies: abundances – galaxies: elliptical and lenticular, cD – galaxies: fundamental parameters.

1 INTRODUCTION

A great effort has been made in the last few years to understand how early-type galaxies formed. The relatively recent discoveries that ellipticals are not merely a one-parameter family (Djorgovski & Davis 1987; Dressler et al. 1987; see also the reviews by Kormendy & Djorgovski 1989; de Zeeuw & Franx 1991; Bertin & Stiavelli 1993 and references therein) and of many ellipticals showing signatures of interaction with the environment (e.g. Bender 1988; Franx & Illingworth 1988; Jedrzejewski & Schechter 1988; Schweizer et al. 1990; Schweizer & Seitzer 1992) have suggested that these galaxies may have different star formation histories, with stellar populations differing in metallicity, age or both (Worthey, Faber & Gonzalez 1992, hereafter WFG). Major scenarios for elliptical galaxy formation, e.g. dissipationless (e.g. van Albada 1982) or dissipative (Larson 1975) collapse, merging of late-type galaxies (Toomre 1977), and cooling flows in a pre-existing potential well (Nulsen, Stewart & Fabian 1984) are able to account for *some* observational facts, but none of these simple pictures seems able to accommodate *all* facts. Given the relatively large number of free parameters in any of these models, the need for more and stronger experimental constraints has become urgent.

Crucial information has been derived from metal line-strength indices (e.g. Davies et al. 1987, hereafter D87) and their radial variations inside the galaxies (e.g. Baum, Thomsen & Morgan 1986; Peletier 1989, hereafter PE89; Gorgas, Efstathiou & Salamanca 1990, hereafter GES; WFG; Davies, Sadler & Peletier 1992, hereafter DSP). The Mg_2 line-strength gradients in early-type galaxies, for example, can vary considerably, ranging from very featureless to structured profiles showing e.g. changes of slope possibly associated with kinematically decoupled cores (Bender 1992), or anomalies in the stellar populations of some ellipticals (Carollo & Danziger 1993, hereafter CD). Their dependence on primary physical parameters is, however, very uncertain: a positive correlation between Mg_2 gradients and luminosity was found by PE89 and GES, which seemed to favour a picture in which early-type galaxies were formed by dissipative collapse; however, DSP found no evidence for such a trend in a different sample.

More information comes from comparison of different metallicity indices with models of old stellar populations, which indicate that [Mg/Fe] in giant ellipticals is higher than in the most metal-rich stars of the solar neighbourhood (WFG). Moreover, the ⟨Fe⟩–Mg_2 relation within ellipticals is steeper than the relation linking the elliptical nuclei (e.g.

WFG; CD; DSP). WFG suggest three possible scenarios to explain this result, namely a variable star formation time-scale, a variable initial mass function (IMF), or a selective mass loss from the galaxies of Fe compared to Mg. The aim of understanding which of these scenarios (if any) is the most likely to explain such a result justifies the present effort.

Here we present, for a sample of 42 galaxies, line-strength gradients for seven metallicity indices (Mg_2, Mg_1, Hβ, Na D, TiO_1, TiO_2 and Fe_{5270}), together with velocity and velocity dispersion profiles. Section 2 describes the sample of objects, the observations and the basic steps of data reduction. In Section 3 we describe further specific steps of data analysis devoted to obtaining radial velocity and velocity dispersion profiles, and kinematic results. Radial line-strength gradients are analogously described in Section 4. Finally, the results are discussed in Section 5.

2 THE OBSERVATIONS

2.1 The sample

The sample consists of 42 galaxies embracing a large variety of photometric and kinematic properties and environmental conditions; it is, however, neither complete nor unbiased. The original selection of the sample, consisting of a large proportion of emission-line galaxies, was based on the intention to compare and contrast abundance gradients in the gaseous component with those in the stellar component. A control sample of already studied galaxies without emission lines was added.

According to RC3, 30 are elliptical galaxies, 11 are lenticular and one is a suspected spiral, although misclassifications might be present. For example, a few objects classified as lenticulars in the surface photometry catalogue of the ESO–Uppsala galaxies (Lauberts & Valentijn 1989, hereafter ESOLV) are ellipticals in the RC3 or in the RSA catalogue, or vice versa. The galaxy ESO 381 − 29, classified as elliptical in ESOLV, has $[O\,III]_{4958,5007}$ in emission and $[N\,II]_{6583}$ stronger than Hα; it is possibly a spiral, as suggested in RC3.

NGC 4684, classified as lenticular in ESOLV and RC3, shows Hα predominating over $[N\,II]_{6583}$. It also shows $[O\,III]_{4958}$, $[O\,III]_{5007}$ and Hβ emission; it is probably an Sa–SBa galaxy, as our (unpublished) NTT images suggest. These two suspected spirals were excluded from our

Table 1(a). Physical parameters for the 42 galaxies.

name	type	R_e	m_b	V_{hel}	V_{grp}	ϵ	$(B-V)_o$	SB_e	a_4	V_{max}
ESO 208-21	L	38	11.45	1099	1675	.32	.83	20.8	-	-
ESO 323-16	L	16	12.95	3410	-	.02	.95	21.6	-	-
ESO 381-29	S?	6	13.01	2618	-	.49	.76	18.9	-	-
IC 1459	E	35	10.83	1734	2225	.25	.95	20.8	-.002	23
IC 2006	L	21	12.29	1364	1422	.12	.91	21.5	-	-
IC 2035	L	7	12.61	1454	-	.23	.71	18.0	-	95*
IC 3370	E	33	11.59	2924	2232	.16	.86	21.5	-	98
IC 4889	L	18	11.91	2539	2349	.33	.88	20.7	.01	60*
IC 4943	E	10	13.54	2753	2328	.08	.89	21.6	-	-
NGC 1052	E	30	11.33	1475	1723	.32	.91	21.1	.005	76
NGC 1209	E	20	12.26	2619	2297	.36	.91	20.5	-	175
NGC 1298	E	42	13.89	6528	-	.09	.83	-	-	-
NGC 1947	L	39	11.50	1100	-	.12	.96	-	-	40
NGC 2502	L	20	12.10	1003	-	.28	.98	-	-	-
NGC 2663	E	50	10.23	2130	2235	.27	-	22.1	-	-
NGC 2974	L	24	11.79	1924	2122	.35	.95	21.3	.0042	-
NGC 3078	E	29	11.86	2492	2593	.21	.95	20.8	-.015	110*
NGC 3100	L	35	11.80	2640	-	.30	-	-	-	-
NGC 3108	L	33	12.25	2678	3260	.12	.91	21.4	-	-
NGC 3136	E	35	10.71	1696	2107	.17	.78	22.5	-	-
NGC 3136B	E	45	10.82	1770	2107	.44	-	22.6	-	-
NGC 3226	E	34	12.22	1275	2460	.13	.88	22.6	-	-
NGC 3250	E	22	11.56	2871	3488	.23	.90	21.2	-.002	-
NGC 3260	E	13	13.40	2413	3488	.31	.97	22.0	-	-
NGC 3557	E	39	10.79	2944	2399	.23	.87	21.0	0.	153
NGC 3706	E	27	11.87	3045	3036	.32	.92	20.9	-	-
NGC 4374	E	50	9.91	1033	1333	.13	.94	20.8	-.006	8
NGC 4684	S?	24	12.35	1589	-	.60	-	-	-	-
NGC 4696	E/cD	85	10.75	2983	2221	.25	-	23.6	-	-
NGC 4832	L	14	12.70	3750	-	.25	.90	-	-	-
NGC 5011	E	35	11.83	3071	2927	.16	.89	20.9	-	-
NGC 5044	E	34	11.32	2771	2982	.03	.95	22.7	-	-
NGC 5077	E	23	12.21	2593	2982	.31	.99	21.2	-.009	90
NGC 5090	E	31	11.97	3421	3987	.16	-	21.7	0	80
NGC 5266	L	38	11.45	3049	-	.36	-	-	-	210
NGC 5796	E	19	11.98	2946	2819	.36	.93	20.5	-	70*
NGC 5846	E	50	10.87	1709	2336	.08	.96	22.3	0	20
NGC 5903	L	37	11.66	2547	2460	.12	.87	21.5	-.007	-
NGC 6849	E	34	12.6	5952	4620	.32	.79	23.0	-	-
NGC 6868	E	40	11.42	2876	2328	.17	.95	21.3	.005	-
NGC 7097	E	16	12.57	2606	-	.29	.89	21.2	.005	-
NGC 7200	L	8	13.71	2897	4244	.27	.88	21.6	-	-

Notes: column (1) = name; (2) = morphological type; (3) = effective radius in arcsec; (4) = apparent B magnitude, corrected for reddening and internal galactic extinction; (5) = heliocentric velocities in km s^{-1}; (6) = corrected velocities, in km s^{-1}, from Faber et al. (1989); (7) = ellipticity; (8) = $(B-V)$ colours corrected for reddening and internal galactic extinction; (9) = B surface brightness inside a de Vaucouleurs effective diameter, from Davies et al. (1987); (10) = boxiness parameter a_4, from Bender et al. (1989) and van der Marel (1991); (11) = maximum rotational velocities in km s^{-1}, from van der Marel (1991) and this work (asterisks). When not explicitly stated, parameters are from the ESOLV or RC3 catalogue.

Table 1(b). The central velocity dispersion and mass for each object.

name	$-M_B$	Log(Mass)	σ_0	err_{σ_0}
ESO 208-21	19.4	10.53	143	21
ESO 323-16	20.3	10.74	162	14
ESO 381-29	19.7	9.87	114	14
IC 1459	21.0	11.31	296	10
IC 2006	19.0	10.24	128	9
IC 2035	18.8	9.63	109	11
IC 3370	21.4	11.20	203	12
IC 4889	20.7	10.76	190	8
IC 4943	19.3	10.44	165	15
NGC 1052	20.1	10.85	203	8
NGC 1209	20.5	11.01	223	17
NGC 1298	20.8	11.59	191	14
NGC 1947	19.3	10.50	140	13
NGC 2502	18.5	10.15	135	10
NGC 2663	22.0	11.48	269	20
NGC 2974	20.3	10.84	195	14
NGC 3078	20.8	11.18	238	14
NGC 3100	20.9	11.20	209	11
NGC 3108	20.5	11.16	209	16
NGC 3136	21.1	11.07	224	13
NGC 3136B	21.0	11.00	182	9
NGC 3226	18.9	10.83	201	14
NGC 3250	21.4	11.24	266	17
NGC 3260	19.1	10.72	205	19
NGC 3557	22.2	11.52	279	24
NGC 3706	21.2	11.38	279	19
NGC 4374	20.8	11.29	314	17
NGC 4684	19.3	10.25	111	10
NGC 4696	22.2	11.81	256	11
NGC 4832	20.8	10.55	130	17
NGC 5011	21.2	11.4	258	22
NGC 5044	21.5	11.32	240	13
NGC 5077	20.5	11.17	252	12
NGC 5090	21.3	11.48	270	15
NGC 5266	21.6	11.28	195	10
NGC 5796	21.0	11.19	269	26
NGC 5846	20.9	11.32	252	17
NGC 5903	21.0	11.26	223	13
NGC 6849	21.9	11.60	221	11
NGC 6868	21.5	11.5	274	11
NGC 7097	20.1	10.95	237	9
NGC 7200	19.2	10.58	195	19

Notes: column (1) = name; (2) = absolute blue magnitude (corrected for reddening); (3) = logarithm of masses used in our analysis (in solar units); heliocentric velocities have been used (results do not change when *corrected* distances from Faber et al. 1989 are used instead), and $H_0 = 75$ here and in column (1); (4) = central velocity dispersion (in km s^{-1}) derived from our data; (5) = error on central velocity dispersion. When more than one measurement was available, errors were computed with a quadrature of the errors on the single measurements. When only one measurement was available, errors indicate the rms of the averaged points.

analysis. The morphological classification adopted in this work is listed in Table 1(a), together with other known properties of the galaxies in our sample.

2.2 Basic steps of data reduction

Long-slit spectra were taken, for most of the objects at two position angles (270° EW and 360° NS), using the Boller and Chivens Cassegrain spectrograph at the ESO 3.6-m telescope on four separate observing runs during the nights of 1985 August 10–13, 1986 March 13–16, 1986 June 1–3 and 1987 February 28–March 2. The characteristics of the detectors and the instrumental set-ups are given in Table 2. In order to reduce cosmic ray events on the CCD, exposures were limited to 20 min; for many objects, several spectra were taken during the same run to increase the signal-to-noise ratio. The slit was always centred on the galaxy nucleus (determined visually on the TV finder). He–Ar calibration spectra were taken for each object to determine the wavelength scale. The average resolution of our spectra, as computed by measuring the FWHM of the emission lines in the He–Ar spectra and of the sky lines in the science frames, was about 9 Å. G and K giants and spectrophotometric standard stars were also observed. The stars were slightly defocused to avoid saturation effects. The observing log for the galaxies and the calibration stars is given in Tables 3(a) and (b).

The data were reduced using the ESO MIDAS system. For each set of data, a bias frame was subtracted from all other frames and a dark-current correction was then applied to all galaxy frames. Raw quartz lamp continuum spectra were normalized with corresponding smoothed frames to determine the small-scale sensitivity variations of the CCD (removed from the science frames). Sky emission lines along the slit, extracted from the galaxy spectra, were used to generate a correction frame for the variable vignetting along the slit. Results are not affected by this correction. Science frames were cleaned from cosmic rays and bad pixels and calibrated in wavelength by fitting, row by row, a third-order polynomial to the positions of the emission lines of the corresponding He–Ar lamp frames. Wavelength calibration was checked on the sky lines of science frames. A sky spectrum for each galaxy frame was generated by averaging the outermost 10 rows on each side of the CCD; this sky was then subtracted from the science frames. We have restricted our measurements to within radii at which Poissonian errors are dominant, so that errors in sky subtraction do not influence

Table 2. The characteristics of the detectors and the instrumental set-up.

Run	CCD [1]	ron (e^-/pix)	Range (Å)	Slit Width (″) [2]	Pixel Size (Å ×″)
Aug 1985	ESO RCA #5	33	4700–7100	1.7	5 × 1.1
March 1986	"	"	4300–6700	1.3	"
June 1986	"	"	"	"	"
"	"	"	3700–6100	"	"
Feb–March 1987	ESO RCA #3	11	3900–6800	1.6	6 × 1.1

[1]Both 30 $\mu m^2 \times (337 \times 520)$ red sensitive detectors. The finally available area was always about 140 pixel in the spatial direction and 480 pixel along the dispersion direction.
[2]Slit length = 2.9 arcmin.

Table 3(a). The observing log for the galaxies.

name	Run	P.A. (deg)	exposure time (min)
ESO 208-21	March 1986	270	20
ESO 323-16	March 1986	270	20
	June 1986 (setup 1)	360	20
	June 1986 (setup 2)	270	20
	Feb-Mar 1987	180	20
ESO 381-29	March 1986	270	20
	June 1986 (setup 2)	270	20
	Feb-Mar 1987	180	20
IC 1459	Aug 1985	270	15+7.5+15+7.5+20
	June 1986 (setup 1)	360	20
	June 1986 (setup 2)	270	20
IC 2006	Aug 1985	270	20
	March 1986	270	20
IC 2035	Aug 1985	270	20
	March 1986	270	20
IC 3370	March 1986	270	20
	June 1986 (setup 1)	360	20
	June 1986 (setup 2)	270	20
	Feb-Mar 1987	180	15
IC 4889	June 1986 (setup 1)	360	20
	June 1986 (setup 2)	270	20
IC 4943	Aug 1985	270	15+15+20+20
	June 1986 (setup 1)	360	20
	June 1986 (setup 2)	270	20
NGC 1052	Aug 1985	270	10+15+15
NGC 1209	Aug 1985	270	10+10+20
NGC 1298	Aug 1985	270	15+15+20
NGC 1947	Aug 1985	270	20
	March 1986	270	20
	Feb-Mar 1987	180	20
NGC 2502	March 1986	270	20
NGC 2663	March 1986	270	20+20
NGC 2974	March 1986	270	20
NGC 3078	March 1986	270	20
	Feb-Mar 1987	180	20
	June 1986 (setup 2)	270	20
NGC 3100	March 1986	270	20
	Feb-Mar 1987	180	20
	June 1986 (setup 1)	360	20
	June 1986 (setup 2)	270	20
NGC 3108	March 1986	270	20
	Feb-Mar 1987	180	20
	June 1986 (setup 1)	360	20
	June 1986 (setup 2)	270	20
NGC 3136	March 1986	270	20+20
NGC 3136B	March 1986	270	20
	Feb-Mar 1987	180	20
	June 1986 (setup 1)	360	20
	June 1986 (setup 2)	270	20
NGC 3226	March 1986	270	20
	Feb-Mar 1987	180	20
NGC 3250	March 1986	270	20+20
	Feb-Mar 1987	180	20
	June 1986 (setup 2)	270	20
NGC 3260	March 1986	270	20
NGC 3557	March 1986	270	20+20
	Feb-Mar 1987	180	20
	June 1986 (setup 2)	270	20
NGC 3706	March 1986	270	20+20
	Feb-Mar 1987	180	20
	June 1986 (setup 2)	270	20
NGC 4374	March 1986	270	20
	June 1986 (setup 2)	270	20
	Feb-Mar 1987	180	10
NGC 4684	March 1986	270	20
	Feb-Mar 1987	180	15
NGC 4696	March 1986	225	20
	March 1986	270	20+20
	March 1986	300	20
	March 1986	330	20
	March 1986	360	20
NGC 4832	Feb-Mar 1987	180	20
NGC 5011	March 1986	270	20+20
	June 1986 (setup 2)	270	20
NGC 5044	March 1986	270	20+20
	Feb-Mar 1987	180	15
	June 1986 (setup 1)	360	20
	June 1986 (setup 2)	270	20
NGC 5077	March 1986	270	20
	Feb-Mar 1987	180	15
NGC 5090	March 1986	270	20
	Feb-Mar 1987	180	20
	June 1986 (setup 1)	360	20
	June 1986 (setup 2)	270	20
NGC 5266	March 1986	270	20
	Feb-Mar 1987	180	20
	June 1986 (setup 1)	360	20
	June 1986 (setup 2)	270	20
NGC 5796	March 1986	270	20+20
	June 1986 (setup 2)	270	20

Table 3(a) – *continued*

name	Run	P.A. (deg)	exposure time (min)
NGC 5846	Aug 1985	270	5+10+15+15+20+20+20
	Feb-Mar 1987	180	20
	June 1986 (setup 1)	360	20
NGC 5903	March 1986	270	20+20
	June 1986 (setup 2)	270	20
NGC 6849	Aug 1985	270	15+20+20
	June 1986 (setup 1)	360	20
	June 1986 (setup 2)	270	20
NGC 6868	Aug 1985	270	15+15+20
	June 1986 (setup 1)	360	20
	June 1986 (setup 2)	270	20
NGC 7097	Aug 1985	270	15+15+20
	June 1986 (setup 1)	360	20
	June 1986 (setup 2)	270	20
NGC 7200	Aug 1985	270	15+15+15+15+20
	June 1986 (setup 1)	360	20
	June 1986 (setup 2)	270	20

Notes. Data taken in 1987 February–March, i.e. at PA 180°, have been inverted in the spatial direction and analysed together with those at 360°. In the figures, east at PA 270° and north at PA 360° are on the left.

Table 3(b). Observing log for the stars.

name	Run	P.A. (deg)	exposure time (sec)
HR 5582	Aug 1985	270	40+40+40
HR 5690	Aug 1985	270	40+40+40+40
HR 7317	Aug 1985	270	30+30+40+40+40
HR 7430	Aug 1985	270	40+40+40+40
HR 8924	Aug 1985	270	30+30+30+30+30
L870-2	Aug 1985	360	20+20+20+30+30
HR 2429	March 1986	270	5+5+5+5
HR 2701	March 1986	270	5+5
HR 2970	March 1986	270	5+5+5+5
L970-30	March 1986	270	60+60
HR 7149	June 1986 (setup2)	270	5+5+5+5
HR 7317	June 1986 (setup2)	270	7+7+7+7
HR 7430	June 1986 (setup2)	270	5+5+5+5+5
L745-4	Feb-Mar 1987	180	60+60

significantly the determination of the metallic features (as checked by over- and undersubtracting the sky by 15 per cent). Extended objects such as NGC 4696, filling in principle all the CCD, have in any case been excluded from our analysis (see Section 4). Finally, the spectra were flux-calibrated and corrected for Galactic extinction by using, when available, Burstein & Heiles's (1984) values, and the cosecant approximation for the remaining objects. For the 1986 June run, the spectrophotometric standards could not be used. We calibrated the spectra of this run comparing, for four galaxies, the uncalibrated spectrum with a flux-calibrated spectrum (taken from a different run) of the same object. Uncertainties in the flux calibration affect central Mg_2 values by 12 per cent, but leave gradients unaffected.

3 KINEMATIC PARAMETERS: ROTATION VELOCITY AND VELOCITY DISPERSION PROFILES

3.1 Data reduction

A Fourier quotient package (Sargent et al. 1977) was run on the fully reduced spectra, after rebinning so as to maintain the signal-to-noise ratio above the fixed threshold of 30. Kinematic properties of the galaxies obtained using different stellar templates were compatible within the errors. Because no templates were available for the first grating position of 1986 June, we used those of the same run taken with the other grating angle; similarly, for the 1987 run, we used those of 1985 August convolved with a Gaussian to reproduce the slightly lower resolution. Template linewidths are obviously fundamental in deriving the velocity dispersions of the galaxies, but should not influence the rotation curves. We checked that velocity dispersions derived from both the 1986 June (first set-up) and the 1987 spectra were in good agreement with those from other runs when the same galaxy was observed. Galaxies not present in any of our other runs, and for which no other measurement appears in the literature, had velocity dispersions inside the range scanned by the above comparison, so that a reliable velocity dispersion determination could also be expected for these galaxies. Because velocity dispersions of stellar templates derived by applying the Fourier quotient to different stars are of the order of 70 km s^{-1}, velocity dispersions larger than about 150 km s^{-1} should be reliably measured with 10 per cent accuracy, and those between 150 and 110 km s^{-1} with an accuracy of 20 per cent. Smaller values are reported as upper limits. For each object, all available velocity dispersion measurements inside the inner 5 arcsec were averaged to estimate the central velocity dispersion σ_0. Results (Table 1b) are in good agreement with D87 [over the 33 galaxies in common, we measure an rms $= (1/\sqrt{32}) \sum_{i=1}^{33} (\sigma_0 - \sigma_{D87})^2 \simeq 17$ km s^{-1}; see also Danziger et al. 1993, and Fig. 1, where the differences between our σ_0 and the D87 values are plotted against σ_0].

3.2 Results

In Figs 2.1–2.42 (a and b) are shown rotation velocity and velocity dispersion profiles for all the galaxies in our sample. For each galaxy, data taken in different runs at the same position angle are plotted in the same figure (and listed together in Appendix A (on Microfiche MN265/1), where the individual measurements at different radii are presented).

For several objects, good kinematic data were already present in the literature. In Fig. 3 we show, for IC 1459, NGC 1052, NGC 4374 and NGC 5846, a comparison between our kinematic profiles and those measured by Davies & Birkinshaw (1988) and Franx & Illingworth (1988). For IC 1459 our position angles are too different from either of the two axes (for which published data are available) to allow a quantitative comparison, but important features, such as e.g. the counter-rotating core, are evident in our data. For the remaining three galaxies, the difference between our position angle and that of the other authors is always less than 20°, so that a direct comparison can be made. Good agreement is found with the above-mentioned kinematical studies.

Except for ESO 323–16, IC 2035, IC 4889, NGC 3078, NGC 4696 and NGC 5796, whose major axis is within $\simeq 5°$ of one of our two position angles, the slit was actually

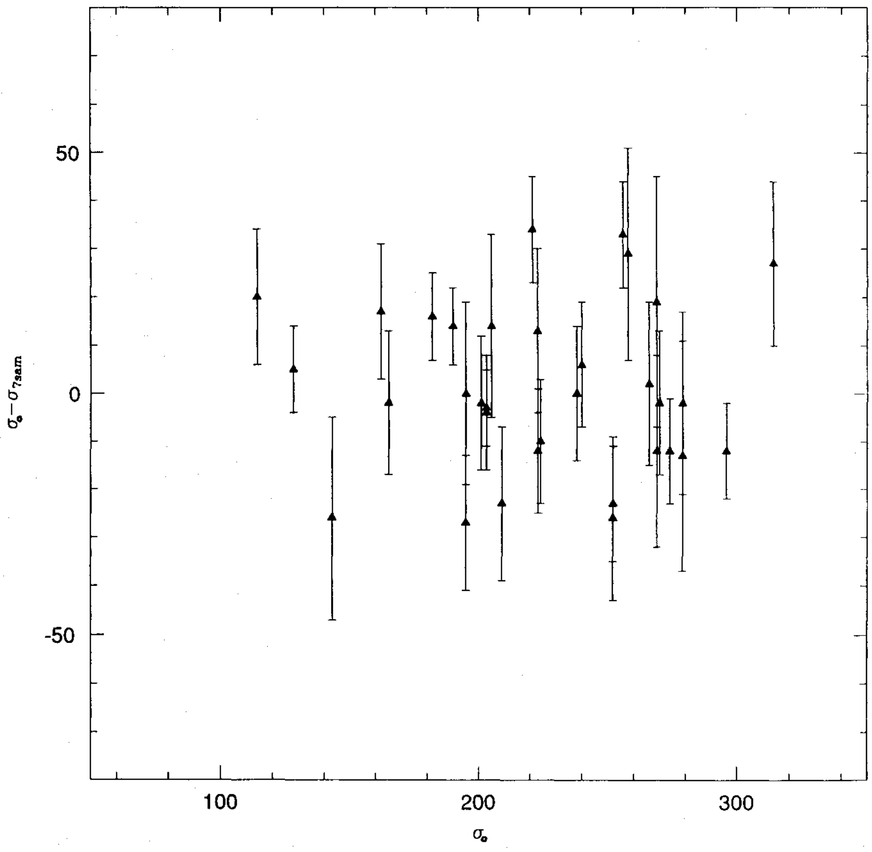

Figure 1. Differences between our and the D87 central velocity dispersion values plotted against our own measurements (in km s^{-1}).

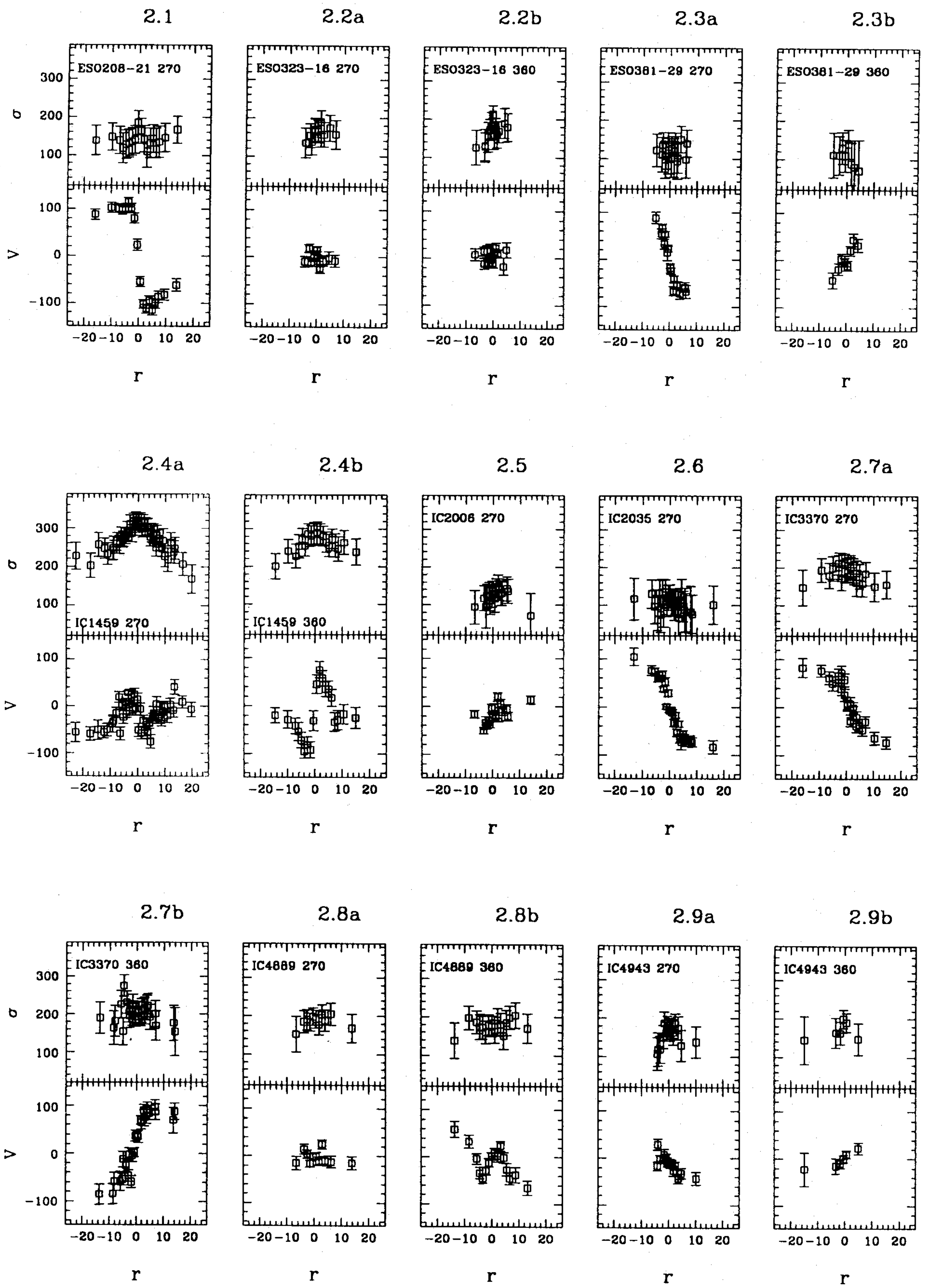

Figure 2. Rotation velocities and velocity dispersion profiles for the 42 galaxies. Numbers from 1 to 42 refer to the different galaxies, as listed in the tables. 'a' and 'b' refer to different position angles (respectively 270° and 360°), when available. For NGC 4696, five position angles (225°, 270°, 300°, 330°, 360°) were available. They are labelled with letters from a to e in Fig. 2.29.

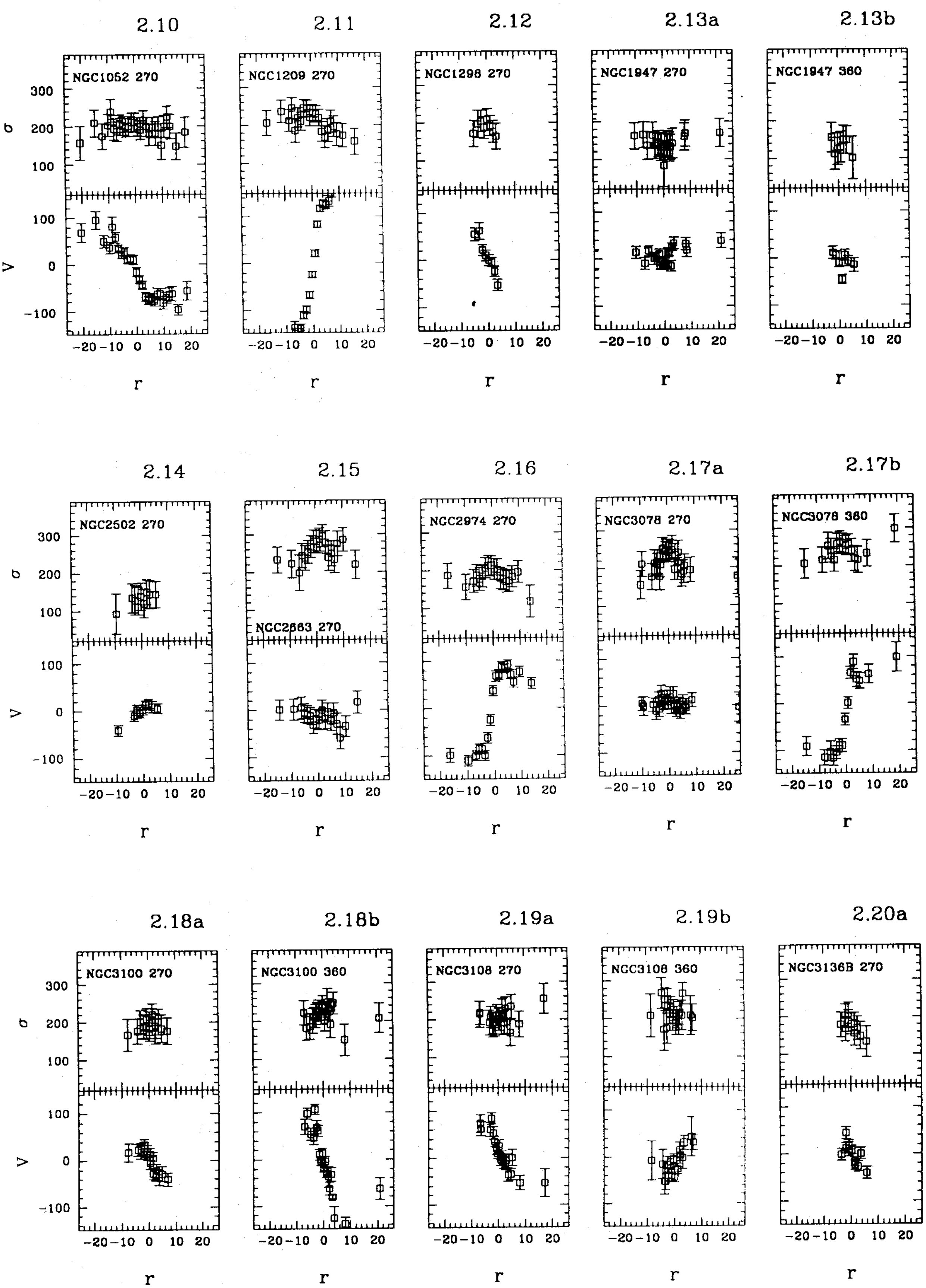

Figure 2 – *continued*

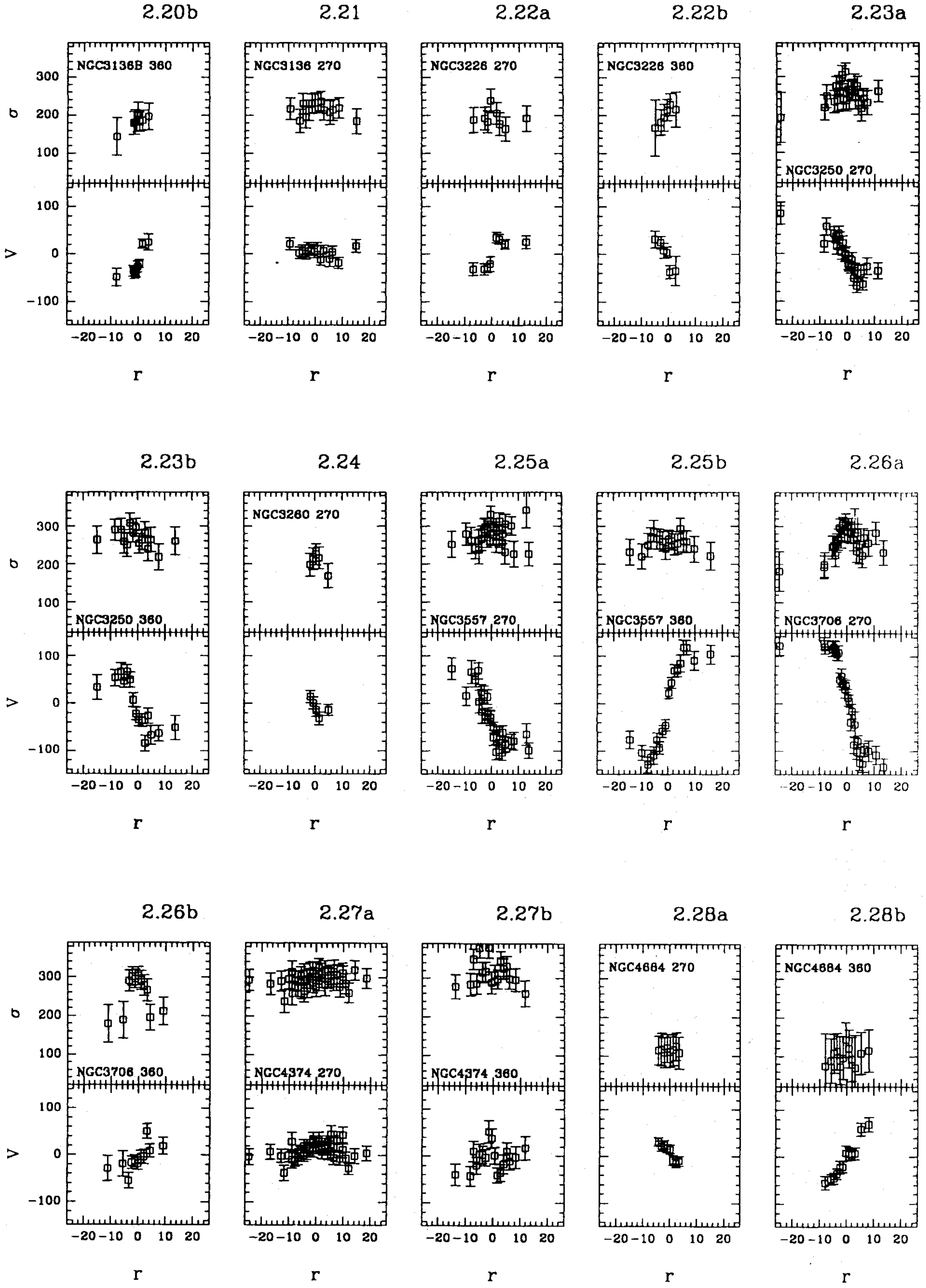

Figure 2 – *continued*

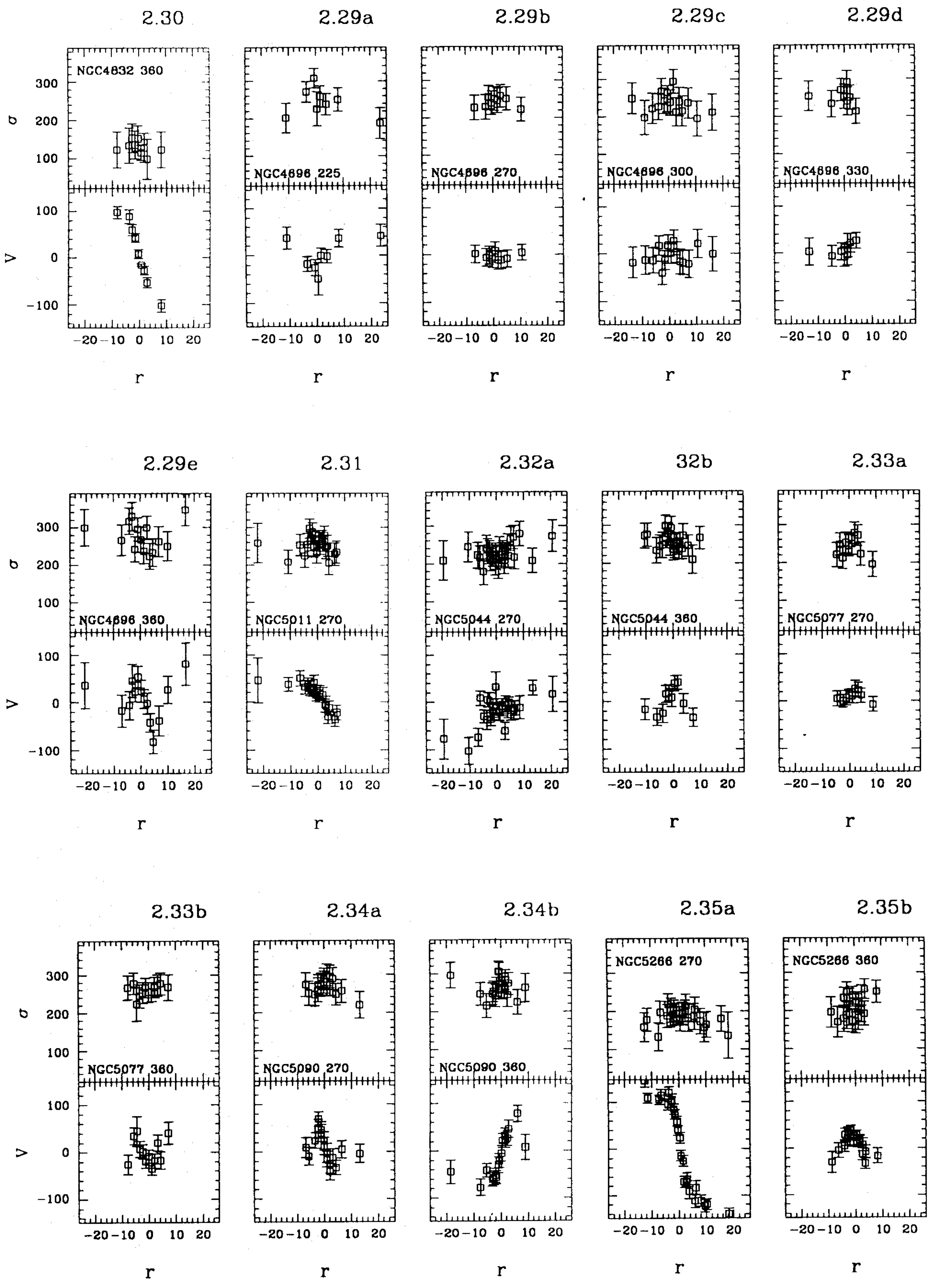

Figure 2 – *continued*

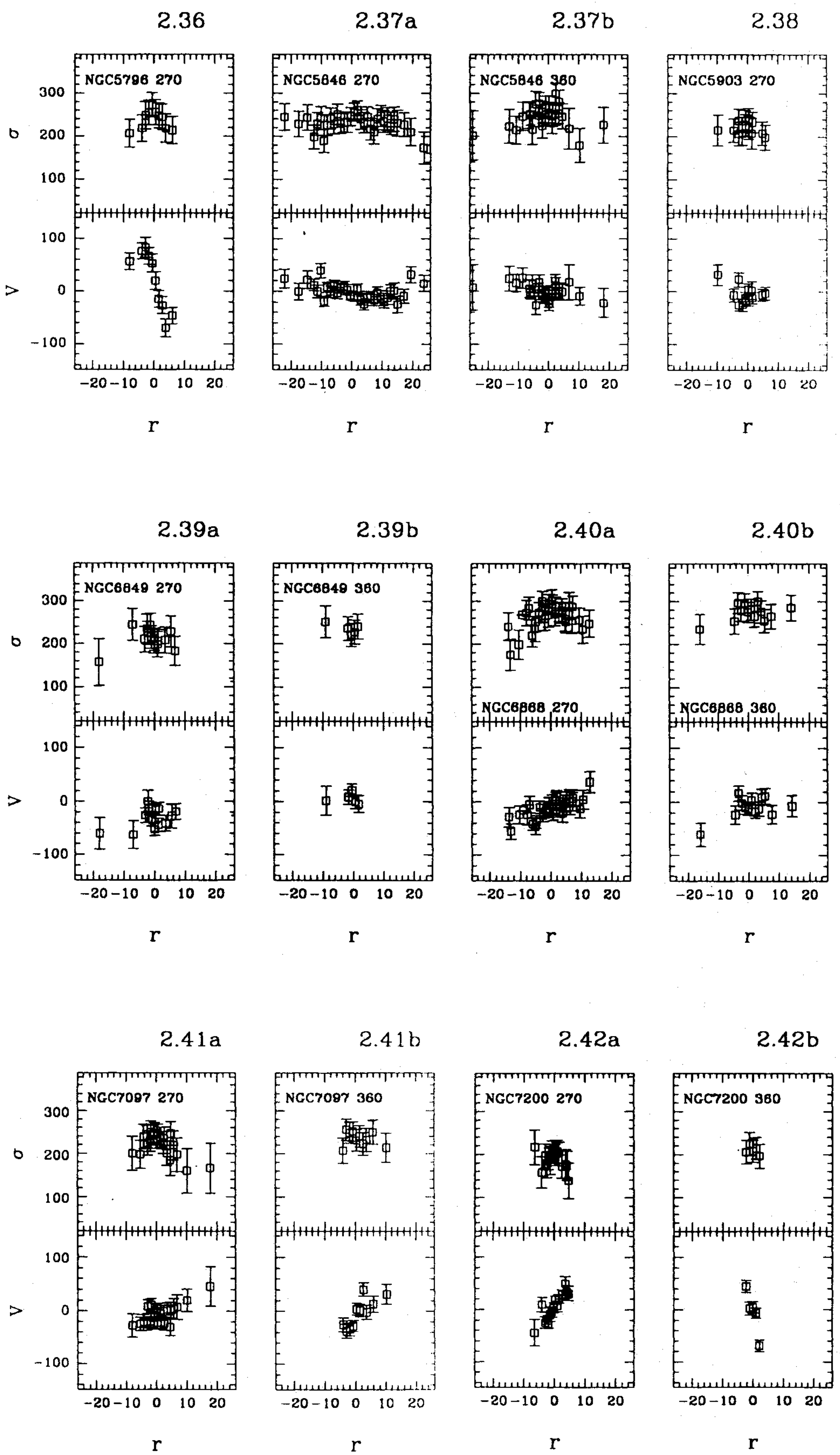

Figure 2 – *continued*

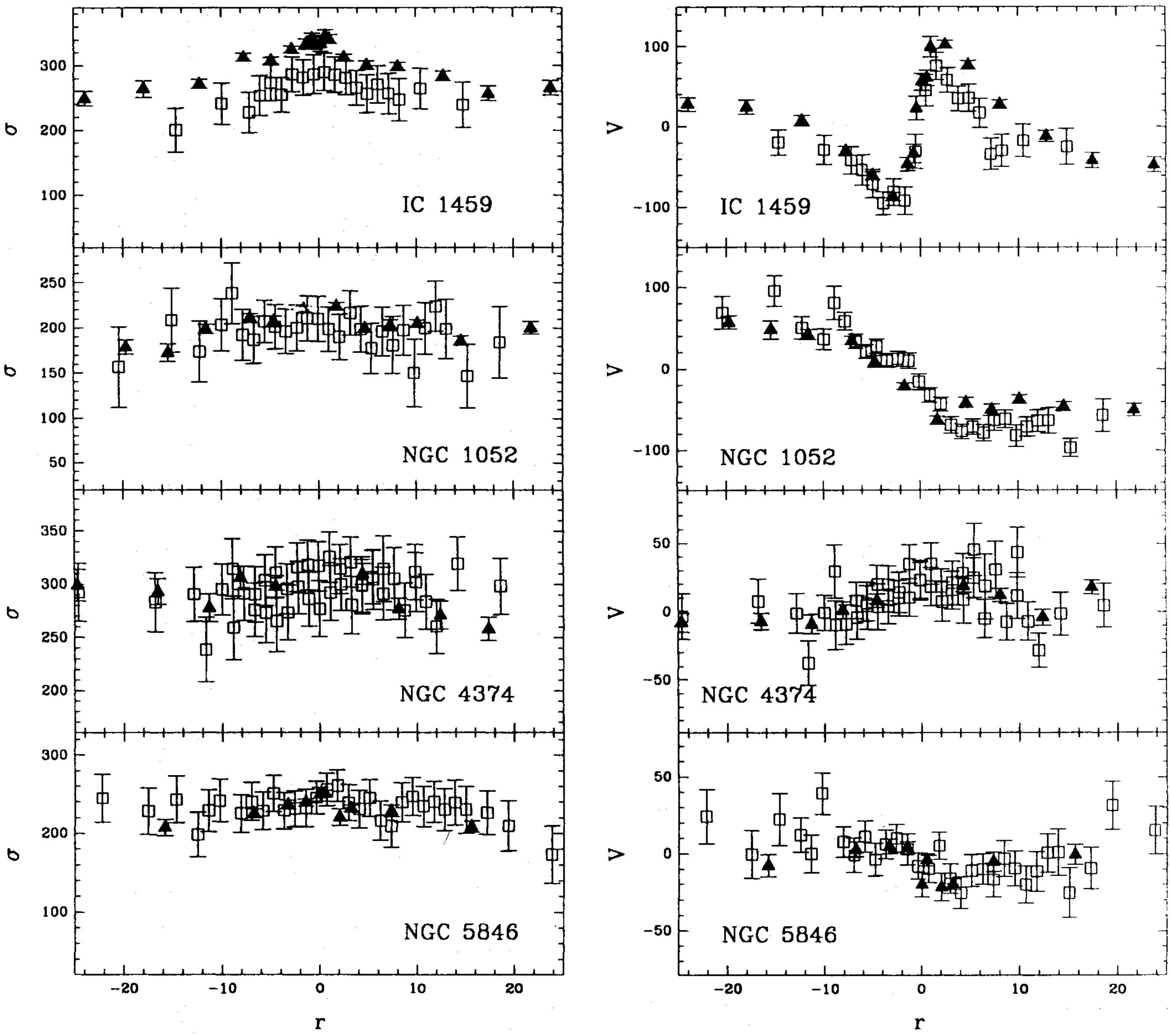

Figure 3. A comparison between our kinematic profiles (open squares) and those of Davies & Birkinshaw (1988, DB) and Franx & Illingworth (1988, FI) (in both cases filled triangles). The following position angles are plotted: IC 1459, 360°_{our} and 39°_{FI}; NGC 1052, 270°_{our} and 73°_{DB}; NGC 4374, 270°_{our} and 97°_{DB}; NGC 5846, 270°_{our} and 80°_{FI}.

never coincident with either of the two principal photometric axes. For four of the six galaxies listed above, we checked that no rotation appeared at the position angle nearer to the minor axis (when available), and we used the extreme values reached by our quasi-major-axis rotation curves to estimate the maximum rotational velocity (V_{max} in Table 1a; ESO 323−16 and NGC 4696 were excluded due to the very small radial range sampled).

Peculiar core kinematics appear in the rotation curves of IC 4889, NGC 4374, NGC 4696 and NGC 5090. However, in view of the low resolution and restricted radial range of our data and, especially in the case of NGC 4696, strong emission lines and problems in sky subtraction, these results need to be confirmed.

In Table 4 we summarize the kinematical properties of the 42 galaxies.

4 LINE STRENGTH GRADIENTS

4.1 Data reduction

The definitions introduced by Burstein et al. (1984, hereafter B84) were used to compute, on the deredshifted (and rebinned so as to maintain a signal-to-noise ratio ≥ 30) spectra, radial line-strength gradients of Mg_2, Mg_1, TiO_1, TiO_2, Hβ, Na D and Fe_{5270}. Measurements were standardized to a 9-Å resolution. Errors due to photon statistics were computed according to the relation

$$\epsilon_i = \frac{\sqrt{OBJ + 2\times DK + [1+(1/N_{rows})]\times SKY + ron^2}}{OBJ}, \tag{1}$$

where *OBJ* is the total number of counts from the object, *SKY* is that from the sky, *DK* is that from the dark frame, and

Table 4. The kinematical properties of the 42 galaxies.

name	P.A.	V_{270}	R^{*}_{270}	V_{360}	R^{*}_{360}	comments
ESO 208-21	108	120	16	-	-	
ESO 323-16		0	7	0	7	almost round
ESO 381-29	44	80	6	45	5	
IC 1459	43	60	23	90	15	counter-rotating core
IC 2006	39	35 ?**	14	-	-	
IC 2035	84	95	16	-	-	
IC 3370	51	85	16	95	14	
IC 4889	1	0	14	60	14	PCK?***, this work
IC 4943		30 ?	18	0	17	almost round
NGC 1052	120	95	20	-	-	
NGC 1209	80	190	16	-	-	
NGC 1298	70	55	5	-	-	almost round
NGC 1947	49	0	21	0	5	? (dust lane)
NGC 2502	117	0	10	-	-	
NGC 2663	111	0	15	-	-	
NGC 2974	42	100	16	-	-	
NGC 3078	176	0	10	110	18	
NGC 3100	146	40	8	120	20	
NGC 3108	48	80	17	40	9	
NGC 3136	12	0	15	-	-	
NGC 3136B	30	0	6	40 ?	8	
NGC 3226	15	40 ?	12	30 ?	5	
NGC 3250	136	70 ?	11	80	15	
NGC 3260	8	0	5	-	-	
NGC 3557	32	100	15	130	15	
NGC 3706	74	130	13	50	11	
NGC 4374	135	35 ?	20	60 ?	19	PCK?, this work
NGC 4684	23	20 ?	5	60	8	
NGC 4696	94	0	23	80 ?	20	PCK?, this work
NGC 4832	39	75	8	-	-	
NGC 5011	158	50 ?	22	-	-	
NGC 5044		70 ?	20	40 ?	10	almost round
NGC 5077	10	0 ?	9	40 ?	8	
NGC 5090	110	55	13	75 ?	18	PCK?, this work
NGC 5266	105	120	18	40 ?	9	
NGC 5796	95	70	8	-	-	
NGC 5846		0	24	0 ?	18	almost round
NGC 5903	165	0	10	-	-	
NGC 6849	23	0	18	0	9	
NGC 6868	76	70 ?	14	0	16	
NGC 7097	20	40 ?	17	0	10	
NGC 7200	35	50 ?	7	60 ?	4	

Notes: column (1) = name; (2) = position angle of major axis (in degrees); (3) = amplitude of rotation at PA = 270° (in km s^{-1}); (4) = maximum radius of measurement at PA = 270° (in arcsec); (5) = amplitude of rotation at PA = 360° (in km s^{-1}); (6) = maximum radius of measurement at PA = 360° (in arcsec).
*For some galaxies, due to the limited radial range covered, amplitudes of rotation at our two position angles might be lower limits to actual rotation along these axes.
**Question marks indicate uncertain determination of V_{rot}.
***PCK? = hints for peculiar core kinematics from our data.

ron is the read-out noise of the CCD. The term $(1/N_{rows}) \times SKY$ arises from having subtracted a sky averaged on $N_{rows}(=20)$ rows from the galactic spectra. The error on the line-strength index is then set equal to the quadrature

$$\epsilon = coeff \times \sqrt{\sum_{i=c_1, c_2, b} \epsilon_i^2}, \qquad (2)$$

where c_1, c_2 and b indicate respectively the two continua and the index band. The coefficient *coeff* is equal to $1.08(=-2.5 \times \log_{10} e)$ for indices measured in magnitudes (Mg_2, Mg_1, TiO_1, TiO_2) and to $(C_{feat} \times W_{pix})/C_{cont}$ for indices measured in equivalent widths (Hβ, Na D and Fe_{5270}; C_{feat} is the total number of counts from the feature, W_{pix} is the pixel width in Å, and C_{cont} is the average continuum).

The line strengths were standardized to zero velocity dispersion by correcting for velocity dispersion broadening. The correction laws were derived by convolving the available template spectra with Gaussians mimicking values of sigma in the range 100–400 km s^{-1}, averaging the results for different templates, and fitting the obtained index–sigma average relations. Even at a value of $\sigma \simeq 300$ km s^{-1}, these corrections are negligible for the Mg_2 index and always much less than 10 per cent for the other molecular bands, while they rise to about 20 per cent for Hβ, Na D and Fe_{5270}. All available Fe_{5270} measurements, as well as all the line strengths measured for IC 1459, NGC 2663, NGC 2974, NGC 3078 and NGC 3706 (galaxies that show a significant velocity dispersion gradient over the measured radial range), were corrected by using the (smoothed) measured velocity dispersion profiles. For the remaining galaxies, whose velocity dispersion profiles show very shallow slopes, central velocity dispersions were used to correct all other indices over the measured radial range.

Data referring to the same position angle were initially grouped together. Central values were obtained by averaging

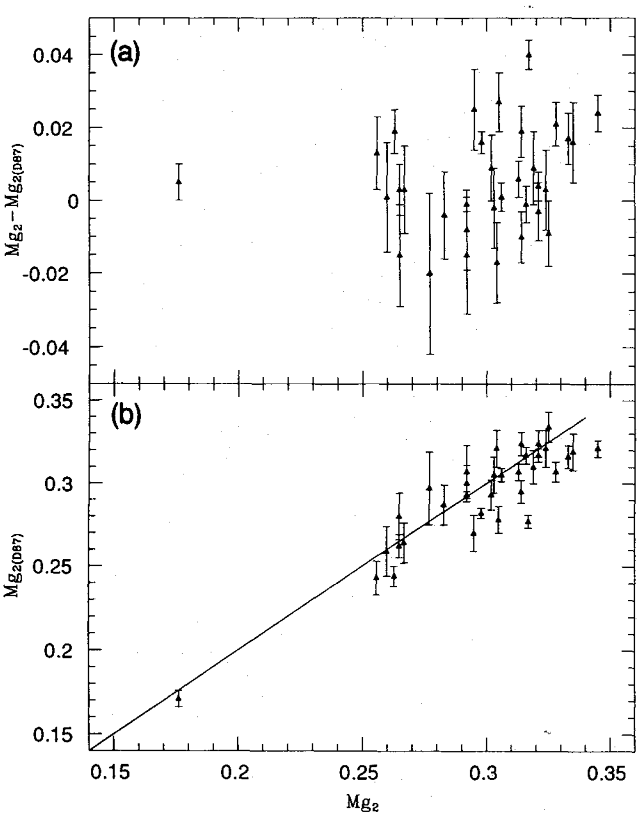

Figure 4. (a) Differences between our and the D87 central Mg_2 values plotted against our own measurements. (b) The D87 measurements of central Mg_2 plotted against the values derived from this work.

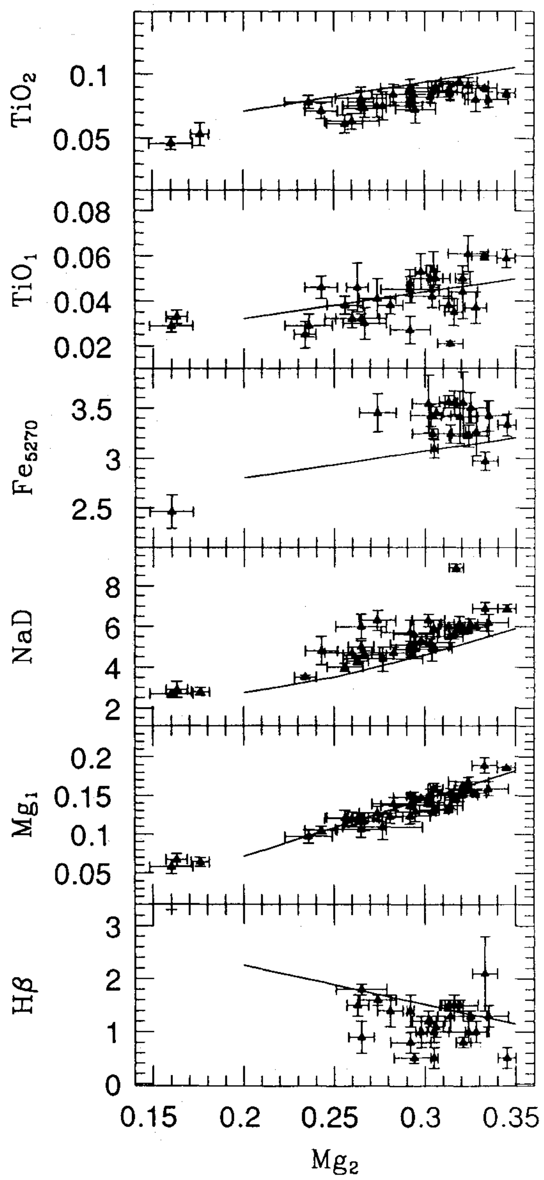

Figure 5. Various line strengths versus Mg_2 index. Symbols are measurements from this work, solid lines the fits of B84.

the inner 3 arcsec, and nominal errors equal to the relative rms were attributed to these measurements. The Mg_2 central values showed no significant shift with respect to those of D87 (rms ≃ 0.02 mag). In Figs 4(b) and (a) we plot, respectively, the D87 Mg_2 values, and the differences between our and the D87 Mg_2 values, against our Mg_2. For all other indices, for which individual measurements on the Lick system were not available, we derived the differences

$$\delta\, \text{index} = \text{index} - \text{index}_{\text{fitB84}}$$

between our measurements and the average fits to the (index versus Mg_2) relationships reported in B84. In Fig. 5 we plot our measurements of the various line strengths and the B84 fits against our Mg_2; in Fig. 6, the differences (δ index) between our measurements and the B84 fits are plotted against our measurement of the specific index. Linear fits to the (δ index versus index) relationships were then obtained. The Mg_1 index turns out already to be on the Lick system, while for the other line strengths the corrections are

$$\delta TiO_2 = 0.44(\pm 0.13) \times TiO_2 - 0.048(\pm 0.010),$$

$$\delta TiO_1 = 0.92(\pm 0.08) \times TiO_1 - 0.040(\pm 0.006),$$

$$\delta Fe_{5270} = 0.87(\pm 0.07) \times Fe_{5270} - 2.67(\pm 0.02),$$

$$\delta H\beta = 0.72(\pm 0.13) \times H\beta - 1.17(\pm 0.03),$$

$$\delta \text{Na D} = 0.36(\pm 0.06) \times \text{Na D} - 1.11(\pm 0.04).$$

Since our sample is highly biased towards galaxies with strong emission lines, resulting in Hβ emission, and with dust, producing interstellar Na D absorption, there may be, for these two lines, valid physical reasons for the significant offset of our sample from the average fits of B84. The corrections above have *not* been applied to data shown later in figures and tables.

Radial logarithmic slopes of the indices were computed by a linear least-squares fit; points inside 2.5 arcsec were discarded to avoid seeing effects. Reliable estimates of line-strength gradients, especially for weak or narrow lines, were not possible for some galaxies owing to the small radial range of the measurement or to a large scatter in the data. For example, the Fe_{5270} line in the outer galactic regions often had such large errors as to lead to a formal error in the gradient comparable to the measured slope. Gradients computed within equal radial ranges (2.5 arcsec $< r < 0.4 R_e$) were consistent with those measured on all external points, but were available for only a few objects and could not be used to study the statistical properties of the sample (galaxies

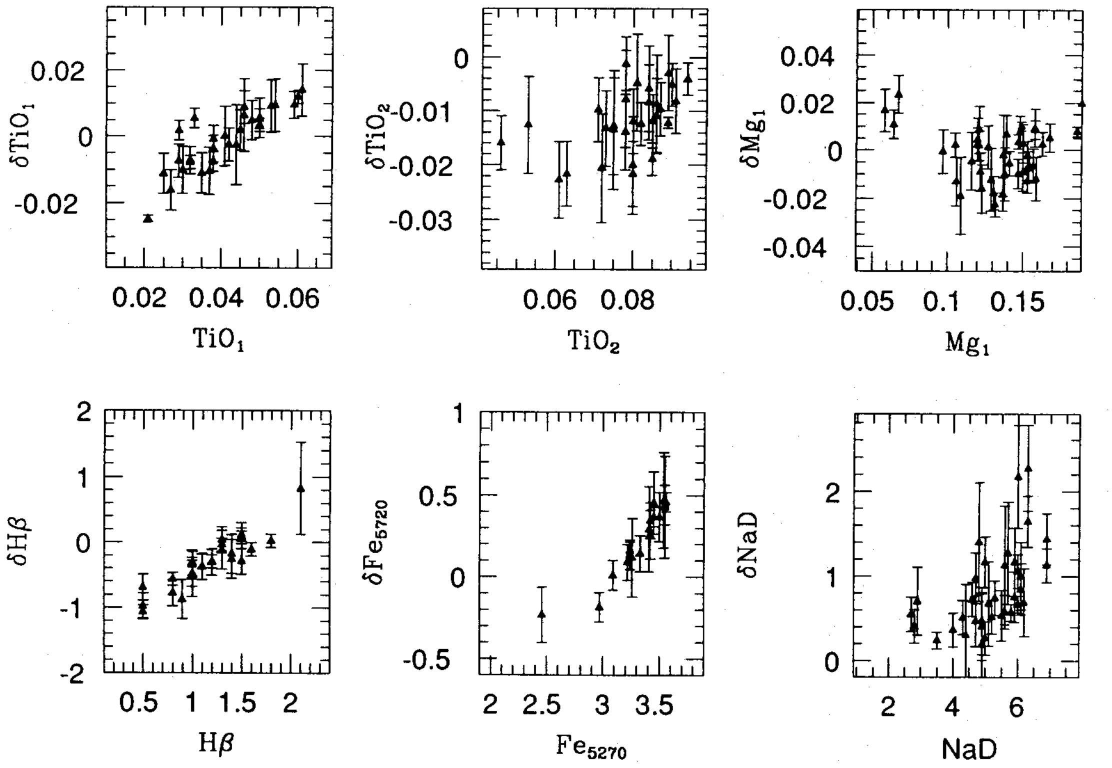

Figure 6. Differences (δ index) between our measurements and the fits of B84 plotted against our measurements of the various line strengths.

Table 5. The central values of all metallicity indices.

name	Mg_2	err_{Mg_2}	Mg_1	err_{Mg_1}	NaD	err_{NaD}	Fe_{5270}	$err_{Fe_{5270}}$	$H\beta$	$err_{H\beta}$	TiO_1	err_{TiO_1}	TiO_2	err_{TiO_2}
ESO 208-21	.304	.011	.138	.011	4.9	.6	3.24	.05	-	-	.042	.005	.086	.009
ESO 323-16	.267	.012	.116	.012	4.6	.2	-	-	-	-	.030	.007	.073	.007
ESO 381-29	.176	.005	.064	.006	2.8	.2	-	-	-	-	-	-	.053	.009
IC 1459	.345	.005	.186	.002	6.9	.2	3.33	.11	.5	.2	.059	.004	.085	.003
IC 2006	.292	.002	.149	.002	4.9	.4	-	-	1.4	.3	.048	.006	.080	.006
IC 2035	.160	.012	.058	.009	2.7	.2	2.46	.17	3.5	.2	.029	.003	.046	.005
IC 3370	.265	.007	.121	.006	5.0	.3	-	-	.9	.3	-	-	.078	.009
IC 4889	.263	.006	.120	.007	4.3	.2	-	-	1.5	.2	.046	.011	-	-
IC 4943	.256	.010	.121	.010	4.0	.2	-	-	-	-	.038	.004	.061	.007
NGC 1052	.333	.007	.189	.010	6.9	.3	2.97	.09	-2.1	.7	.060	.002	.089	.001
NGC 1209	.303	.011	.150	.008	5.2	.2	3.42	.11	1.2	.1	.050	.006	.082	.004
NGC 1298	.234	.006	-	-	3.5	.1	-	-	-	-	.025	.006	-	-
NGC 1947	.243	.009	.105	.005	4.8	.7	-	-	-	-	.046	.005	.071	.006
NGC 2502	.281	.007	.122	.008	-	-	-	-	1.4	.3	.038	.004	-	-
NGC 2663	.314	.007	.137	.007	5.5	.3	-	-	1.3	.3	.021	.001	.086	.007
NGC 2974	.292	.011	.123	.010	5.1	.5	-	-	.8	.2	.027	.006	.078	.007
NGC 3078	.325	.009	.157	.007	6.1	.3	3.50	.15	1.3	.1	-	-	-	-
NGC 3100	.294	.011	.148	.007	5.6	.7	-	-	.5	.1	-	-	.084	.007
NGC 3108	.302	.009	.141	.005	6.3	.3	3.54	.29	1.2	.2	-	-	-	-
NGC 3136	.265	.014	.106	.010	6.0	.6	-	-	1.8	.1	.032	.002	.081	.009
NGC 3136B	.283	.012	.139	.008	4.7	.3	-	-	-	-	-	-	.084	.008
NGC 3226	.292	.016	.137	.017	5.7	.6	-	-	-	-	.045	.006	.089	.007
NGC 3250	.316	.005	.147	.006	5.6	.2	3.55	.12	1.5	.2	.035	.006	-	-
NGC 3260	.277	.022	.109	.016	4.4	.6	-	-	-	-	-	-	.075	.011
NGC 3557	.313	.005	.132	.005	6.0	.2	3.56	.06	1.5	.1	.038	.003	.087	.005
NGC 3706	.319	.010	.150	.008	6.1	.4	3.41	.26	1.5	.1	-	-	.094	.003
NGC 4374	.306	.004	.158	.004	-	-	3.45	.06	1.1	.2	.050	.003	.090	.004
NGC 4684	.163	.006	.067	.008	2.9	.4	-	-	-	-	.033	.003	-	-
NGC 4696	.317	.004	-	-	8.9	.2	-	-	-	-	-	-	-	-
NGC 4832	.236	.013	.097	.009			-	-	-	-	.029	.005	.078	.005
NGC 5011	.305	.008	.131	.007	5.0	.2	-	-	1.0	.2	-	-	-	-
NGC 5044	.321	.008	.154	.006	-	-	-	-	-	-	.044	.012	-	-
NGC 5077	.314	.007	.153	.006	-	-	3.24	.09	-	-	-	-	.085	.005
NGC 5090	.328	.006	.153	.005	6.0	.1	3.26	.24	1.0	.2	.037	.007	.080	.009
NGC 5266	.274	.010	.127	.009	6.3	.5	3.45	.19	1.6	.1	.041	.009	.075	.009
NGC 5796	.335	.011	.159	.009	6.2	.4	3.42	.15	1.3	.2	-	-	.080	.006
NGC 5846	.324	.011	.168	.006	5.8	.1	3.22	.11	1.0	.2	.061	.008	.091	.006
NGC 5903	.295	.011	.129	.013	4.9	.4	-	-	-	-	-	-	.072	.010
NGC 6849	.260	.015	.120	.009	4.7	.3	-	-	-	-	.032	.004	.063	.006
NGC 6868	.321	.004	.163	.005	5.9	.3	3.55	.31	.8	.1	.050	.002	-	-
NGC 7097	.305	.002	.158	.008	5.9	.4	3.09	.09	.5	.2	.054	.008	-	-
NGC 7200	.298	.003	.147	.003	5.3	.2	-	-	1.0	.3	.053	.008	-	-

Table 6. The radial logarithmic gradients of all metallicity indices.

name	$-\frac{dMg_2}{dLogr}$	err $\frac{dMg_2}{dLogr}$	$-\frac{dMg_1}{dLogr}$	err $\frac{dMg_1}{dLogr}$	$-\frac{dNaD}{dLogr}$	err $\frac{dNaD}{dLogr}$	$-\frac{Fe_{5270}}{dLogr}$	err $\frac{Fe_{5270}}{dLogr}$	$-\frac{dH\beta}{dLogr}$	err $\frac{dH\beta}{dLogr}$	$-\frac{dTiO_1}{dLogr}$	err $\frac{dTiO_1}{dLogr}$	$-\frac{dTiO_2}{dLogr}$	err $\frac{dTiO_2}{dLogr}$
ESO 208-21	.090	.010	.062	.008	2.36	.19	.66	.40	-	-	-	-	-	-
ESO 323-16	.058	.012	.059	.018	-	-	-	-	-	-	-	-	-	-
ESO 381-29	-	-	.033	.020	-	-	-	-	-	-	-	-	-	-
IC 1459	.080	.009	.057	.005	2.6	.10	.44	.21	-.62	20	0074	.0030	.0037	0018
IC 2006	.075	.009	.038	.008	3.35	.34	-	-	-	-	-	-	-	-
IC 2035	.020	.012	-	-	1.48	.23	1.02	.5	.83	.50	-	-	-	-
IC 3370	.026	.010	-	-	1.10	.30	-	-	-.91	.50	-	-	-	-
IC 4889	.062	.010	.054	.009	1.72	.44	-	-	-	-	-	-	-	-
IC 4943	.066	.018	-	-	1.5	.4	-	-	-	-	-	-	-	-
NGC 1052	.074	.004	.074	.004	4.01	.14	.56	.27	-3.53	.29	0169	.0040	.0099	0040
NGC 1209	.078	.007	.037	.007	1.07	.29	1.13	.55	-.45	.27	-	-	.0171	0095
NGC 1298	-	-	-	-	-	-	-	-	-	-	-	-	-	-
NGC 1947	-	-	.033	.010	-	-	-	-	-	-	-	-	-	-
NGC 2502	.033	011	.047	.016	-	-	-	-	-	-	-	-	-	-
NGC 2663	.091	014	.052	.010	2.58	.31	-	-	-	-	-	-	.0112	.0065
NGC 2974	.074	009	.045	.008	-	-	-	-	-.24	.20	-	-	.0078	.0046
NGC 3078	.071	.006	.052	.008	1.81	.36	.92	50	.35	.28	-	-	-	-
NGC 3100	.078	.011	.055	.008	2.66	.51	-	-	-.99	.70	-	-	-	-
NGC 3108	.059	.020	.057	.010	2.66	.73	.53	.40	-	-	-	-	-	-
NGC 3136	-	-	.035	.011	2.48	.65	-	-	-	-	-	-	-	-
NGC 3136B	-	-	-	-	-	-	-	-	-	-	-	-	-	-
NGC 3226	-	-	-	-	-	-	-	-	-	-	-	-	-	-
NGC 3250	.058	.009	049	.017	1.0	.4	.76	45	.87	.45	0420	.0200	-	-
NGC 3260	-	-	-	-	-	-	-	-	-	-	-	-	-	-
NGC 3557	.045	.007	-	-	1.55	.25	-	-	0.	.20	0230	.0101	-	-
NGC 3706	.095	009	.075	.008	2.13	.47	.44	.37	-	-	-	-	-	-
NGC 4374	.050	.004	.045	.005	1.39	.25	.33	.25	-.45	.20	0131	.0038	.0077	.0035
NGC 4684	-	-	-	-	2.07	.78	-	-	-	-	-	-	-	-
NGC 4696	-	-	-	-	-	-	-	-	-	-	-	-	-	-
NGC 4832	.058	.013	.032	.012	-	-	-	-	-	-	-	-	-	-
NGC 5011	.067	.013	.044	.008	-	-	-	-	-.74	.45	-	-	-	-
NGC 5044	.034	.012	.045	.007	1.35	.40	-	-	-	-	.0195	.0086	-	-
NGC 5077	.056	.013	.073	.009	-	-	.64	.50	-2.40	.70	-	-	.0218	.0110
NGC 5090	.045	.012	-	-	1.64	.40	.69	.51	-	-	-	-	-	-
NGC 5266	.081	.010	.057	.010	3.40	.41	1.07	.50	-	-	-	-	-	-
NGC 5796	.059	003	.043	.014	-	-	.65	.42	-1.02	.60	-	-	-	-
NGC 5846	.003	007	.016	.008	.70	05	71	27	-.55	.28	-.0083	.033	-.0590	.0021
NGC 5903	-	-	-	-	-	-	-	-	-	-	-	-	-	-
NGC 6849	-	-	-	-	-	-	-	-	-	-	-	-	-	-
NGC 6868	062	013	-	-	.87	.16	.36	20	-.98	.40	.0377	.0102	-	-
NGC 7097	.115	010	.084	.008	2.90	.32	1.88	.45	-1.34	.50	.0300	.0090	-	-
NGC 7200	-	-	.093	.017	-	-	-	-	-	-	.0528	.0201	-	-

1993MNRAS.265..553C

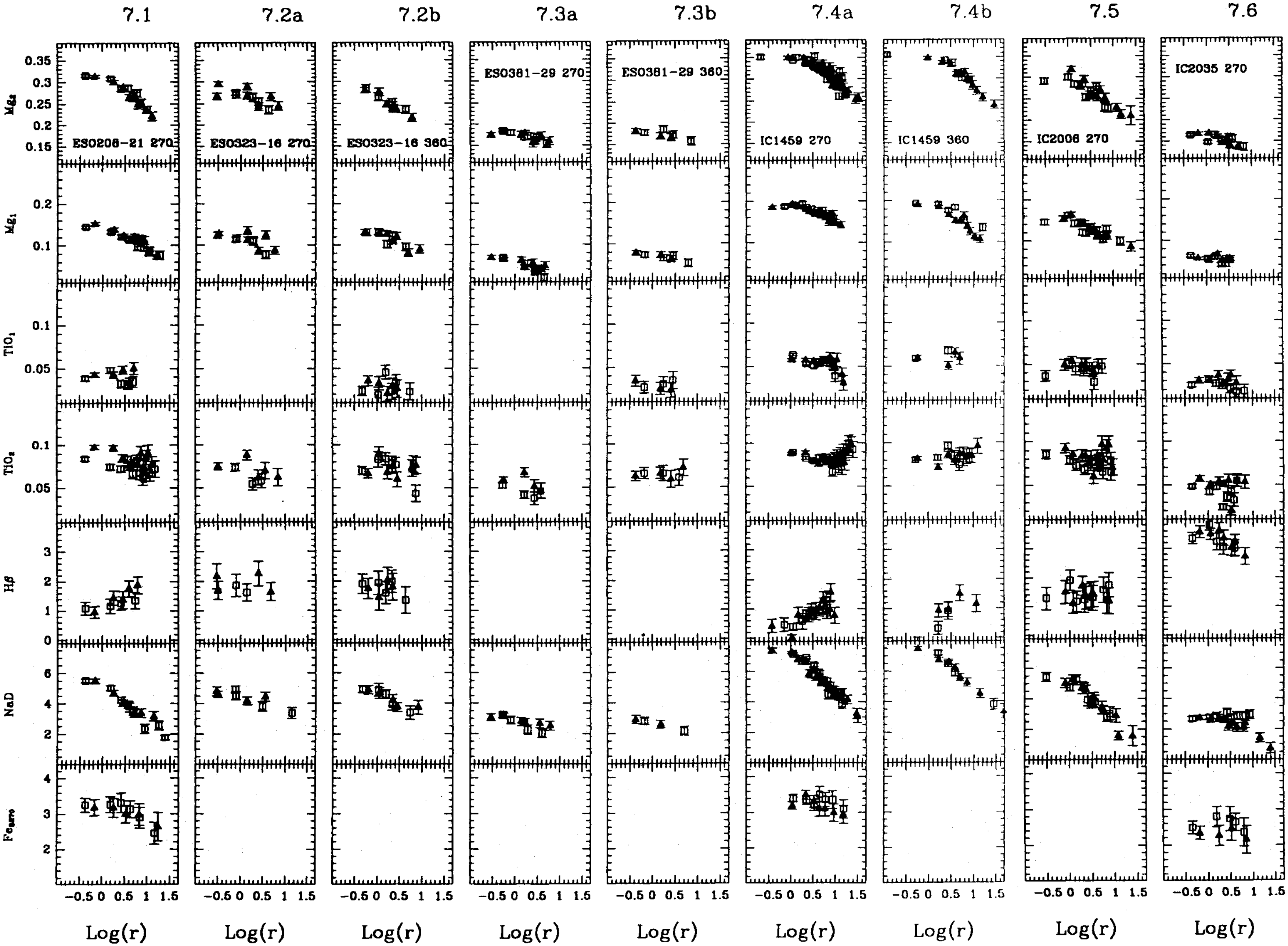

Figure 7. Radial profiles of, from top to bottom, Mg_2, Mg_1, TiO_1, TiO_2, Hβ, Na D and Fe_{5270} indices. Numbers and letters are as in Fig. 2.

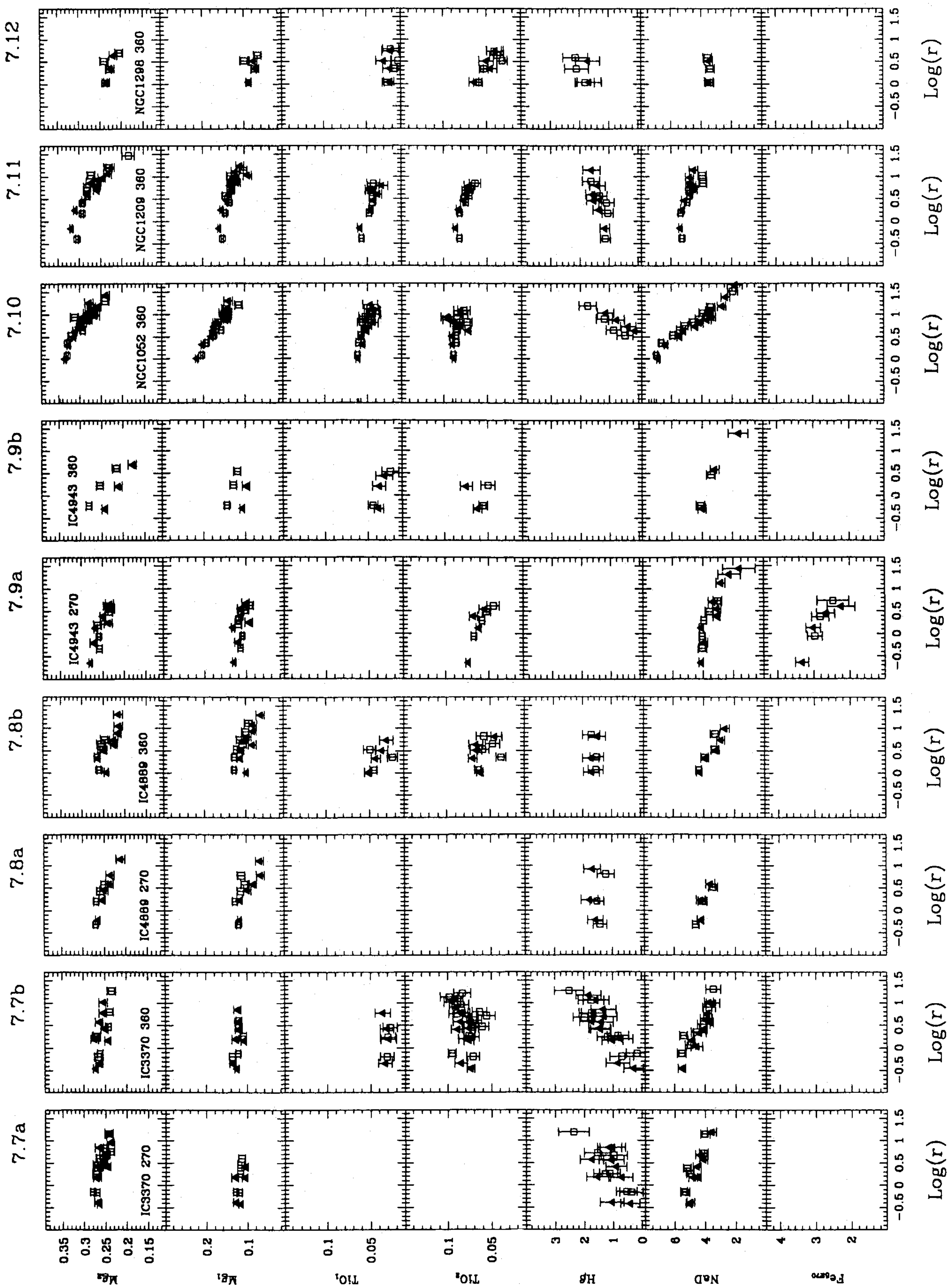

Figure 7 – *continued*

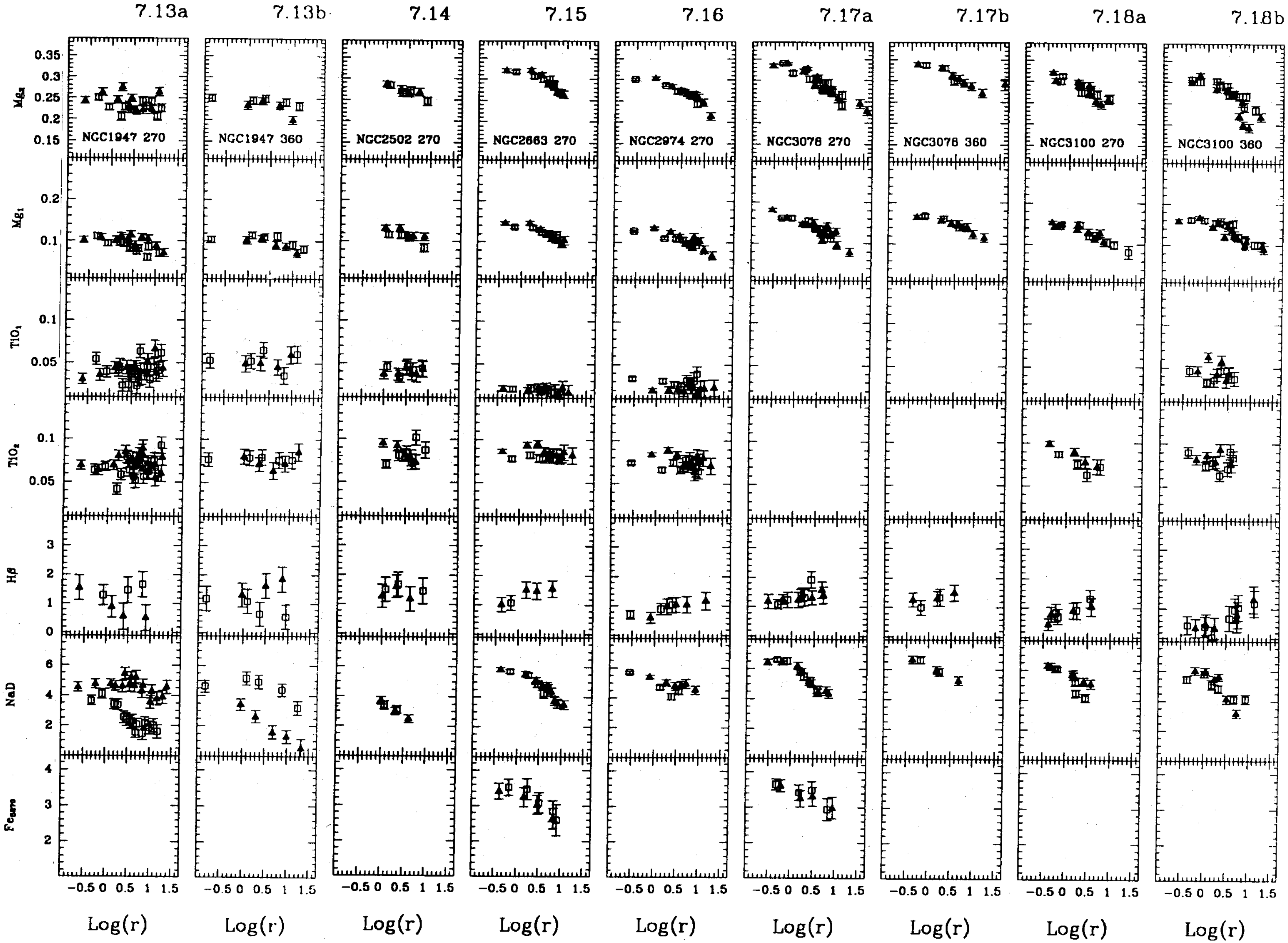

Figure 7 – *continued*

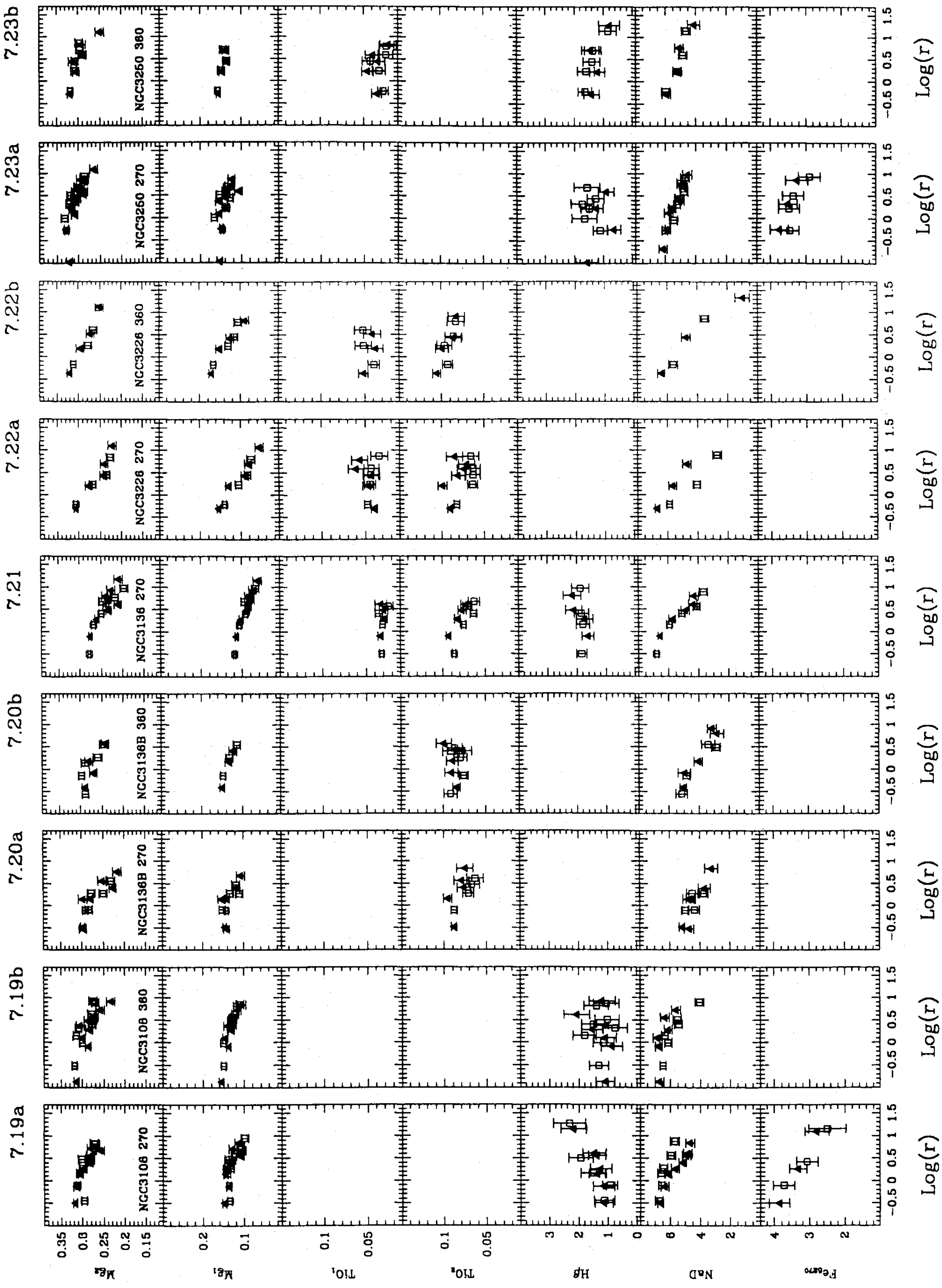

Figure 7 – *continued*

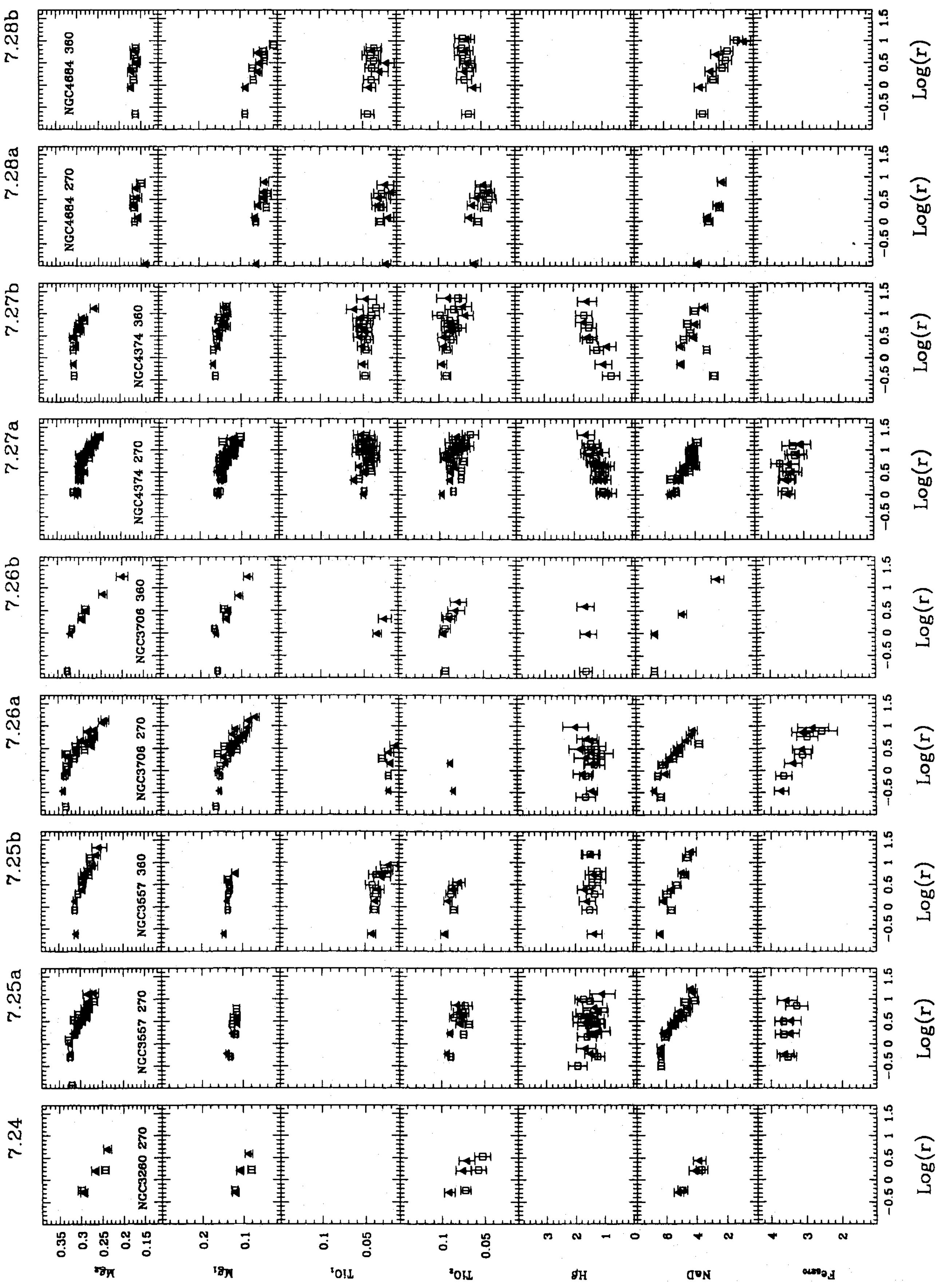

Figure 7 – continued

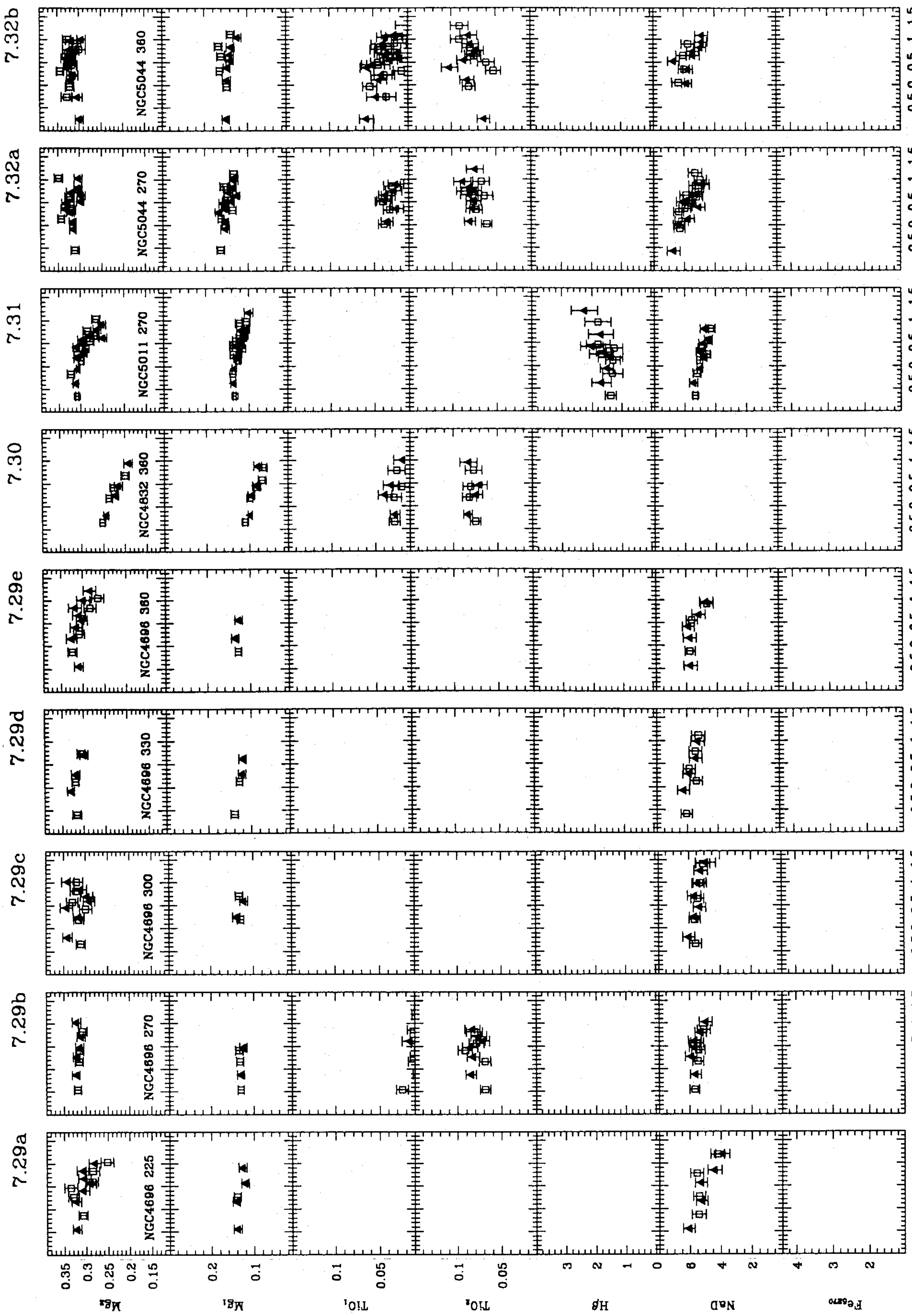

Figure 7 – *continued*

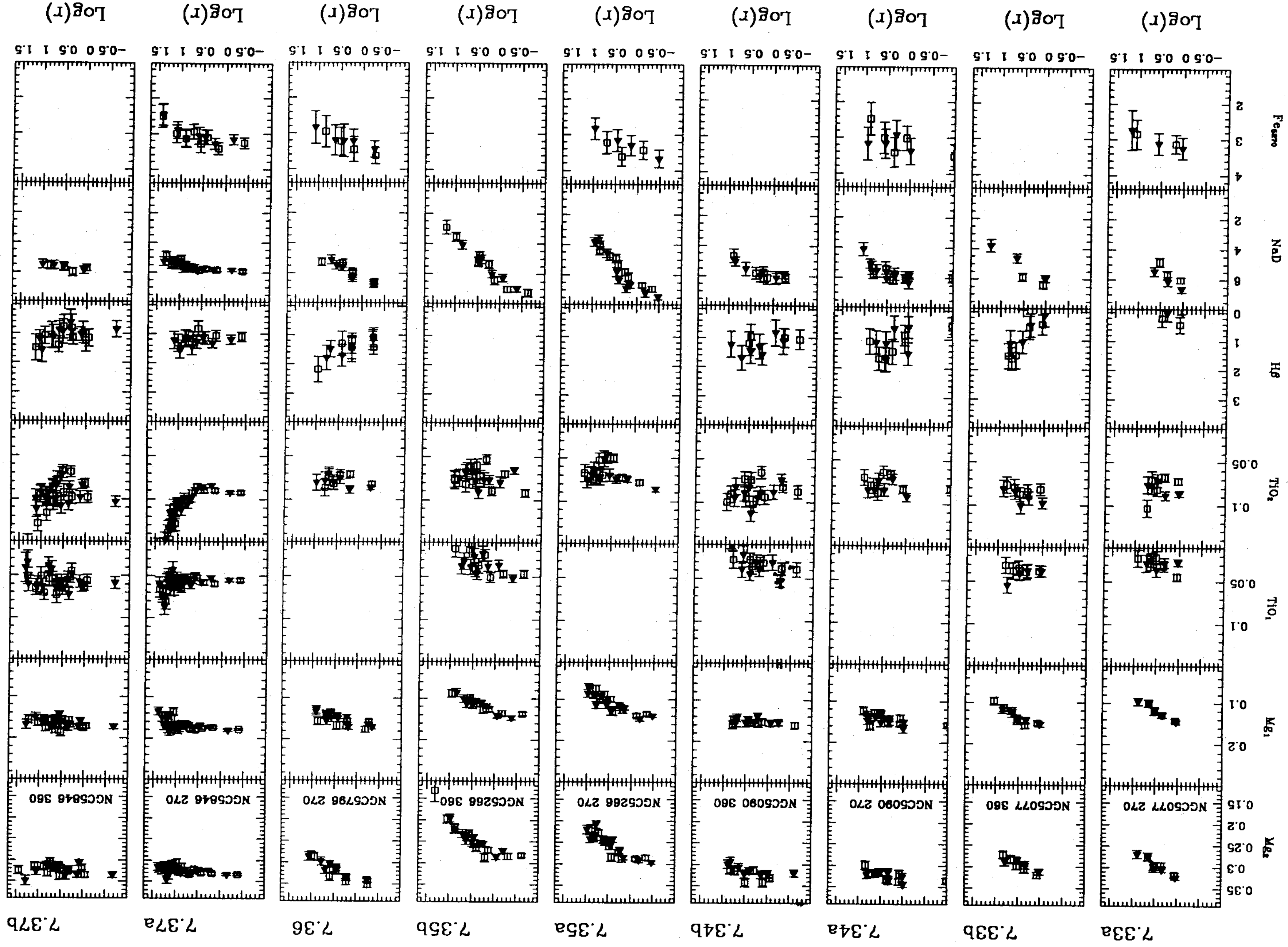

Figure 7 – *continued*

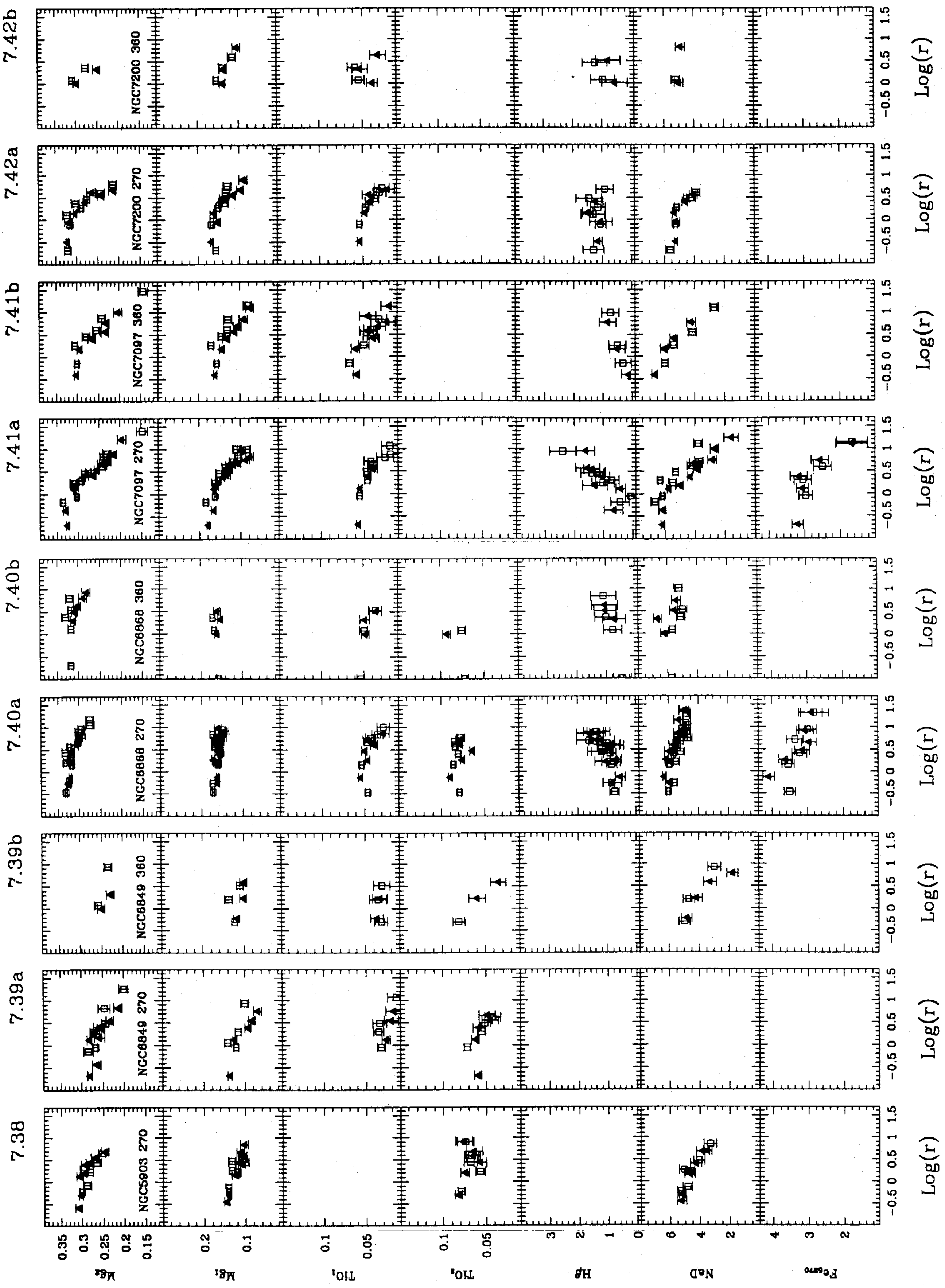

Figure 7 – *continued*

for which this measurement was possible were all high-mass ellipticals: see discussion below). We finally used, for our analysis, gradients derived from a fit to all measured points outside 2.5 arcsec. After exclusion of the two suspected spirals, Mg_2 gradients were available for 30 galaxies. For each object present at two position angles, a comparison of both the central values and the slopes derived in the two measurements showed no significant difference. For these galaxies we used, throughout our analysis, averages for both the central values and the gradients. Standard errors obtained by treating the two single measurements as independent were attributed to the final average values.

4.2 Results

For each galaxy, the central values and radial logarithmic gradients of all metallicity indices are listed in Tables 5 and 6 respectively, while radial profiles are shown in Figs 7.1–7.42 (a and b; data taken in different runs at the same position angle are shown overplotted). For the best determined indices, i.e. Mg_2, Mg_1, Na D and Fe_{5270}, the individual measurements at different radii are listed in Appendix B (on Microfiche MN265/1).

Correlations between different metallicity gradients were studied, and correlation coefficients and the associated probabilities P were computed to estimate the significance of the results. At a high level of significance, the Mg_1 and Na D gradients positively correlate with the Mg_2 ones ($P \geq 99$ per cent; see Figs 8a and b). Although the lack of correlation between the other line-strength gradients and the Mg_2 ones may indeed have an astrophysical origin and consequence, our data are not adequate to investigate any such relationships, or any trend between e.g. the TiO and Fe gradients, properly. This is because gradients for these indices were available for only a few galaxies; in many of our galaxies Hβ is filled with emission; and the scatter in both TiO features is large in our data.

Correlations between Mg_2 gradients and various physical parameters were then explored. When available, homogeneous collections of data were used, to avoid additional sources of scatter (see Table 1a).

No obvious features appear in the Mg_2 gradients that can be associated with the presence of shells, emission lines, of X-ray or radio emission. In addition, gradients in galaxies showing any of the above features have normal values when compared to those of the whole sample. Asymmetric metallicity profiles were instead measured in NGC 1947, possibly due to the presence of the dust lanes seen in this galaxy.

No significant dependence of the Mg_2 gradient on $(B-V)$, on deviations from ellipticity (a_4) or on V/σ [or $(V/\sigma)^*$] was found. However, although not statistically significant, a hint appears in our sample that fast-rotating galaxies show higher Mg_2 gradients than slowly rotating objects (Fig. 9b). This disappears when GES and DSP galaxies are added, although galaxies with high rotation velocities and low Mg_2 gradients are still absent in all three samples (Fig. 9b). A significant correlation appears instead with ellipticity ($P \geq 99$ per cent),

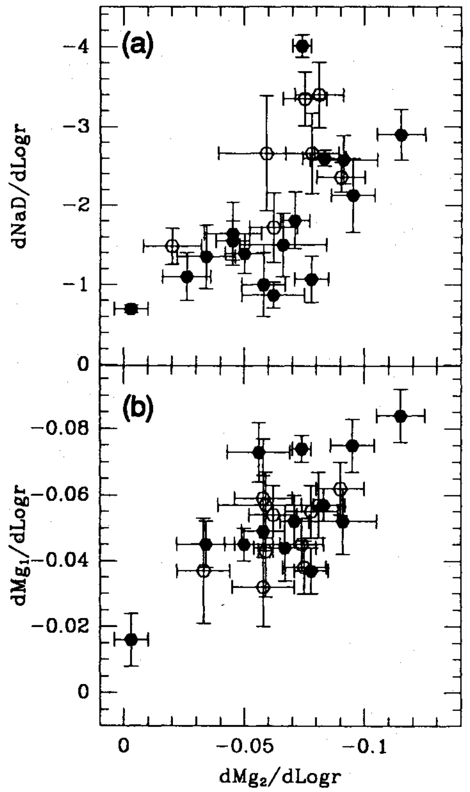

Figure 8. The radial logarithmic gradient of (a) Na D and (b) Mg_1 versus the radial logarithmic gradient of Mg_2. Filled symbols indicate elliptical and open symbols lenticular galaxies.

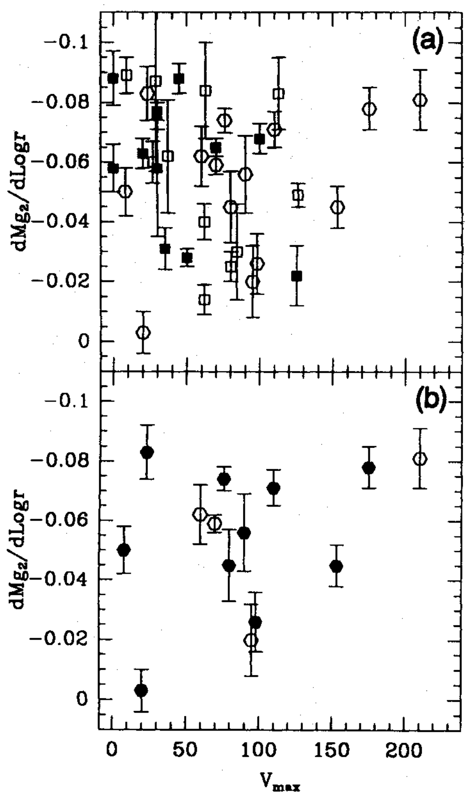

Figure 9. The Mg_2 gradient versus maximum radial velocity. (a) Open circles indicate all our 30 galaxies, open squares GES data and filled squares DSP data. (b) The 30 galaxies of our sample for which $(d\,Mg_2)/(d\log r)$ has been measured. Filled symbols indicate elliptical and open symbols lenticular galaxies.

with rounder galaxies showing in our data shallower Mg_2 gradients (Fig. 10b). Indeed, projection effects may play some role here, but they are not easy to disentangle; moreover, this correlation disappears when the enlarged sample containing our data plus that of DSP and GES is considered (Fig. 10a). It is therefore not yet clear whether (at least part of) the correlation is a physical effect, which is obscured when scattered, inhomogeneous measurements are used, or whether it is a 'conspiracy' in our data.

The dependence of metallicity gradients on 'fundamental' parameters was investigated. Galactic masses were computed assuming a Jaffe law for the density distribution (Jaffe 1983), and spherical symmetry, so that

$$M_{tot} = 4\pi \rho_0 r_m^3, \qquad (3)$$

where $r_m \simeq 10^{0.13} R_e$ (van Albada 1982), with R_e the effective radius, and ρ_0 is the central density.

For $r \ll r_m$, the isothermal sphere approximation can be used to relate ρ_0 to σ_0, so that

$$M_{tot} = 3 \times 10^3 \left(\frac{\sigma_0}{1\ \mathrm{km\ s^{-1}}}\right)^2 \left(\frac{D}{1\ \mathrm{Mpc}}\right)\left(\frac{R_e}{1\ \mathrm{arcsec}}\right) \mathrm{M}_\odot. \qquad (4)$$

Masses derived from the above definition are listed in Table 1(b).

The Mg_2 gradient shows a bimodal trend with mass, i.e. for objects less massive than about $10^{11}\ \mathrm{M}_\odot$ the Mg_2 gradient increases with increasing mass ($P \geq 99$ per cent), while more massive objects show no obvious pattern in the gradient–mass plane (Fig. 11a). This result is confirmed and strengthened by adding the DSP and GES data to our

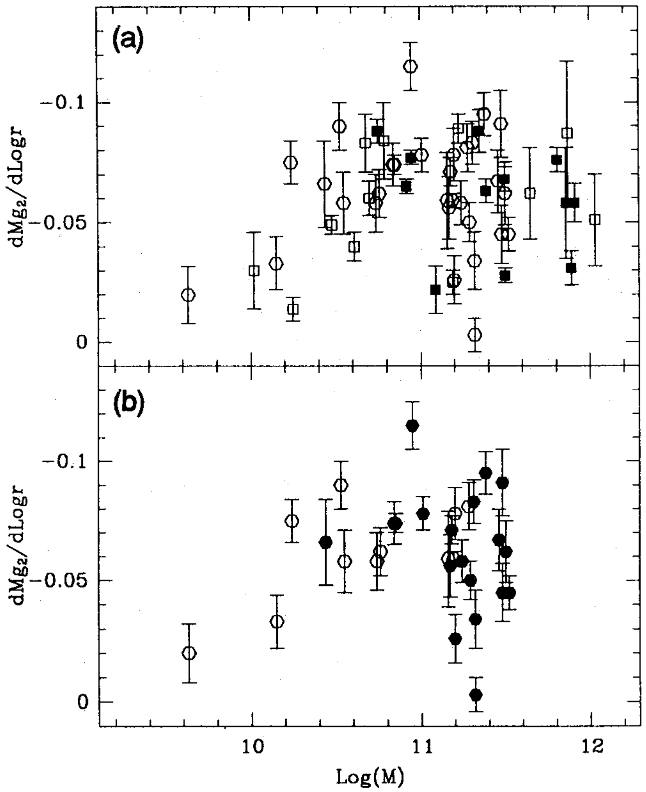

Figure 11. The Mg_2 gradient versus logarithm of galactic mass. (a) and (b) are as in Fig. 9.

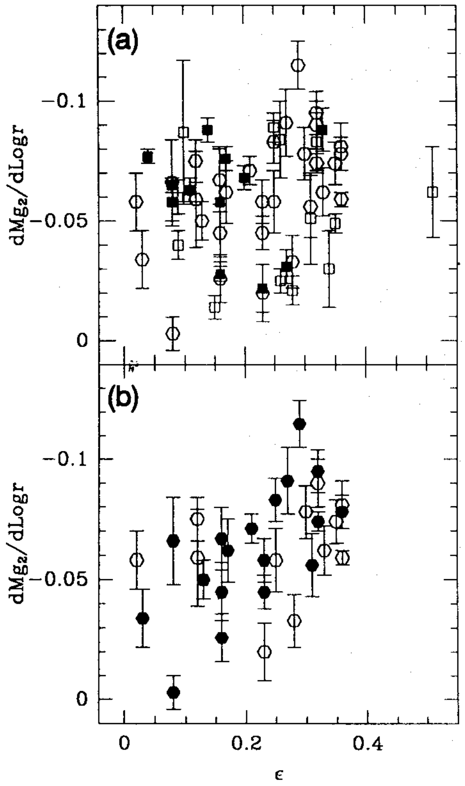

Figure 10. The Mg_2 gradient versus ellipticity. (a) and (b) are as in Fig. 9.

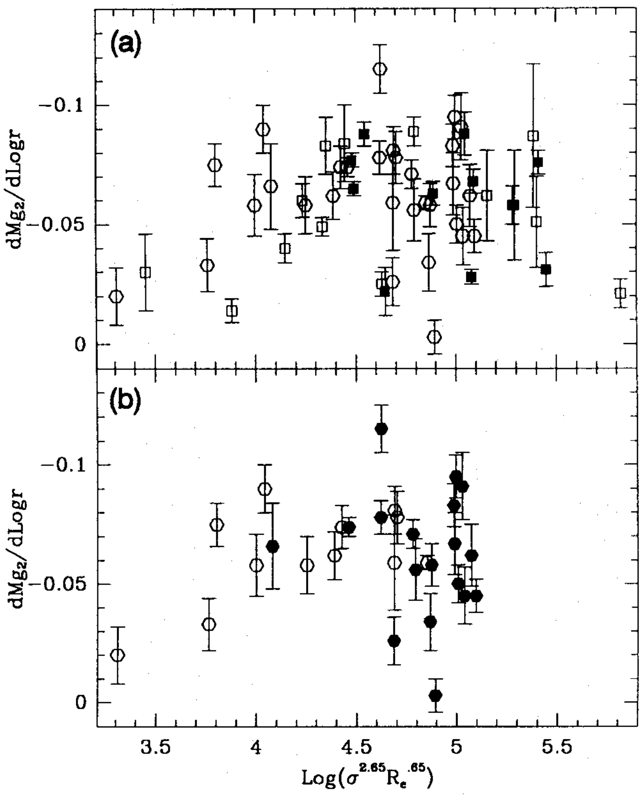

Figure 12. The Mg_2 gradient versus log(fundamental plane luminosity). (a) and (b) are as in Fig. 9.

sample, as shown in Fig. 11(b) [see also Figs 12a and 12b, where (d Mg_2)/(d log r) is plotted versus the 'fundamental plane' luminosity, $\sigma^{2.65}R_e^{0.65}$; again, $P>99$ per cent].

The Mg_2 gradient of low-mass galaxies consistently correlates, although with more scatter, with the central velocity dispersion σ_0 (Figs 13a–c) and the central Mg_2 value (Figs 14a–c; in both cases $P \simeq 98$ per cent). The same positive trend at low masses is observed in the M_B(d Mg_2)/(d log r) plane (with M_B the absolute B magnitude), although here the correlation is significant at less than the 90 per cent level. All these correlations disappear when high-mass galaxies also (or only) are considered.

Contradictory information on the relationship of Mg_2 gradients with M_B, Mg_2 and σ_0 is found in the literature, e.g. PE89 reports a positive correlation with M_B: GES report positive correlations with Mg_2 and σ_0; and DSP report instead no correlation with any fundamental parameter. Indeed, of the 13 GES galaxies, seven have small masses, while nine out of the 12 DSP galaxies are bright radio ellipticals populating the high-mass branch. Our results suggest therefore that previous discrepancies are due to too-small samples and/or to different selection effects, biasing the analysed samples towards different classes of galaxy.

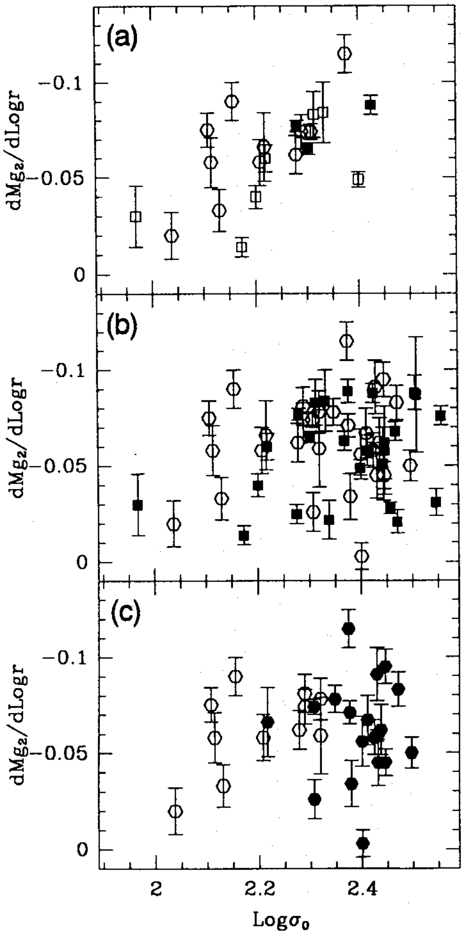

Figure 13. The Mg_2 gradient versus log(σ_0). (a) Galaxies with $M<10^{11}$ $M_\odot$. Open circles indicate our galaxies, open squares GES data and filled squares DSP data. (b) All galaxies of the three samples mentioned above. Symbols as in (a). (c) The 30 galaxies of our sample. Filled symbols indicate elliptical and open symbols lenticular galaxies.

In Fig. 15 we plot, for each of the 17 galaxies for which we were able to compute the Fe_{5270} index, a straight line connecting central (filled symbols) to outermost values in the Fe_{5270}–Mg_2 plane. In agreement with WFG (who first presented such a diagram) and with other studies (see e.g. Efstathiou & Gorgas 1985; DSP; CD), we find, on average, a steeper Fe-versus-Mg slope within galaxies than that obtained using a sample of galactic nuclei. In addition, galactic mass seems not to influence this diagram, e.g. no particular trend in the positions (and slopes) is found with increasing mass (even when only the subsample of 'low-mass' galaxies is considered). Also, no obvious trend is found with other parameters such as colours or M/L, though these results should be confirmed with higher quality data.

5 DISCUSSION

In simple models of dissipative collapse coupled with supernova-induced winds (Larson 1974; Carlberg 1984; Arimoto & Yoshii 1987; Matteucci & Tornambè 1987; Brocato et al. 1990), a galactic wind is generated when the thermal energy of the gas exceeds its potential energy. In this scenario, galaxies with smaller masses develop a wind earlier than massive ones and, as a consequence of this, a mass–metallicity relation is produced. Moreover, since star formation lasts longer and becomes faster as the radius decreases, a metallicity gradient is expected to form which should steepen as the masses and luminosities of the galaxies increase. This scenario seems to be the natural explanation for the observed

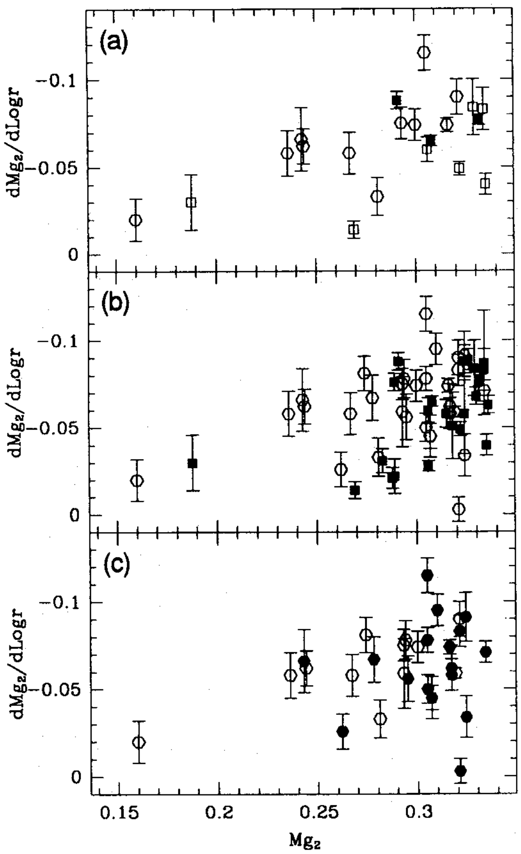

Figure 14. The Mg_2 gradient versus central Mg_2. (a), (b) and (c) are as in Fig. 13.

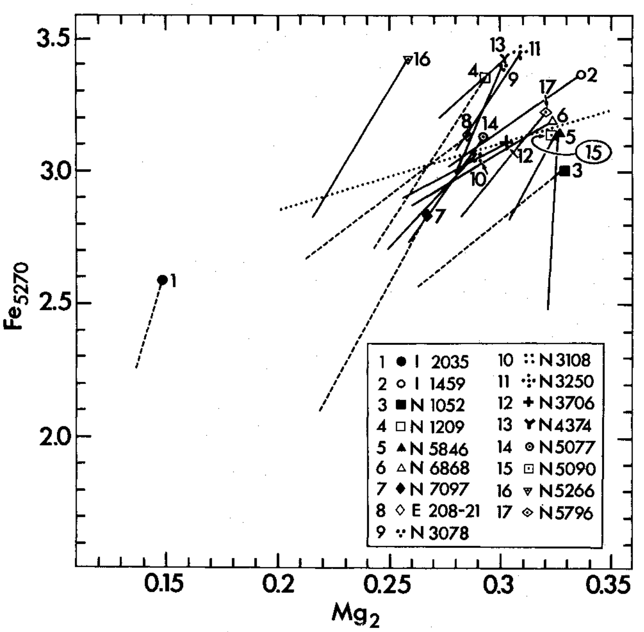

Figure 15. Fe_{5270} versus Mg_2 for the 17 galaxies for which the iron measurement is listed in Table 6. Symbols indicate central values. The straight lines describing Fe–Mg slopes within individual galaxies are obtained connecting, for each galaxy on the Fe–Mg plane, the central values to the average of the outermost 2.5 arcsec. Low-mass galaxies are identified with dashed lines. Overplotted (dotted line) is the fit to the galactic nuclei, taken from B84.

properties of small early-type galaxies in the $(d\,Mg_2)/(d \log r)$–mass plane. Indeed, many of the galaxies of our sample populating the low-mass branch are lenticular galaxies, i.e. galaxies with a fast-rotating stellar disc that testifies to the occurrence of a dissipative collapse in the gaseous protocloud. Small ellipticals do, however, fall on the same path in the $(d\,Mg_2)/(d \log r)$–mass plane, thus suggesting that (i) they have possibly originated through the same mechanism, and (ii) they should show, with a deeper investigation, the signature of dissipative collapse, e.g. a stellar disc (even if faint) detectable photometrically through discy isophotes. In fact, Nieto & Bender (1989) find that less massive galaxies have preferentially positive values of a_4. The fact that we do not observe any feature in the gradient–a_4 diagram might be a spurious result, as we have not accumulated an homogeneous collection of data on a_4 for our galaxies, and different radial ranges used in computing the parameter might strongly influence its value.

In this simple chemical enrichment scheme, the increasing amount of dissipation with galactic mass, which produces the correlation of mass with metallicity gradient, affects also the star formation time-scales, i.e. star formation should go slower as the mass increases. This would allow a larger number of type I supernovae (SNe) relative to type II, and would lead to an increase of iron content with galactic mass. In the Fe–Mg plane, this should be manifested in a systematic shift of the position of the galaxy (and maybe in an increasing slope) with mass, a trend that is not evident in our data. These data are, however, far from satisfactory for studying this point, as we have only five low-mass objects in the Fe–Mg plane and errors in the slopes are rather large. Even if this lack of trend were confirmed by better data, local inhomogeneities in the gas distribution could play an important role in explaining this point. Such a test (limited to galaxies smaller than the 'transition' mass) should, however, be tried.

Despite the possible success in explaining formation of smaller early-type galaxies, the simple dissipative collapse scenario with galactic winds, because of its predictions concerning the behaviour of [Mg/Fe] as a function of increasing mass (Matteucci & Tornambé 1987), has recently been shown to be inadequate for describing giant ellipticals. Observations (see e.g. WFG) show in fact a much higher [Mg/Fe] ratio in the nuclei of galaxies than would be expected for giant ellipticals under the most reasonable assumptions concerning the conversion of line indices into abundances. Our demonstrated absence of a positive correlation between mass and line-strength gradients for massive galaxies ($M > 10^{11}\,M_\odot$) supports the view that, above this critical mass, dissipative collapse in the current 'simple' formulation cannot explain the formation and evolution of giant ellipticals. Moreover, this might point to merging of smaller galaxies as the dominant mechanism in the formation of massive galaxies (see also Kormendy & Djorgovski 1989 for similar evidence based on colour gradients).

A flatter IMF (i.e. weighted towards more massive stars) has been invoked by WFG, in the context of merging during which starburst activity is provoked, to explain the results in the Fe_{5270} versus Mg_2 plane. It would also explain, with the higher number of dark remnants resulting from the increased occurrence of type II SNe, the observed weak correlation of M/L with mass (see e.g. Kormendy & Djorgovski 1989 and references therein).

The variety of slopes in the Fe–Mg plane presented here (and by WFG and DSP) might reflect the possibility that the sites of enhanced star formation, with the flatter IMF triggered by a merger, could be distributed somewhat randomly throughout the galaxy. This randomization might also be responsible for the observed lack of dependence of the Mg_2 gradient on mass above $10^{11}\,M_\odot$, where a great number of mergers might be expected. In this context, the observed transition on the $(d\,Mg_2)/(d \log r)$–mass plane also implies that the minimum mass for merging to create massive ellipticals cannot be much smaller than $10^{11}\,M_\odot$. So far, there is little quantitative evidence (both observational and theoretical) that the starburst phenomenon gives rise to any peculiarly flat IMF. Although it may seem intuitively to be a possible explanation, detailed modelling is still required to demonstrate its validity.

An alternative explanation would require that during their formation the more massive objects suffer less dissipation than the smaller ones. This would imply either (i) that merging becomes more stellar and less gaseous in these objects (Bender, Burstein & Faber 1992), or (ii) that, in the case of collapse, massive objects have a higher star formation rate, which quickly consumes all the available gas before dissipation becomes important. The fact that a tight correlation between the Mg_2 index and velocity dispersion exists in stellar systems covering a range of 15 mag, from dwarf spheroids to giant elliptical galaxies (Bender 1992), perhaps makes the collapse hypothesis appealing. In fact, if different mass systems are formed by different mechanisms, it seems a remarkable coincidence that this correlation remains intact (and with no change of slope) over the complete range.

In any case, if a less dissipative formation process is acting in more massive ellipticals, the idea that their longer dynamical time-scales might influence their chemical enrichment is not supported by our results in the $(d\,Mg_2)/(d\log r)$–mass plane, or by the results in the Fe_{5270}–Mg_2 plane (WFG, DSP and this work). The significance of a transition mass of $10^{11}\,M_\odot$ also requires an explanation.

It is known that ellipticals cover *at least* a two-parameter manifold (Djorgovski & Davis 1987; Dressler et al. 1987), the first being a 'size' parameter such as e.g. the mass, the second depending somehow on the star formation history and on the properties of the galactic stellar population (e.g. Terlevich et al. 1981; Dressler et al. 1987; Bender, Burstein & Faber 1992; Djorgovski 1992). What we are observing in the metallicity gradients of early-type galaxies might be a reflection of the second parameter or, to be consistent with what is observed in their colour gradients (Djorgovski, private communication), even of something external to the 'fundamental plane' of elliptical galaxies. Mass appears to be a basic parameter influencing the strength of metallicity gradients, but alone is not able to explain the observed variety of metallicity gradients. Abundance ratios and metallicity gradients in high-mass galaxies must depend on some still-unidentified property or phenomenon.

ACKNOWLEDGMENTS

The authors thank E. Brocato and F. Matteucci for their help during the initial phase of this work, and L. Lucy, R. F. Peletier and P. T. de Zeeuw for many interesting comments on a preliminary version of this paper. CMC wishes to thank G. Djorgovski, F. Matteucci, R. F. Peletier, M. Stiavelli, P. T. de Zeeuw and W. W. Zeilinger for innumerable elucidating discussions.

REFERENCES

Arimoto N., Yoshii Y., 1987, A&A, 173, 23
Baum W. A., Thomsen B., Morgan B. L., 1986, ApJ, 301, 83
Bender R., 1988, A&A, 202, L5
Bender R., 1992, in Barbuy B., Renzini A., eds, The Stellar Population of Galaxies. Kluwer, Dordrecht, p. 267
Bender R., Burstein D., Faber S. M., 1992, ApJ, 399, 462
Bender R., Surma O., Döbereiner S., Möllenhof C., Madejsky R., 1989, A&A, 217, 35
Bertin G., Stiavelli M., 1993, Rep. Prog. Phys., 56, 493
Brocato E., Matteucci F., Mazzitelli F., Tornambé A., 1990, ApJ, 349, 458
Burstein D., Heiles C., 1984, ApJS, 54, 33
Burstein D., Faber S. M., Gaskell C. M., Krumm N., 1984, ApJ, 287, 586 (B84)
Carlberg R. C., 1984, ApJ, 286, 403
Carollo M., Danziger I. J., 1993, MNRAS, submitted (CD)
Danziger I. J., Carollo C. M., Buson L., Matteucci F., Brocato E., 1993, in Danziger I. J., Zeilinger W. W., Kjär K., eds, Structure, Dynamics and Chemical Evolution of Early-Type Galaxies. ESO, Garching bei München, p. 399
Davies R. L., Birkinshaw M., 1988, ApJS, 68, 409
Davies R. L., Burstein D., Dressler A., Faber S. M., Lynden-Bell D., Terlevich R. J., Wegner G., 1987, ApJS, 64, 581 (D87)
Davies R. L., Sadler E. M., Peletier R., 1992, MNRAS, 262, 650 (DSP)
de Zeeuw P. T., Franx M., 1991, ARA&A, 29, 239
Djorgovski S., 1992, in Busarello G., Capaccioli M., Longo G., eds, Morphological Classification of Galaxies. Springer-Verlag, Berlin, p. 337
Djorgovski S., Davis M., 1987, ApJ, 313, 59
Dressler A., Lynden-Bell D., Burstein D., Davies R. L., Faber S. M., Terlevich R. J., Wegner G., 1987, ApJ, 313, 42
Efstathiou G., Gorgas J., 1985, MNRAS, 215, 37P
Faber S. M., Wegner G., Burstein D., Davies R. L., Dressler A., Lynden-Bell D., Terlevich R. J., 1989, ApJ, 69, 763
Franx M., Illingworth G. D., 1988, ApJ, 327, L55
Gorgas J., Efstathiou G., Salamanca A., 1990, MNRAS, 245, 217 (GES)
Jaffe W., 1983, MNRAS, 202, 995
Jedrzejewski R. J., Schechter P. L., 1988, ApJ, 330, L87
Kormendy J., Djorgovski S., 1989, ARA&A, 27, 235
Larson R. B., 1974, MNRAS, 166, 385
Larson R. B., 1975, MNRAS, 173, 671
Lauberts A., Valentijn E. A., 1989, The Surface Brightness Catalogue of the ESO–Uppsala Galaxies. ESO, Garching bei München
Matteucci F., Tornambé A., 1987, A&A, 185, 51
Nieto J.-L., Bender R., 1989, A&A, 215, 266
Nulsen P. E. J., Stewart G. C., Fabian A. C., 1984, MNRAS, 208, 185
Peletier R. F., 1989, PhD thesis, Groningen (PE89)
Sargent W. L. W., Schechter P. L., Boksenberg A., Shortridge K., 1977, ApJ, 212, 326
Schweizer F., Seitzer P., 1992, AJ, 104, 1039
Schweizer F., Seitzer P., Faber S. M., Burstein D., Dalle Ore C. M., Gonzalez J. J., 1990, ApJ, 364, L33
Terlevich R., Davies R. L., Faber S. M., Burstein D., 1981, MNRAS, 196, 381
Toomre A., 1977, in Tinsley B. T., Larson R. B., eds, The Evolution of Galaxies and Stellar Populations. Yale Univ. Press, New Haven, CI
van Albada T. S., 1982, MNRAS, 201, 939
van der Marel R., 1991, MNRAS, 248, 515
White S. D. M., 1980, MNRAS, 191, 1
Worthey G., Faber S. M., Gonzalez J. J., 1992, ApJ, 398, 69 (WFG)

Monthly Notices
of the
ROYAL ASTRONOMICAL SOCIETY
Vol. 265 No. 3

Metallicity gradients in early–type galaxies

C. M. Carollo, I. J. Danziger and L. Buson

Published for
The Royal Astronomical Society
by
Blackwell Scientific Publications
23 Ainslie Place
Edinburgh
EH3 6AJ

The microfiche are 105 x 148 mm archivally permanent silver halide film produced to internationally accepted standards in the NMA 98–image format.
Microfiche produced by Micromedia, Bicester, Oxon

APPENDIX A: INDIVIDUAL MEASUREMENTS AT DIFFERENT RADII FOR EACH GALAXY

Column (1) = radial distance from the centre (in arcsec).
Column (2) = amplitude of rotation (in km s^{-1}).
Column (3) = formal Fourier quotient error on the amplitude of rotation (in km s^{-1}).
Column (4) = velocity dispersion (in km s^{-1}).
Column (5) = formal Fourier quotient error on velocity dispersion (in km s^{-1}).

eso208_270

-15.9	88.3	11.2	138.5	38.0
-9.9	102.6	10.9	147.8	35.6
-7.0	101.2	9.6	139.0	35.2
-5.9	97.2	9.2	118.8	39.5
-4.8	100.7	9.3	127.9	37.2
-3.7	114.1	9.7	131.6	37.0
-2.6	101.7	9.7	135.7	36.1
-1.5	80.5	10.6	141.0	36.5
-0.4	23.4	12.1	184.8	31.4
0.7	-54.5	11.0	163.5	33.0
1.8	-102.1	9.5	142.4	34.3
2.9	-112.1	9.0	110.1	41.9
4.0	-94.7	10.3	132.2	38.0
5.1	-114.6	10.6	143.3	36.0
6.2	-101.1	10.3	132.1	38.1
7.3	-86.7	12.1	135.1	40.5
9.5	-82.1	11.7	146.4	37.1
13.9	-61.6	13.3	166.8	35.8

eso323_270

-4.2	-10.2	11.2	134.4	38.5
-2.5	18.1	9.0	153.2	31.0
-1.9	-11.5	9.1	137.8	34.0
-0.8	0.3	9.4	167.3	29.5
-0.8	3.4	9.8	169.4	29.9
0.3	13.7	8.8	164.2	28.9
0.3	1.0	10.0	168.6	30.3
1.4	-24.9	10.0	156.2	32.1
1.4	-8.7	11.4	188.8	29.5
2.5	-9.3	10.0	156.5	32.0
4.7	-2.2	13.1	173.4	33.9
6.9	-8.6	13.2	156.3	36.9

eso323_360

-6.6	7.5	12.5	125.5	44.9
-3.3	15.0	9.5	128.6	36.0
-3.3	-11.6	11.9	130.6	42.4
-2.2	14.3	13.1	153.4	39.0
-1.6	-11.7	8.9	173.0	27.4
-1.1	17.6	13.1	183.6	33.8
-0.5	-0.5	8.3	212.5	22.9
0.0	-10.2	10.6	155.4	34.4
0.6	12.1	8.2	176.6	26.0

	1.1	22.4	10.5	159.4	33.8
	1.7	9.6	8.5	167.1	27.6
	3.9	-17.6	18.4	189.1	39.2
	5.0	17.6	16.5	178.9	36.6
eso381_270					
	-5.1	88.6	12.1	122.1	42.5
	-3.0	55.0	10.8	110.7	45.0
	-2.7	66.9	8.3	136.1	32.0
	-1.9	33.1	10.1	98.0	48.5
	-1.6	53.7	6.1	107.0	34.0
	-0.8	15.0	16.6	114.8	53.8
	-0.5	22.7	6.4	122.0	31.0
	0.3	-18.1	10.0	99.0	47.8
	0.6	-24.1	7.1	126.5	31.6
	1.4	-66.9	9.7	102.6	50.6
	1.7	-41.7	7.3	136.8	29.9
	2.5	-67.7	8.4	93.0	46.6
	2.8	-54.2	8.0	103.2	40.3
	3.9	-72.2	11.1	150.1	34.1
	5.8	-58.3	9.9	98.0	48.0
	6.1	-67.9	13.5	140.0	35.0
eso381_360					
	-5.1	-42.6	16.9	111.5	57.9
	-2.9	-18.5	12.4	110.8	49.9
	-1.8	3.5	11.0	129.8	41.0
	-0.7	-3.3	8.7	110.1	42.1
	0.4	-11.2	10.1	139.5	37.0
	1.5	20.8	10.3	88.5	55.7
	2.6	43.7	13.5	80.6	69.6
	4.3	32.4	13.7	70.7	79.5
i1459_270					
	-22.5	-55.9	20.3	226.9	34.5
	-17.2	-59.3	14.5	202.3	31.5
	-14.4	-50.7	20.3	256.7	31.6
	-12.1	-55.6	13.1	246.5	26.1
	-11.0	-50.7	13.5	232.8	27.6
	-9.1	-37.4	18.3	247.6	31.0
	-8.8	-33.4	11.2	241.9	24.5
	-7.7	-14.6	11.4	265.4	23.3
	-6.6	18.7	11.5	257.1	23.9
	-6.2	-58.9	13.5	277.3	24.8
	-5.5	3.1	9.8	270.4	21.3
	-5.1	-23.7	13.8	276.6	25.0
	-4.4	6.3	10.0	279.0	21.1
	-4.0	-10.8	14.2	291.9	24.6
	-3.3	28.9	3.4	287.2	11.1
	-2.9	3.0	13.3	310.7	22.9
	-2.2	23.6	11.5	285.7	22.4
	-1.8	-8.1	12.2	317.6	21.7
	-1.1	25.3	12.6	303.0	22.6
	-0.7	-6.0	13.0	320.3	22.2
	0.0	14.3	13.0	316.3	22.5
	0.4	-51.9	13.8	312.2	23.2
	1.1	-6.9	13.0	317.7	22.3

	1.5	-57.4	13.4	299.9	23.6
	2.2	-31.4	12.3	312.9	21.9
	2.6	-50.5	13.1	304.3	23.0
	3.3	-40.2	11.3	301.4	21.4
	3.7	-55.4	13.8	300.8	23.7
	4.4	-36.9	11.3	276.0	22.6
	4.8	-75.6	14.2	288.0	24.8
	5.5	-25.8	10.7	282.4	21.7
	5.9	-15.7	15.1	284.9	25.7
	6.6	-18.3	10.2	248.7	22.8
	7.0	4.6	15.7	281.4	26.3
	7.7	-27.0	10.9	273.0	22.3
	8.8	-31.5	11.7	250.1	24.5
	9.2	-11.3	20.0	267.9	30.7
	9.9	-1.5	12.0	226.4	26.4
	11.0	-21.1	15.0	217.6	30.3
	12.1	3.3	13.6	262.6	25.6
	13.2	-8.8	15.1	237.6	28.8
	13.6	41.7	16.0	247.1	28.8
	16.5	9.1	13.6	206.9	29.9
	19.8	-6.8	15.2	168.6	36.7
	27.5	33.0	17.4	196.5	35.2
i1459_360					
	-30.8	-39.9	46.1	188.3	58.7
	-14.6	-19.7	15.7	200.4	33.4
	-10.0	-28.8	18.3	240.9	31.7
	-7.1	-41.7	16.7	227.6	31.5
	-6.0	-53.7	18.8	253.3	31.1
	-4.9	-71.7	16.3	273.2	27.7
	-3.8	-95.0	14.1	254.6	26.9
	-2.7	-81.1	16.8	286.4	27.2
	-1.6	-91.7	16.8	281.3	27.6
	-0.5	-30.7	21.1	286.5	30.6
	0.6	45.1	19.5	290.1	29.2
	1.7	75.5	17.2	285.9	27.6
	2.8	57.9	15.5	280.6	26.5
	3.9	34.8	15.3	265.4	27.3
	5.0	35.8	16.9	256.3	29.2
	6.1	17.1	18.1	270.8	29.2
	7.2	-33.7	19.3	256.5	31.3
	8.3	-29.4	20.1	246.8	32.7
	10.5	-17.1	20.2	264.2	31.4
	14.9	-24.6	22.2	238.9	35.1
i2006_270					
	-6.6	-16.4	8.3	94.0	44.6
	-3.2	-50.7	6.8	117.3	32.8
	-2.5	-34.2	13.2	95.3	55.7
	-2.1	-40.1	6.7	123.0	31.3
	-1.4	-30.2	9.3	121.9	37.3
	-1.0	-37.5	7.4	110.6	36.2
	-0.3	-3.8	9.2	128.5	35.3
	0.1	-22.4	5.8	137.4	26.5
	0.8	-1.0	7.7	115.9	35.4
	1.2	-18.6	5.5	144.4	24.9
	1.9	20.1	8.9	148.8	30.9
	2.3	-25.2	6.8	140.8	28.3

	3.0	6.9	8.6	131.6	33.5
	3.4	-11.3	7.2	130.1	31.1
	5.2	-5.1	9.0	142.5	32.0
	5.6	-20.7	8.5	136.0	32.5
	14.0	13.9	8.4	72.0	57.9
	27.6	-4.4	14.4	101.3	54.8
i2035_270					
	-13.1	105.1	18.3	116.8	55.3
	-6.6	76.5	10.8	130.4	38.0
	-5.5	72.8	8.7	96.9	44.3
	-4.4	59.5	6.7	80.3	46.2
	-3.7	65.9	9.2	131.8	35.6
	-3.3	59.8	5.8	75.2	46.1
	-2.6	66.9	9.0	135.1	34.5
	-2.2	37.8	5.8	84.4	41.2
	-1.5	53.1	8.2	135.6	32.3
	-1.1	1.4	5.3	103.6	32.5
	-0.4	29.5	7.3	120.2	33.3
	0.0	-5.2	6.3	123.9	30.3
	0.7	-6.9	7.0	108.9	34.8
	1.1	-11.0	5.8	108.0	32.7
	1.8	-33.1	7.6	99.6	38.3
	2.2	-16.4	5.8	106.0	33.3
	2.9	-53.7	7.7	108.3	36.5
	3.3	-34.9	6.7	66.7	55.2
	4.0	-66.1	8.7	106.7	38.8
	4.4	-72.3	16.8	128.6	40.5
	5.1	-57.4	8.4	97.6	40.7
	5.5	-63.6	7.7	87.7	58.4
	6.2	-70.8	10.3	81.6	49.5
	7.7	-68.3	9.0	83.4	67.3
	8.4	-73.2	9.8	76.9	50.3
	16.0	-82.9	13.8	101.4	50.3
i3370_270					
	-34.8	111.9	24.3	114.0	65.7
	-16.1	82.4	19.5	147.5	46.9
	-9.3	76.5	13.0	193.7	31.1
	-6.4	61.2	13.5	179.5	33.5
	-5.1	49.6	14.9	198.3	32.6
	-2.9	59.2	13.3	211.4	29.5
	-2.9	66.3	14.1	202.5	31.2
	-1.8	38.1	12.5	173.5	33.0
	-1.8	72.3	14.4	209.7	30.9
	-0.7	26.3	12.6	191.2	30.9
	-0.7	57.3	13.7	208.3	30.2
	0.4	9.1	13.3	194.8	31.3
	0.4	4.8	12.0	204.9	28.7
	1.5	-27.3	12.5	198.7	29.8
	1.5	7.5	13.7	203.4	30.8
	2.6	-10.5	13.7	193.1	32.0
	2.6	0.0	11.6	185.4	30.1
	3.7	-38.8	13.4	186.5	32.2
	3.7	-20.4	12.4	160.5	34.9
	4.8	-35.9	12.5	176.9	32.5
	5.9	-47.6	11.3	157.8	33.8
	7.0	-30.0	12.0	183.8	30.9

	10.3	-63.8	13.1	149.7	37.9
	14.7	-72.8	12.9	155.4	36.6
	36.7	-119.3	31.0	177.0	50.8
i3370_360					
	-13.7	-85.3	21.3	189.9	42.2
	-8.6	-84.4	21.1	163.2	44.3
	-8.2	-58.8	19.1	181.7	41.3
	-6.0	-57.6	19.7	226.0	35.7
	-5.2	-53.9	12.0	153.4	35.2
	-4.9	-11.8	16.5	275.5	28.3
	-3.8	-24.7	14.1	230.7	29.7
	-3.0	-46.1	11.9	206.7	28.0
	-2.7	-1.1	13.3	195.3	32.4
	-1.9	-59.1	12.2	198.4	29.1
	-1.6	-3.8	13.3	221.6	29.7
	-0.8	3.0	9.8	193.6	26.6
	-0.5	37.6	11.6	205.1	29.4
	0.3	38.5	8.7	207.8	23.8
	0.6	35.1	12.6	203.1	30.8
	1.4	69.7	9.3	194.4	25.8
	1.7	64.9	13.6	208.9	31.3
	2.5	90.3	12.1	214.0	27.5
	2.8	75.1	17.3	208.8	35.5
	3.6	79.3	17.2	216.5	32.5
	3.9	92.2	15.0	222.4	31.3
	4.7	84.9	15.3	191.9	33.4
	6.8	97.3	15.7	200.1	34.8
	6.9	87.2	16.6	169.0	38.3
	13.6	69.8	26.3	176.4	46.6
	14.1	87.9	17.3	153.1	63.1
i4889_270					
	-6.7	-15.1	14.3	152.5	45.8
	-3.8	15.0	10.9	184.6	29.0
	-2.7	4.3	9.4	190.1	26.4
	-1.6	-16.0	7.1	184.0	23.6
	-0.5	-1.4	7.3	198.2	22.6
	0.6	0.3	7.4	191.5	23.3
	1.7	-10.8	8.6	176.6	26.6
	2.8	25.4	9.7	202.9	25.7
	3.9	-10.6	10.1	188.2	27.5
	6.1	-12.4	12.3	204.7	28.7
	13.8	-14.5	13.9	168.3	37.0
i4889_360					
	-13.7	58.7	16.6	138.6	45.8
	-8.4	33.1	13.7	198.0	31.2
	-5.6	-3.6	11.3	186.0	29.7
	-4.5	-33.8	12.1	174.2	32.6
	-3.4	-45.7	9.9	172.3	29.6
	-2.3	-29.2	8.7	160.5	29.3
	-1.2	-11.4	8.6	179.0	26.7
	-0.1	2.0	8.3	175.3	26.6
	1.0	10.0	9.0	162.7	29.4
	2.1	2.8	13.0	191.1	31.6
	3.2	23.8	10.2	180.2	29.1

	4.3	-1.1	10.9	150.8	34.4
	5.4	-26.7	13.6	184.9	33.0
	6.5	-45.5	12.7	198.1	30.3
	8.7	-37.8	16.1	204.0	33.4
	13.1	-65.3	15.4	170.7	37.4
i4943_270					
	-4.2	-16.9	9.3	106.8	41.9
	-3.9	29.3	11.4	118.6	43.4
	-3.1	-1.1	7.7	118.5	34.7
	-2.0	-3.0	8.4	150.7	29.8
	-1.6	7.1	11.9	186.2	30.6
	-0.9	2.6	6.7	165.1	24.5
	-0.5	-8.8	10.0	175.3	29.3
	0.2	-10.2	6.4	174.6	23.1
	0.6	-11.7	9.8	170.2	29.6
	1.3	-11.3	6.7	171.3	24.0
	1.7	-27.3	11.2	163.2	33.0
	2.4	-16.4	8.5	185.6	25.4
	3.5	-43.8	10.3	173.8	29.5
	4.6	-32.7	11.7	128.1	40.1
	10.1	-43.7	13.8	137.8	40.9
i4943_360					
	-15.0	-22.3	35.8	144.4	61.8
	-3.4	-15.4	16.1	163.4	38.5
	-1.7	-9.8	9.2	162.8	29.3
	-0.6	0.0	8.7	199.8	24.4
	0.5	9.8	8.5	190.1	25.1
	4.9	22.7	12.1	147.6	40.8
	24.7	-9.0	51.[illegible]	145.9	63.9
n1052_270					
	-20.4	69.1	20.3	156.7	44.4
	-15.0	95.6	18.9	208.8	35.3
	-12.2	50.2	13.5	174.3	33.7
	-10.0	36.4	12.4	203.4	28.9
	-8.9	81.2	20.5	238.5	33.8
	-7.8	58.3	10.9	192.6	28.1
	-6.7	34.2	8.8	186.8	25.9
	-5.6	21.3	8.3	207.4	23.3
	-4.5	27.8	8.7	201.3	24.4
	-3.4	10.5	8.6	196.3	24.8
	-2.3	12.6	9.4	200.3	25.5
	-1.2	10.2	9.8	210.7	25.1
	-0.1	-15.9	9.7	210.1	25.0
	1.0	-32.2	8.9	198.7	24.8
	2.1	-43.2	8.4	190.0	25.0
	3.2	-68.9	9.9	216.5	24.8
	4.3	-76.6	9.3	198.8	25.4
	5.4	-71.1	9.5	177.6	27.9
	6.5	-78.5	10.2	196.2	27.0
	7.6	-62.9	12.6	181.1	31.7
	8.7	-61.4	10.8	197.5	27.7
	9.8	-82.0	13.3	150.2	37.6
	10.9	-70.9	11.9	199.7	28.7
	12.0	-63.6	13.5	224.1	28.1

	13.1	-63.1	15.7	199.0	32.7
	15.3	-96.9	11.4	146.8	35.3
	18.6	-56.7	20.1	184.3	39.6
	27.4	-40.1	31.7	171.3	52.8
n1209_270					
	-29.6	-259.4	23.3	202.2	41.7
	-16.3	-170.1	14.5	206.1	32.6
	-10.9	-190.8	14.2	235.7	29.4
	-8.1	-167.6	12.1	212.1	29.2
	-7.0	-137.0	12.9	244.2	27.6
	-5.9	-151.4	11.8	185.1	31.4
	-4.8	-139.3	9.6	219.7	25.4
	-3.7	-111.3	8.0	210.0	24.0
	-2.6	-98.8	8.2	245.0	21.9
	-1.5	-68.2	8.2	243.0	21.9
	-0.4	-24.2	7.0	219.0	21.8
	0.7	20.7	7.5	232.8	21.5
	1.8	83.5	7.4	229.1	21.7
	2.9	116.9	7.5	219.7	22.4
	4.0	127.8	8.0	182.7	26.2
	5.1	123.9	8.5	168.3	28.5
	6.2	132.8	10.8	185.9	30.0
	7.3	152.2	11.7	209.8	28.9
	8.4	180.3	9.6	196.7	27.3
	9.5	173.5	10.0	176.1	30.1
	11.7	162.1	10.5	172.4	31.0
	16.1	163.9	11.2	157.0	34.4
	40.3	201.0	15.8	128.0	47.0
n1298_270					
	-24.9	59.1	61.8	194.9	69.5
	-5.0	54.5	13.8	171.7	34.9
	-3.3	62.1	17.6	197.0	35.9
	-2.2	21.0	11.7	204.1	28.4
	-1.1	9.6	11.0	187.2	29.2
	0.0	-0.2	12.0	207.9	28.4
	1.1	-4.3	9.5	192.5	26.6
	2.2	-23.8	10.3	177.1	29.4
	3.3	-53.1	12.1	164.2	33.9
	38.5	-104.3	34.4	152.9	60.4
n1947_270					
	-35.0	34.3	27.6	212.3	42.6
	-26.2	-3.3	20.0	165.0	42.7
	-10.5	14.0	12.8	162.9	34.8
	-7.3	-9.9	12.7	165.9	34.0
	-5.9	16.9	10.3	136.9	36.3
	-3.8	0.5	12.6	164.4	33.8
	-3.1	3.4	9.6	136.3	35.0
	-2.0	10.0	10.3	141.1	35.3
	-1.6	-14.2	8.9	144.8	31.5
	-0.9	-4.6	10.2	133.4	36.9
	-0.5	-14.9	8.0	140.3	30.8
	0.2	-8.5	9.8	83.0	55.8
	0.6	-13.1	8.7	133.6	33.4
	1.3	13.9	10.1	140.7	35.0

	1.7	13.4	6.9	137.5	29.0
	2.4	-15.3	10.9	133.5	38.1
	2.8	25.1	8.6	133.1	33.3
	3.5	33.4	12.6	142.9	38.8
	7.9	31.8	12.9	159.8	35.8
	8.3	18.0	14.1	168.9	35.2
	21.1	38.6	15.7	170.3	37.7
	37.6	105.7	24.0	161.7	47.8
n1947_360					
	-2.4	11.0	13.2	155.8	38.7
	-1.3	5.5	9.3	112.3	42.7
	-0.2	-10.9	9.3	124.7	42.0
	0.9	-45.7	9.6	129.5	41.2
	2.0	5.7	11.8	150.3	37.5
	3.1	-6.9	10.9	149.1	36.3
	5.3	-15.0	14.0	101.4	57.4
n2502_270					
	-9.5	-40.5	11.4	93.2	54.2
	-3.4	-10.0	11.2	134.8	38.4
	-2.3	2.6	10.7	129.0	39.0
	-1.2	-4.3	9.6	127.4	37.4
	-0.1	2.6	10.4	138.7	36.1
	1.0	12.4	9.3	120.4	38.5
	2.1	15.9	10.0	150.5	32.9
	3.2	9.0	11.4	144.0	36.5
	5.4	4.9	10.2	143.3	34.7
n2663_270					
	-36.4	-10.4	28.0	207.2	43.4
	-14.4	0.3	21.2	233.0	34.0
	-9.0	1.4	22.5	221.8	36.8
	-6.2	4.4	23.1	197.8	47.7
	-5.1	-6.7	20.1	243.6	32.7
	-4.0	-9.5	18.6	237.4	31.8
	-2.9	-12.8	17.7	253.2	30.0
	-1.8	-32.0	17.7	266.6	29.1
	-0.7	-18.4	19.8	281.7	29.8
	0.4	-21.7	19.5	280.8	29.7
	1.5	0.0	21.0	286.4	30.4
	2.6	-19.1	21.1	295.7	30.0
	3.7	-4.9	19.5	279.4	29.6
	4.8	-23.2	20.3	237.1	33.4
	5.9	-6.7	21.6	248.7	33.4
	7.0	-29.8	22.3	232.9	33.3
	8.1	-59.3	23.2	274.4	32.5
	10.3	-34.6	21.9	285.7	31.2
	14.7	15.9	24.1	219.3	37.7
	35.6	73.6	32.7	189.2	49.5
n2974_270					
	-37.8	6.6	28.5	162.6	51.1
	-16.4	-98.3	14.5	186.6	32.9
	-9.7	-110.1	11.3	156.5	33.3
	-6.9	-100.0	10.6	172.0	30.0

-5.8	-85.7	10.7	186.4	28.4
-4.7	-85.3	11.0	177.2	29.9
-3.6	-99.8	10.3	184.3	28.1
-2.5	-62.7	11.0	206.2	26.8
-1.4	-25.2	11.5	211.8	26.9
-0.3	36.5	10.7	212.6	25.9
0.8	68.0	11.2	202.9	27.5
1.9	70.7	10.8	201.7	27.0
3.0	88.5	10.0	178.7	28.3
4.1	83.9	9.1	175.9	27.3
5.2	92.8	9.6	170.1	28.8
6.3	71.1	9.9	172.7	28.9
7.4	54.6	10.3	183.3	28.1
9.6	76.8	11.6	195.0	28.5
14.0	52.5	11.3	117.7	42.5
38.2	77.8	18.9	113.5	56.7

n3078_270

-10.1	4.4	14.3	155.6	38.4
-9.5	-0.5	19.9	211.0	33.0
-6.0	2.2	14.2	176.8	34.4
-4.9	-11.2	18.4	213.1	34.7
-4.1	13.3	15.9	210.1	29.4
-3.8	-7.2	16.4	216.6	32.2
-3.0	24.9	19.4	177.3	36.2
-2.7	16.7	14.8	207.8	31.6
-1.9	12.6	19.8	249.7	29.9
-1.6	7.4	16.1	252.0	28.8
-0.8	16.4	15.4	243.4	26.2
-0.5	8.9	16.0	246.2	29.3
0.3	24.6	15.0	241.3	26.6
0.6	-0.3	16.9	245.7	30.1
1.4	25.0	15.1	247.0	25.9
1.7	0.5	17.5	255.9	29.9
2.5	-9.8	13.7	196.0	27.7
2.8	-2.7	15.6	235.0	29.8
3.6	2.1	14.8	197.3	28.9
3.9	-9.6	18.1	240.7	31.6
5.0	7.9	14.5	184.6	34.0
5.8	-1.5	16.1	190.4	30.7
6.1	-5.1	14.3	205.5	31.0
8.3	11.5	15.2	194.6	33.3
25.6	-4.4	31.0	178.0	48.8
36.9	-8.4	28.1	161.8	52.0

n3078_360

-14.7	-91.2	20.4	206.1	39.3
-8.1	-115.0	16.4	215.6	34.0
-5.9	-102.4	21.6	252.9	34.9
-4.8	-116.4	16.5	240.6	31.5
-3.7	-104.8	13.5	215.0	30.9
-2.6	-89.8	13.8	258.7	27.4
-1.5	-89.8	13.9	264.1	27.3
-0.4	-34.5	12.8	259.2	26.4
0.7	1.2	12.2	253.3	26.1
1.8	66.2	12.8	256.6	26.6
2.9	88.9	15.7	240.3	30.6
4.0	51.4	16.1	219.2	33.2

	5.1	48.3	17.1	215.8	34.6
	8.5	63.0	19.7	232.6	35.1
	19.0	98.8	31.3	298.1	37.2
n3100_270					
	-31.2	-3.1	33.4	181.1	53.6
	-7.6	17.7	19.3	166.5	42.3
	-4.0	22.8	12.8	175.9	33.0
	-2.9	18.6	14.0	200.2	31.3
	-2.8	24.5	13.1	201.0	30.4
	-1.8	26.7	13.5	189.4	32.0
	-1.7	33.7	12.1	186.3	30.8
	-0.7	20.6	12.6	189.5	30.9
	-0.6	13.5	12.5	208.3	28.8
	0.4	13.6	13.0	182.4	32.4
	0.5	-4.6	13.5	197.5	31.3
	1.5	5.7	12.7	207.0	29.2
	1.6	-28.3	12.9	220.3	28.3
	2.6	-31.4	12.8	175.4	33.0
	2.7	-21.2	14.2	190.3	32.9
	3.7	-36.5	16.3	201.2	34.0
	4.9	-28.8	16.3	183.0	36.4
	7.0	-40.5	14.2	176.2	34.6
	36.7	-54.2	40.9	251.6	45.3
n3100_360					
	-7.0	69.9	15.5	221.7	32.0
	-6.1	97.6	11.9	180.7	30.9
	-4.8	53.9	13.5	185.3	34.1
	-3.7	45.6	14.3	200.1	33.1
	-3.3	106.6	11.0	210.1	26.5
	-2.6	69.1	13.9	213.1	31.2
	-2.2	61.4	11.0	224.1	25.4
	-1.5	10.2	11.5	228.6	27.0
	-1.1	-3.1	9.7	224.5	23.9
	-0.4	13.9	10.7	217.9	26.8
	0.0	-16.4	10.5	242.9	23.5
	0.7	-4.1	11.3	202.1	29.3
	1.1	-28.7	10.3	226.8	24.5
	1.8	-37.6	21.8	249.9	35.5
	2.2	-63.0	13.9	230.5	28.1
	2.9	-32.0	14.9	190.4	35.1
	3.3	-80.8	4.2	242.4	13.7
	4.0	-126.5	25.3	246.6	29.4
	8.1	-138.8	14.3	149.6	41.7
	20.9	-63.0	23.4	207.0	39.1
n3108_270					
	-32.4	122.4	32.5	43.1	194.2
	-6.7	73.6	18.7	214.2	34.8
	-6.5	62.9	14.8	217.9	30.5
	-3.0	60.8	14.8	192.0	33.3
	-2.6	84.0	12.0	207.1	28.5
	-1.9	53.4	13.3	185.8	32.4
	-1.5	35.3	11.3	191.3	29.3
	-0.8	20.6	12.2	186.3	30.8
	-0.4	10.1	12.2	211.8	28.3

	0.3	25.4	13 0	200.4	30.2
	0.7	-2.7	13.3	201.4	30.7
	1.4	1.8	13.7	192.3	31.9
	1.8	-7.6	14.5	224.7	29.6
	2.5	-12.6	13.3	191.0	31.7
	2.9	-5.2	14.7	229.8	29.3
	3.6	-35.9	14.3	194.7	32.5
	4.7	-34.6	12.4	164.4	34.2
	5.1	0.9	17.5	234.4	31.5
	8.0	-53.2	15.3	187.5	34.3
	17.2	-53.5	30.3	254.8	39.9
	37.7	-52.7	36.1	186.7	55.5
n3108_360					
	-8.4	-8.0	42.1	208.0	56.8
	-4.3	-15.8	31.6	267.0	40.0
	-3.6	-52.2	28.7	171.7	56.5
	-3.2	-53.6	16.5	250.1	30.3
	-2.5	-16.7	18.0	173.9	40.2
	-2.1	-38.9	13.3	251.3	27.1
	-1.4	-11.7	11.6	212.9	27.2
	-1.0	-39.9	11.9	229.7	27.4
	-0.3	-5.0	10.8	196.3	27.7
	0.1	-43.4	11.1	221.9	27.0
	0.8	-7.5	13.7	189.0	32.0
	1.2	-25.9	11.3	203.5	29.3
	1.9	15.0	15.8	190.2	34.0
	2.3	3.8	12.7	214.2	29.8
	3.0	-2.0	23.5	208.5	39.0
	3.4	30.7	15.7	266.2	28.4
	6.3	42.9	42.2	208.1	50.9
	6.9	31.4	16.5	202.4	35.5
n3136B_270					
	-3.6	-1.2	12.5	178.8	33.3
	-1.9	44.4	12.7	202.9	29.8
	-1.9	12.3	11.1	167.4	32.7
	-0.8	19.2	10.3	189.1	28.3
	-0.8	10.3	15.6	203.6	34.2
	0.3	8.1	9.5	180.6	28.0
	1.4	-16.8	10.0	155.7	32.3
	1.4	-24.0	9.8	182.2	29.2
	2.5	-26.5	10.6	169.8	32.0
	3.6	1.1	12.2	149.3	36.7
	5.8	-40.1	12.9	133.7	41.1
n3136B_360					
	-8.0	-48.7	18.6	143.9	49.2
	-1.8	-35.4	11.5	179.7	30.4
	-1.4	-39.2	12.4	182.0	33.2
	-0.7	-40.0	9.1	183.2	26.7
	-0.3	-27.3	11.8	204.6	29.7
	0.4	-20.6	8.8	183.1	26.2
	1.5	21.2	9.3	186.8	26.6
	2.5	-22.6	65.3	156.2	87.7
	3.7	24.5	17.1	196.4	34.8

n3136_270

-34.5	-15.2	24.7	246.2	36.2
-9.3	21.5	12.8	217.1	28.0
-5.8	2.1	12.2	185.5	30.5
-4.7	5.9	12.8	230.6	27.0
-3.6	0.5	11.7	196.1	28.7
-2.5	13.2	11.7	213.6	27.0
-1.4	8.7	11.6	231.1	25.5
-0.3	4.3	12.4	233.6	26.2
0.8	12.3	12.2	233.7	25.9
1.9	-11.7	11.9	237.6	25.4
3.0	6.6	12.0	214.1	27.2
5.2	-10.8	15.4	208.0	31.5
6.3	3.7	12.3	214.3	27.7
8.5	-18.6	12.0	219.4	27.0
15.1	17.0	13.7	184.7	32.5

n3226_270

-34.0	54.4	45.1	251.7	50.3
-6.9	-31.6	13.2	188.4	33.3
-2.8	-31.9	11.4	191.8	30.3
-1.7	-29.2	9.9	183.2	29.1
-0.6	-20.8	15.4	238.4	30.6
1.6	34.9	11.1	205.5	28.5
2.7	31.6	10.5	177.2	30.7
4.9	20.7	9.9	164.5	31.3
12.6	25.0	13.8	191.4	33.5
36.8	-92.1	27.7	135.6	60.5

n3226_360

-5.1	31.8	17.8	167.9	74.0
-2.9	24.9	13.0	182.6	33.9
-1.8	8.0	15.9	194.8	35.8
-0.7	4.1	11.6	214.5	28.4
0.4	-36.9	13.5	228.8	29.4
2.6	-34.7	30.5	215.9	46.0

n3250_270

-34.1	72.2	32.2	207.9	46.8
-24.5	84.7	23.1	191.8	65.9
-8.4	19.8	17.7	217.8	33.1
-7.7	56.4	17.8	248.1	30.3
-4.9	41.1	15.2	233.3	29.6
-4.2	35.9	13.6	275.2	24.8
-3.8	15.1	16.6	237.8	30.5
-3.1	42.8	14.8	278.3	25.7
-2.7	28.3	16.5	256.4	29.1
-2.0	2.8	14.7	304.7	24.3
-1.6	21.7	14.6	241.1	28.1
-0.9	-3.0	13.9	313.0	23.2
-0.5	-0.3	14.6	237.4	28.7
0.2	-22.5	10.7	267.8	22.4
0.6	-20.4	16.0	243.7	29.7
1.3	-28.3	12.1	263.5	24.0
1.7	-13.6	16.1	264.7	28.2
2.4	-51.3	15.5	281.4	26.1

	2.8	-35.7	16.1	244.8	29.6
	3.5	-67.3	14.2	275.4	25.4
	3.9	-40.2	17.7	230.6	32.4
	5.0	-41.5	16.8	215.2	32.9
	5.7	-63.9	12.9	242.5	26.2
	7.2	-26.6	17.1	230.6	31.8
	11.2	-35.9	16.8	261.6	28.5
	36.9	-48.4	22.0	222.8	36.8
n3250_360					
	-14.9	33.2	25.8	262.9	36.2
	-8.3	53.5	17.4	289.7	28.1
	-6.1	66.9	19.2	290.5	29.6
	-5.0	46.4	14.0	258.3	30.8
	-3.9	67.0	14.7	249.9	31.4
	-2.8	49.9	15.8	307.9	25.8
	-1.7	7.2	14.1	282.4	25.9
	-0.6	-21.8	13.2	295.8	24.3
	0.5	-34.5	12.2	253.9	25.9
	1.6	-35.9	13.3	262.4	26.4
	2.7	-84.6	16.9	282.3	28.3
	3.8	-25.9	16.0	238.7	30.8
	4.9	-66.7	20.1	263.4	32.3
	7.8	-62.9	16.8	217.4	33.8
	13.8	-50.8	25.4	260.4	36.5
n3260_270					
	-29.6	63.4	41.6	148.1	65.6
	-1.7	13.9	13.0	197.5	29.9
	-0.6	0.8	12.9	213.3	28.5
	0.5	-14.2	12.8	225.2	27.4
	1.6	-31.3	13.3	215.3	28.7
	4.9	-13.8	11.5	169.1	31.7
	36.8	-61.8	29.7	59.0	132.1
n3557_270					
	-34.6	125.9	36.3	337.4	36.3
	-14.8	73.2	22.8	251.2	34.1
	-9.5	15.7	19.4	279.0	30.1
	-7.5	66.0	24.5	262.1	34.5
	-6.0	49.1	14.7	241.5	28.3
	-4.9	68.4	17.5	260.1	29.6
	-4.7	4.0	23.8	236.2	35.9
	-3.8	23.1	16.4	263.2	28.4
	-3.6	-17.9	23.9	266.9	33.4
	-2.7	18.5	17.9	290.1	28.2
	-2.5	-27.9	13.3	298.0	23.4
	-1.6	13.3	15.3	270.1	27.0
	-1.4	-20.0	11.2	291.8	21.7
	-0.5	-30.6	15.8	278.3	27.1
	-0.3	-29.2	13.1	330.4	21.9
	0.6	-72.4	16.0	275.9	27.4
	0.8	-50.2	11.9	297.9	22.1
	1.7	-102.5	15.6	258.1	28.2
	1.9	-72.3	13.4	287.2	24.1
	2.8	-98.9	17.0	271.0	28.6
	3.0	-62.1	13.6	312.4	23.0

3.9	-103.5	15.8	257.8	28.4
4.1	-60.9	15.3	278.7	26.1
5.0	-86.9	16.8	230.7	31.4
5.2	-85.3	15.9	305.5	25.2
7.4	-79.7	15.0	300.2	24.6
8.3	-79.0	19.1	226.1	33.8
12.9	-64.8	23.4	342.4	47.8
13.8	-99.0	16.1	226.1	[illegible]
36.9	-147.0	22.1	185.6	41.9

n3557_360

-14.1	-76.1	18.4	231.1	34.0
-9.7	-103.9	15.8	219.6	32.7
-7.5	-129.2	17.1	249.4	31.1
-6.4	-113.4	15.6	267.1	28.3
-5.3	-109.3	18.7	286.9	29.5
-4.2	-76.1	14.4	266.3	27.2
-3.1	-93.0	13.6	265.8	26.4
-2.0	-57.9	12.6	259.4	26.0
-0.9	-45.1	12.1	239.7	26.8
0.2	22.3	11.5	265.6	24.4
1.3	43.5	12.0	261.0	25.0
2.4	68.7	13.7	251.5	27.5
3.5	68.8	12.9	252.9	26.6
4.6	84.4	18.3	292.4	28.7
5.7	[illegible]	15.6	259.6	28.8
6.8	118.3	14.8	258.7	28.1
9.7	90.4	19.7	239.2	34.2
15.7	104.1	19.9	221.2	36.4

n3706_270

-33.6	126.5	27.6	213.8	41.9
-24.3	122.2	19.7	181.4	51.0
-8.1	127.4	12.3	193.0	29.8
-8.0	119.6	14.6	199.3	32.3
-5.2	115.8	16.0	244.5	29.5
-4.7	120.3	13.3	249.1	26.1
-4.1	117.2	11.8	224.9	29.8
-3.6	103.7	11.9	256.5	24.3
-3.0	107.5	16.4	265.6	28.2
-2.5	51.0	14.7	295.9	24.7
-1.9	57.9	16.7	271.3	28.2
-1.4	41.4	12.0	303.3	22.0
-0.8	28.8	16.8	289.1	27.3
-0.3	37.6	12.7	312.0	22.3
0.3	13.3	17.1	285.3	27.8
0.8	5.3	12.8	299.6	22.8
1.4	-39.0	17.5	283.5	28.2
1.9	-15.8	15.3	297.4	25.1
2.5	-86.3	17.7	265.4	29.5
3.0	-43.3	27.2	315.9	32.1
3.6	-101.2	15.4	235.1	29.5
4.1	-79.0	12.4	283.9	23.2
4.7	-124.6	15.0	231.5	29.4
5.8	-127.5	16.0	222.8	31.1
6.3	-96.0	12.9	269.6	25.2
8.0	-99.4	21.7	255.6	33.7
10.8	-108.3	19.5	282.7	29.3

13.6	-133.7	17.9	230.5	32.2
36.7	-141.0	22.2	164.8	45.7

n3706_360

-11.1	-28.6	26.9	179.2	49.1
-5.6	-18.7	27.0	189.4	47.6
-3.4	-54.2	16.8	290.6	27.6
-2.3	-16.1	13.5	302.0	24.1
-1.2	-12.8	12.7	295.6	23.9
-0.1	-18.2	13.0	303.4	23.6
1.0	-3.7	13.2	291.6	24.5
2.1	-4.0	15.0	278.3	26.9
3.2	51.0	16.1	266.7	28.6
4.3	9.0	14.1	195.4	33.3
9.1	19.5	18.5	211.8	36.0

n4374_270

-42.7	-6.3	26.7	288.5	34.8
-24.6	-3.5	16.7	292.5	27.3
-16.8	7.7	16.2	283.3	27.7
-12.8	-1.2	14.4	290.7	25.6
-11.7	-37.5	16.3	238.6	30.2
-10.0	-0.8	12.8	295.1	24.0
-8.9	29.4	19.5	314.6	28.4
-8.8	-9.6	17.7	259.3	29.8
-7.8	-9.2	14.4	291.4	25.6
-6.7	8.1	13.2	275.8	25.3
-6.6	-4.1	15.9	290.5	26.3
-5.6	6.1	13.0	303.7	23.7
-5.5	4.3	17.2	273.4	28.4
-4.5	19.8	14.0	310.8	24.2
-4.4	3.5	16.7	265.3	28.6
-3.4	3.8	12.5	295.7	23.5
-3.3	19.2	14.3	273.5	25.8
-2.3	9.9	12.8	316.0	22.9
-2.2	14.2	14.7	297.1	25.0
-1.2	10.2	13.7	318.2	23.6
-1.1	34.8	14.4	286.2	25.3
-0.1	22.9	13.3	317.1	23.3
0.0	23.0	14.5	276.8	26.0
1.0	18.2	14.1	325.4	23.7
1.1	34.9	15.3	292.0	25.9
2.1	18.0	13.2	314.3	23.4
2.2	7.1	14.2	299.6	24.5
3.2	15.5	13.8	320.7	23.6
3.3	20.9	16.0	280.4	27.0
4.3	28.5	14.0	298.7	24.8
4.4	8.7	17.2	299.2	26.9
5.4	24.7	14.5	306.7	24.9
5.5	45.5	19.1	304.5	28.1
6.5	-5.2	13.9	291.2	25.0
6.6	18.5	23.8	314.7	30.8
7.7	30.8	20.5	305.1	29.1
8.7	-7.4	13.5	275.4	25.6
9.8	11.6	16.6	311.4	26.3
9.9	43.4	18.3	301.9	27.7
10.9	-7.0	14.1	283.7	25.7
12.0	-28.1	12.4	260.4	25.4

	14.2	-1.5	15.6	319.2	25.1
	18.6	4.6	15.8	298.2	26.3
	29.6	17.5	15.8	263.2	28.4
n4374_360					
	-13.6	-40.0	23.0	277.6	31.0
	-8.1	-42.8	20.9	283.5	29.1
	-7.0	9.5	21.9	349.3	26.6
	-5.9	-20.5	18.0	284.9	26.9
	-4.8	4.1	21.7	377.2	25.4
	-3.7	2.3	18.4	314.1	25.8
	-2.6	-3.9	17.4	316.5	25.5
	-1.5	51.5	24.1	378.5	27.1
	-0.4	37.2	20.7	287.7	28.7
	0.7	0.7	17.8	308.4	25.6
	1.8	-41.5	15.7	296.8	24.6
	2.9	-36.2	18.2	344.7	24.4
	4.0	-17.3	19.9	324.4	26.4
	5.1	9.9	19.3	330.9	25.7
	6.2	-11.8	17.7	297.9	26.0
	8.4	-2.9	23.3	295.5	29.9
	11.9	16.9	25.3	260.0	33.6
n4684_270					
	-4.3	31.8	9.1	114.8	37.7
	-3.2	22.5	11.5	117.2	43.0
	-2.1	25.2	9.2	109.1	39.6
	-1.0	17.5	9.1	120.4	36.9
	0.1	15.3	9.5	110.5	39.7
	1.2	-7.9	10.4	115.4	40.8
	2.3	-14.4	9.1	124.1	36.1
	3.4	-9.9	9.9	107.6	41.9
n4696_225					
	-10.9	36.8	23.4	201.2	39.9
	-3.5	-18.3	15.8	270.8	27.2
	-0.7	-25.9	16.9	308.1	25.9
	0.4	-49.5	34.5	225.9	45.4
	1.5	-0.3	15.7	259.2	27.6
	3.7	-2.0	14.5	238.3	28.1
	8.1	36.3	19.0	251.1	31.1
	23.5	41.6	23.4	187.7	41.7
n4696_270					
	-33.4	-26.4	21.0	171.7	43.0
	-6.7	1.3	18.3	227.5	32.9
	-2.6	-6.3	18.3	229.2	32.9
	-1.5	-1.7	18.8	255.4	31.1
	-0.4	-10.0	17.8	240.1	31.5
	0.7	7.4	19.2	251.4	31.7
	1.8	-12.0	20.1	246.5	32.9
	2.9	-11.5	18.0	258.6	30.3
	5.1	-8.3	17.8	251.1	30.4
	10.6	4.2	16.8	222.4	32.0
	38.2	38.7	23.4	220.6	38.1

n4696_300

-13.4	-18.6	32.7	249.2	41.1
-8.7	-13.7	30.1	197.7	46.3
-5.9	-14.2	27.0	222.3	40.7
-3.7	17.0	21.2	227.0	35.2
-2.6	-41.0	24.3	268.5	33.9
-1.5	-13.7	20.0	242.4	33.2
-0.4	17.4	22.4	247.9	34.8
0.7	0.3	20.7	238.2	34.1
1.8	27.4	23.0	294.3	31.9
2.9	3.4	21.4	212.8	37.6
4.0	-16.9	25.7	240.3	37.8
5.1	-19.4	25.5	216.0	40.0
7.3	-22.2	29.0	236.7	40.6
10.6	20.8	29.9	195.0	46.8
16.1	-1.1	36.6	211.9	48.8

n4696_330

-13.3	3.1	28.3	254.0	38.8
-4.8	-6.4	21.9	233.0	35.7
-1.3	2.6	17.8	269.9	29.4
-0.2	-8.3	20.3	252.1	32.5
0.9	-4.3	21.3	290.1	30.7
1.1	15.9	25.0	239.4	37.1
2.0	21.2	19.8	249.8	32.4
4.2	26.2	17.1	213.5	33.3

n4696_360

-20.6	35.8	49.1	299.6	48.4
-7.0	-18.2	33.8	266.5	40.8
-4.2	-6.8	29.8	316.8	34.9
-3.1	45.6	35.2	328.7	37.4
-2.0	22.1	20.9	241.9	33.8
-0.9	53.4	22.9	295.5	31.1
0.2	23.6	23.1	267.4	33.5
1.3	6.8	19.5	237.1	33.2
2.4	-2.6	22.0	298.8	30.7
3.5	-42.8	19.7	222.9	34.8
4.6	-82.8	24.4	233.3	37.8
6.8	-39.4	30.8	262.5	39.4
10.1	25.9	29.2	250.1	38.9
16.7	81.0	45.2	346.3	41.0

n4843_360

-8.2	97.4	13.4	122.4	47.5
-3.8	88.6	14.7	133.6	46.3
-2.7	59.4	12.2	153.1	37.5
-1.6	42.3	9.5	135.5	36.8
-0.5	8.0	9.6	152.0	33.5
0.6	-15.5	2.5	115.0	19.8
1.7	-27.5	9.4	127.9	38.4
2.8	-53.6	10.9	97.4	52.8
8.2	-102.6	13.4	122.4	47.5

n5011_270

-35.8	-13.8	44.9	230.9	50.9
-21.8	46.0	48.0	258.5	52.2
-10.7	37.4	15.0	208.4	31.7
-6.3	50.3	16.6	253.5	28.9
-4.6	31.3	15.0	224.1	30.1
-3.5	33.5	17.3	255.3	29.8
-2.9	28.5	15.4	297.2	25.2
-2.4	28.9	16.3	265.4	28.1
-1.8	25.0	13.2	288.6	23.8
-1.3	41.4	15.3	249.8	28.5
-0.7	14.0	11.9	264.3	23.8
-0.2	22.5	13.4	233.0	27.7
0.4	10.8	11.4	268.7	23.0
0.9	19.0	15.6	257.5	28.2
2.0	14.9	15.8	264.0	27.9
2.6	-7.7	13.4	279.2	24.4
3.1	-5.3	17.3	248.0	30.1
3.7	-30.9	15.0	251.4	27.6
4.2	-12.7	14.3	205.3	31.3
6.4	-36.7	15.8	229.2	30.3
7.0	-22.4	15.7	234.4	29.5
37.2	-46.2	22.4	197.4	40.4

n5044_270

-19.5	-77.3	41.7	208.9	51.9
-10.4	-102.2	28.3	244.4	39.4
-6.9	-73.9	18.6	222.7	33.6
-6.1	8.5	15.1	216.7	30.7
-4.7	-29.9	13.8	178.8	34.0
-3.6	-37.2	20.5	241.0	33.4
-3.2	5.2	15.4	235.8	29.5
-2.5	1.8	18.2	230.5	30.2
-2.1	-36.0	13.9	210.5	29.9
-1.4	-19.8	18.3	223.9	30.6
-1.0	-18.5	13.8	220.8	28.9
-0.3	32.0	33.0	212.3	42.1
0.1	-8.4	15.2	215.2	30.9
0.8	-21.7	17.8	196.7	35.8
1.2	-22.2	16.1	240.8	29.7
1.9	-8.8	16.1	224.9	30.9
2.3	-14.1	15.5	231.3	29.9
3.0	-60.4	17.7	208.6	34.7
3.4	-0.9	14.5	218.2	30.1
4.1	-13.6	19.8	246.0	32.5
4.5	-4.5	14.7	221.2	29.9
5.2	-18.1	20.3	265.2	31.6
6.3	-17.3	20.6	270.0	30.8
6.7	-13.0	14.9	216.8	30.5
8.5	-11.4	24.3	278.8	32.5
13.3	30.2	15.7	207.8	32.1
20.5	16.8	37.4	273.1	41.5

n5044_360

-10.4	-16.7	22.2	272.0	33.2
-9.5	211.0	21.7	275.6	31.2
-6.1	-32.9	18.3	233.6	33.5
-4.9	231.6	16.0	243.6	29.2
-3.9	-24.9	19.4	247.3	33.3

	-2.8	16.1	17.7	297.9	28.0
	-2.0	179.9	13.5	283.7	24.3
	-1.7	18.4	17.2	276.3	29.0
	-0.9	207.3	15.2	247.7	28.0
	-0.6	8.3	19.7	292.5	30.0
	0.2	235.0	15.2	236.1	28.9
	0.5	38.1	16.7	244.6	31.0
	1.3	179.4	12.7	253.4	25.3
	1.6	40.4	15.2	251.7	29.0
	2.4	178.0	13.5	239.1	27.2
	3.5	181.8	12.8	237.1	26.4
	3.8	-4.2	20.8	272.2	32.1
	5.7	179.2	15.0	245.8	28.0
	7.3	-33.7	19.1	209.7	37.1
	10.1	235.5	18.8	266.2	30.0
n5077_270					
	-31.0	-36.7	21.8	106.1	65.3
	-4.4	4.9	16.2	220.4	31.4
	-3.3	5.4	16.5	247.7	29.3
	-2.2	-0.1	13.5	212.4	29.3
	-1.1	6.2	15.1	251.8	27.9
	0.0	10.7	14.5	244.3	27.8
	1.1	10.3	15.3	248.2	28.3
	2.2	26.1	17.1	277.7	28.0
	3.3	23.1	15.8	271.1	27.3
	4.4	11.6	15.3	222.2	30.4
	8.8	-7.1	15.4	195.1	33.2
	37.4	-66.0	34.7	126.0	72.8
n5077_360					
	-7.8	-25.8	21.2	266.7	32.0
	-5.6	34.1	18.0	277.8	28.8
	-4.5	44.4	31.6	222.9	43.8
	-3.4	6.9	17.1	244.4	30.4
	-2.3	1.7	14.6	253.2	27.6
	-1.2	-19.8	13.8	266.6	25.9
	-0.1	-8.4	13.8	254.7	26.7
	1.0	-35.3	12.8	255.8	25.6
	2.1	-18.0	15.1	267.3	27.0
	3.2	19.8	16.9	273.2	28.4
	4.3	-17.2	18.0	277.4	28.9
	7.2	40.5	23.5	267.2	33.8
n5090_270					
	-33.8	-29.4	32.9	185.8	51.5
	-6.9	9.1	21.2	273.1	31.8
	-5.8	-9.9	18.9	250.5	31.4
	-3.4	23.4	16.4	246.7	29.6
	-2.3	49.2	19.7	259.4	31.5
	-2.3	68.8	15.4	273.2	26.8
	-1.2	45.9	17.5	274.6	28.7
	-1.2	39.5	18.2	271.0	29.3
	-0.1	22.9	19.2	279.6	29.5
	-0.1	12.5	18.7	287.4	28.5
	1.0	-15.6	17.3	271.9	28.7
	1.0	-2.8	20.4	298.5	29.3

2.1	-25.6	20.0	294.2	29.5
2.1	-42.5	17.6	273.0	28.7
3.2	-12.7	19.1	288.9	29.0
4.3	-33.6	15.6	247.1	28.7
6.5	4.9	18.2	255.8	30.4
13.1	-4.1	19.2	219.7	34.5
36.2	0.7	22.8	221.3	37.4

n5090_360

-18.5	-44.5	25.2	296.0	33.6
-7.5	-77.7	17.4	246.3	30.1
-5.3	-41.6	14.1	215.2	31.2
-3.1	-60.2	14.8	246.1	29.0
-2.7	-57.6	14.4	252.8	27.0
-2.0	-52.5	14.8	241.6	29.4
-1.6	-56.6	13.8	264.6	25.6
-0.9	-30.0	16.6	305.5	26.7
-0.5	-21.2	15.3	304.2	24.7
0.2	-5.7	16.4	260.7	29.3
0.6	21.3	15.0	273.9	26.2
1.3	31.9	15.1	263.0	28.1
1.7	22.7	16.1	284.0	26.5
2.4	26.4	16.2	243.6	30.6
2.8	46.0	18.5	273.9	29.1
6.1	78.3	17.3	224.6	31.9
9.0	7.4	26.7	262.5	37.8

n5266_270

-36.8	108.7	10.9	167.6	31.5
-27.6	212.2	38.8	153.6	65.1
-12.5	146.9	14.1	158.2	37.6
-11.5	108.6	10.5	177.6	29.7
-7.4	105.4	9.9	1[illegible]2.7	36.5
-6.6	115.3	12.2	196.6	29.9
-4.1	94.5	11.6	187.3	30.0
-3.8	120.5	12.8	216.7	28.6
-3.0	101.0	10.9	187.4	29.0
-2.7	103.5	14.4	202.2	31.7
-1.9	85.2	11.3	191.3	29.1
-1.6	73.6	10.5	202.1	27.1
-0.8	58.8	11.1	192.4	28.9
-0.5	39.3	10.4	193.2	27.8
0.3	23.9	11.2	193.0	28.8
0.6	-14.5	11.5	179.5	31.1
1.4	-25.9	11.6	195.1	29.1
1.7	-71.2	12.1	192.7	30.0
2.5	-70.0	11.4	200.0	28.4
2.8	-66.0	14.5	213.0	30.8
3.6	-91.7	15.3	182.4	35.3
5.8	-111.8	14.8	186.2	34.1
6.1	-83.7	15.2	204.4	32.4
8.0	-110.9	12.2	173.3	32.6
9.4	-122.4	13.0	157.2	38.5
10.2	-118.9	11.7	164.9	33.1
15.7	-163.2	13.6	180.6	33.4
18.2	-139.8	12.4	136.2	60.7
35.5	-171.4	20.7	171.0	42.7

n5266_360

-8.8	-30.3	22.7	195.4	40.2
-6.4	-4.5	16.0	170.2	39.7
-4.2	4.7	13.0	178.9	34.6
-4.0	28.2	13.4	233.4	27.3
-3.1	20.5	14.9	187.1	35.8
-2.9	32.7	12.3	248.8	25.2
-2.0	37.8	11.3	191.3	30.4
-1.8	38.9	10.2	233.4	23.9
-0.9	12.8	9.8	173.3	30.6
-0.7	26.5	10.0	240.1	23.3
0.2	27.9	9.9	171.1	31.0
0.4	11.1	9.3	218.7	23.8
1.3	17.9	10.3	179.7	30.4
1.5	16.1	10.8	222.6	25.3
2.4	-12.6	12.7	200.2	31.2
2.6	7.8	13.5	239.5	26.9
3.5	-32.7	12.2	191.7	31.6
3.7	-7.5	14.1	256.0	26.3
8.1	-16.4	16.7	249.4	29.0

n5796_270

-34.2	21.0	38.7	193.9	54.0
-8.0	56.6	15.5	206.4	32.5
-3.8	76.4	15.1	218.0	30.7
-2.7	83.4	19.0	247.9	31.9
-1.6	66.6	15.7	255.3	28.4
-0.5	52.9	17.1	272.1	28.6
0.6	20.1	16.6	255.9	29.2
1.7	-14.7	16.1	247.4	29.2
2.8	-26.8	16.4	244.7	29.8
3.9	-69.8	17.1	218.4	32.8
6.1	-46.8	15.7	213.6	31.7
36.9	-89.5	20.7	169.4	43.0

n5846_270

-36.5	-19.9	27.2	168.7	49.6
-22.2	24.2	17.7	244.8	30.6
-17.5	-0.4	15.5	228.3	29.9
-14.7	22.4	16.9	243.3	30.0
-12.5	12.2	11.2	198.6	28.0
-11.4	0.1	12.3	229.0	26.6
-10.3	39.3	13.6	241.9	27.0
-9.2	-19.0	10.0	189.4	27.3
-8.1	7.9	9.8	225.3	24.0
-7.0	-0.8	11.2	240.5	24.5
-5.9	11.3	10.0	228.7	24.0
-4.8	-3.7	10.5	251.0	23.1
-3.7	6.2	9.5	229.3	23.3
-2.6	10.1	9.1	231.7	22.8
-1.5	2.9	10.1	232.7	23.9
-0.4	-7.8	8.5	245.6	21.1
0.7	-9.8	8.9	256.0	21.0
1.8	5.3	8.7	260.9	20.6
2.9	-16.0	9.6	239.3	22.8
4.0	-25.1	10.3	231.1	24.2
5.1	-10.8	10.4	245.0	23.4

6.2	-9.9	10.0	216.3	25.0
7.3	-16.7	11.1	209.3	26.9
8.4	-3.1	11.8	239.5	25.1
9.5	-9.5	11.4	247.0	24.3
10.6	-19.9	11.9	234.4	25.8
11.7	-11.3	12.7	240.5	26.2
12.8	0.7	12.4	230.3	26.6
13.9	1.2	15.2	239.3	28.7
15.0	-25.1	16.0	230.3	30.1
17.2	-9.2	13.5	226.3	28.0
19.4	31.6	15.5	209.6	31.8
23.8	15.2	15.5	173.2	36.4

n5846_360

-25.1	7.6	43.0	201.8	57.0
-13.0	24.6	23.7	223.6	39.2
-10.7	16.0	16.5	214.2	32.0
-8.6	25.7	19.5	246.3	33.1
-6.4	5.7	17.0	250.0	30.9
-6.1	-1.8	12.8	252.4	25.4
-5.3	14.9	16.4	215.3	33.8
-4.2	-26.0	18.0	275.2	29.9
-3.2	4.0	11.8	248.8	24.7
-3.1	17.3	14.3	276.1	26.4
-2.1	-2.4	13.1	256.6	25.6
-2.0	-7.7	12.1	224.6	28.1
-1.0	-0.1	11.2	250.7	24.0
-0.9	-10.1	12.0	268.8	24.7
0.1	-17.9	11.5	254.8	24.0
0.2	-23.4	13.0	267.4	25.8
1.2	-3.9	10.7	230.8	24.7
1.3	-4.9	12.4	249.7	26.4
2.3	20.0	12.2	251.1	24.9
2.4	11.9	14.6	298.9	25.4
3.4	-4.5	11.7	253.9	24.3
3.5	1.5	15.3	279.8	27.2
4.6	-1.0	15.1	246.4	29.4
6.8	17.8	33.6	218.5	47.6
10.3	-9.0	16.8	179.0	39.2
18.1	-21.6	27.6	226.7	42.0

n5903_270

-32.2	-5.2	41.0	180.3	55.9
-9.7	32.1	19.5	215.1	35.1
-4.5	-7.2	12.4	214.2	27.6
-2.9	22.8	13.2	237.1	26.9
-2.8	-25.7	11.0	206.5	26.9
-1.7	-25.4	11.9	208.0	27.8
-0.7	-11.8	10.4	237.3	23.9
-0.6	-16.5	11.2	226.3	25.5
0.4	4.1	11.5	241.5	24.8
0.5	-15.2	11.6	220.8	26.3
1.5	2.6	16.8	208.1	35.7
1.6	-11.5	10.5	234.0	24.1
4.9	-6.0	11.0	207.9	26.7
5.9	-3.3	12.2	198.2	29.2
36.8	-60.0	19.5	149.8	45.7

n6849_270

	-18.0	-60.0	29.8	157.4	54.1
	-7.0	-62.6	26.5	244.8	37.0
	-3.1	-25.9	14.2	210.0	30.4
	-2.2	-0.6	20.8	234.4	33.9
	-2.0	-12.8	12.6	224.6	27.1
	-1.1	-33.1	13.7	243.5	26.9
	-0.9	-34.9	11.0	215.1	26.1
	0.0	-52.7	12.0	206.0	28.2
	0.2	-15.4	11.0	210.6	26.5
	1.1	-44.4	12.8	198.2	30.0
	1.3	-13.6	11.5	205.4	27.5
	3.5	-41.0	14.9	207.9	31.1
	5.5	-27.3	22.8	228.3	36.3
	6.8	-19.0	14.6	182.9	34.0
	26.6	4.4	31.0	166.3	53.1

n6849_360

	-9.0	1.7	26.9	251.4	37.4
	-1.6	8.3	13.1	235.5	27.3
	-0.5	21.0	11.8	220.4	27.0
	0.6	-0.1	12.9	227.5	27.6
	1.7	-4.3	15.9	240.4	29.5

n6868_270

	-13.7	-28.0	18.4	241.2	31.9
	-13.1	-55.5	15.1	175.3	35.5
	-10.2	-23.8	17.0	198.8	34.4
	-9.1	-15.8	0.0	268.2	0.7
	-7.8	-24.0	19.2	272.7	30.1
	-6.9	-4.9	15.4	283.4	26.0
	-5.8	-41.3	11.5	219.7	26.3
	-4.9	-45.9	15.0	236.0	29.2
	-4.7	-37.0	11.5	252.8	24.1
	-3.6	-9.5	12.1	273.5	23.5
	-2.5	-24.3	12.4	300.9	22.5
	-1.6	-14.3	15.4	260.0	27.8
	-1.4	-14.9	11.1	280.9	22.1
	-0.5	-6.4	15.0	267.3	26.8
	-0.3	-12.6	12.2	293.4	22.6
	0.6	-3.8	17.2	300.3	26.8
	0.8	-21.8	12.2	292.8	22.7
	1.7	3.3	15.2	269.7	26.9
	1.9	10.2	11.5	287.9	22.2
	3.0	-17.1	11.6	276.2	22.9
	3.9	-21.0	16.9	278.8	27.8
	4.1	-4.4	11.9	273.2	23.3
	5.0	-2.4	15.5	258.3	28.1
	5.2	5.7	13.4	252.3	26.0
	6.3	0.1	23.3	289.9	31.4
	7.2	1.4	17.2	255.3	29.5
	7.4	7.4	15.0	287.5	25.4
	9.6	-12.5	16.9	256.4	28.8
	10.7	5.1	17.8	234.1	31.5
	12.9	37.0	19.3	247.6	31.6

n6868_360

	-15.9	-60.4	21.7	235.1	34.9
	-4.5	-23.3	17.5	253.9	29.6
	-3.4	16.6	14.5	296.5	24.5
	-2.3	-1.1	13.2	278.2	24.2
	-1.2	-10.3	12.0	296.2	22.3
	-0.1	-12.7	12.0	274.8	23.3
	1.0	3.8	14.1	281.9	24.8
	2.1	-16.9	12.9	265.8	24.7
	3.2	-12.0	13.5	300.5	23.4
	4.3	10.1	14.5	276.2	25.6
	5.4	11.9	14.6	254.7	27.0
	7.6	-22.6	17.2	264.7	28.5
	14.2	-6.9	19.8	285.4	29.4

n7097_270

	-8.0	-26.8	21.6	200.3	39.9
	-5.3	-24.2	12.7	198.4	32.0
	-4.2	-20.5	15.0	239.8	28.4
	-3.1	-23.1	12.4	239.8	25.8
	-2.9	9.0	12.5	224.6	28.0
	-2.0	-20.0	10.3	229.2	24.2
	-1.8	11.4	12.5	250.3	25.2
	-0.9	-23.3	10.6	242.6	23.7
	-0.7	-7.7	11.0	248.1	23.8
	0.2	4.5	9.7	234.0	23.2
	0.4	-21.6	11.1	244.6	24.2
	1.3	-4.2	10.4	238.1	23.7
	1.5	-21.8	11.8	236.6	25.5
	2.4	-0.3	11.1	225.8	25.5
	2.6	-23.7	12.2	236.5	25.9
	3.5	4.3	11.7	200.7	28.4
	4.6	-30.2	15.8	183.8	35.0
	4.8	1.5	15.1	246.7	28.0
	5.7	4.5	19.3	219.5	34.1
	6.8	7.8	22.6	197.6	39.4
	10.1	20.2	20.7	159.9	51.3
	17.8	46.2	36.9	166.5	57.9

n7097_360

	-4.0	-25.3	13.3	206.8	29.5
	-2.9	-37.6	13.2	255.8	25.5
	-1.8	-34.4	11.7	248.7	24.6
	-0.7	-27.4	10.4	252.2	22.9
	0.4	4.0	11.4	231.3	25.4
	1.5	2.0	11.5	240.6	24.9
	2.6	40.8	12.2	222.8	26.8
	3.7	-1.8	13.2	232.2	27.2
	5.9	13.4	15.5	249.6	28.2
	10.3	31.8	18.2	214.0	33.7

n7200_270

	-6.4	-44.0	25.8	216.6	40.3
	-4.1	9.6	13.7	157.8	36.6
	-3.0	-24.7	11.2	195.9	28.2
	-2.4	-16.5	11.4	175.6	30.7
	-1.9	-26.6	8.9	189.7	25.8

	-1.3	-8.2	13.9	186.1	32.6
	-0.8	-4.8	9.0	207.3	24.3
	-0.2	3.8	10.0	206.0	25.8
	0.3	18.4	8.5	198.0	24.5
	0.9	6.4	10.4	206.0	26.3
	1.4	21.1	8.7	202.8	24.2
	2.5	29.3	8.6	171.5	27.2
	3.6	49.5	13.5	177.4	33.4
	4.2	34.5	11.7	173.3	34.7
	4.7	31.3	13.8	138.3	40.9
n7200_360					
	-2.3	44.3	11.6	205.5	27.7
	-1.2	2.5	12.2	224.7	26.7
	-0.1	4.8	10.7	208.0	26.4
	1.0	-6.6	10.1	214.4	25.2
	2.1	-69.5	11.3	196.2	28.2

APPENDIX B: INDIVIDUAL MEASUREMENTS AT DIFFERENT RADII FOR THE BEST DETERMINED INDICES

Column (1) = radial distance from the centre (in arcsec).
Column (2) = line-strength index.
Column (3) = error on the line-strength index.
[Columns (2) and (3) are in magnitudes for Mg_2 and Mg_1 and in angstroms for Fe_{5270} and Na D.]

ESO208_Fe5270_270

-14.6	2.449	0.308
-6.8	2.899	0.293
-4.2	3.134	0.241
-2.6	3.318	0.272
-1.5	3.266	0.226
-0.4	3.255	0.198
0.7	3.180	0.225
1.8	3.178	0.264
3.3	2.994	0.250
6.7	2.985	0.306
17.4	2.636	0.404

ESO208_Mg1_270

-18.3	0.077	0.010
-11.0	0.084	0.010
-8.1	0.096	0.009
-7.0	0.108	0.010
-5.9	0.096	0.008
-4.8	0.114	0.007
-3.7	0.116	0.006
-2.6	0.121	0.005
-1.5	0.133	0.004
-0.4	0.145	0.003
0.7	0.152	0.003
1.8	0.139	0.004
2.9	0.123	0.005
4.0	0.113	0.007
5.1	0.121	0.008
6.2	0.113	0.009
7.3	0.117	0.008
8.4	0.112	0.009
10.6	0.087	0.009
16.1	0.077	0.010

ESO208_Mg2_270

-9.9	0.237	0.009
-7.0	0.254	0.008
-5.9	0.276	0.009
-4.8	0.263	0.007
-3.7	0.286	0.006
-2.6	0.285	0.005
-1.5	0.308	0.004
-0.4	0.316	0.004
0.7	0.314	0.004
1.8	0.300	0.005
2.9	0.288	0.006
4.0	0.265	0.007
5.1	0.268	0.008
6.2	0.249	0.010
7.3	0.252	0.009
9.5	0.236	0.009
12.8	0.221	0.010

ESO208_NaD_270

-24.6	1.770	0.154
-18.0	2.554	0.293
-8.8	2.353	0.294
-5.9	3.390	0.249
-4.8	3.507	0.276
-3.7	3.941	0.227
-2.6	4.241	0.199
-1.5	5.022	0.176
-0.4	5.512	0.131
0.7	5.493	0.158
1.8	4.701	0.197
2.9	4.050	0.214
4.0	3.758	0.294
5.1	3.364	0.264
7.3	3.382	0.274
13.9	3.170	0.297

ESO323_Mg1_270

-3.6	0.077	0.010
-1.9	0.108	0.009
-1.9	0.112	0.009
-0.8	0.117	0.008
-0.8	0.113	0.006
0.3	0.124	0.007
0.3	0.128	0.005
1.4	0.136	0.009
1.4	0.113	0.007
2.5	0.086	0.008
3.6	0.125	0.010
5.8	0.087	0.010

ESO323_Mg1_360

-4.4	0.095	0.009

-2.2	0.122	0.010
-1.7	0.102	0.009
-1.1	0.132	0.008
-0.6	0.130	0.008
0.0	0.124	0.007
0.5	0.132	0.006
1.1	0.129	0.008
1.6	0.127	0.006
2.2	0.111	0.009
2.7	0.121	0.009
4.9	0.081	0.009
8.9	0.090	0.010

ESO323_Mg2_270

-4.2	0.236	0.010
-2.5	0.254	0.009
-1.9	0.265	0.010
-0.8	0.271	0.008
-0.8	0.276	0.006
0.3	0.267	0.008
0.3	0.295	0.005
1.4	0.268	0.008
1.4	0.289	0.007
2.5	0.243	0.009
4.7	0.266	0.009
6.9	0.245	0.010

ESO323_Mg2_360

-4.4	0.236	0.010
-2.3	0.239	0.009
-2.2	0.253	0.009
-1.1	0.265	0.009
-0.6	0.285	0.009
0.0	0.275	0.008
0.5	0.281	0.007
1.1	0.277	0.009
1.6	0.249	0.007
2.2	0.243	0.010
2.7	0.237	0.008
6.0	0.217	0.010

ESO323_NaD_270

-14.2	3.376	0.368
-3.1	3.826	0.299
-0.8	4.524	0.262
-0.8	4.934	0.242
0.3	4.811	0.284
0.3	4.632	0.207
1.4	4.176	0.266
3.6	4.476	0.292

ESO323_NaD_360

-5.5	3.395	0.435
-2.2	3.928	0.394
-1.6	4.604	0.271
-1.1	4.891	0.421
-0.5	4.937	0.234
0.0	4.621	0.318
0.6	4.885	0.269
1.1	4.696	0.358
2.2	4.207	0.368
2.8	3.756	0.297
8.2	3.745	0.447

ESO381_Mg1_270

-4.5	0.019	0.010
-3.0	0.039	0.009
-2.7	0.035	0.009
-1.9	0.055	0.008
-1.6	0.045	0.006
-0.5	0.069	0.004
0.3	0.070	0.005
0.6	0.064	0.004
1.4	0.063	0.007
1.7	0.045	0.005
2.5	0.055	0.009
2.8	0.041	0.008
3.9	0.042	0.009
4.7	0.049	0.010

ESO381_Mg1_360

-6.2	0.054	0.010
-2.9	0.071	0.010
-1.8	0.066	0.007
-0.7	0.074	0.006
0.4	0.078	0.006
1.5	0.073	0.007
2.6	0.063	0.008

ESO381_Mg2_270

-5.1	0.154	0.010
-3.0	0.169	0.010
-2.7	0.162	0.009
-1.9	0.172	0.008
-1.6	0.170	0.006
-0.8	0.180	0.006
-0.5	0.186	0.004
0.3	0.176	0.006
0.6	0.181	0.004
1.4	0.176	0.007
1.7	0.180	0.006
2.5	0.156	0.010
2.8	0.161	0.008
3.9	0.172	0.010
5.8	0.161	0.010

ESO381_Mg2_360

-7.3	0.157	0.010
-2.9	0.173	0.009
-1.8	0.186	0.008
-0.7	0.178	0.007
0.4	0.182	0.006
1.5	0.170	0.008
2.6	0.167	0.009

ESO381_NaD_270

-4.0	2.044	0.282
-1.9	2.264	0.296
-1.6	2.761	0.262
-0.8	2.907	0.273
-0.5	3.269	0.185
0.3	3.087	0.240
0.6	3.157	0.182
1.4	2.806	0.277
1.7	2.772	0.252
3.6	2.689	0.297
6.1	2.520	0.299

ESO381_NaD_360

-5.1	2.139	0.295
-0.7	2.817	0.254
0.4	2.918	0.288
1.5	2.604	0.264

IC1459_Fe5270_270

-15.3	3.101	0.259
-8.7	3.359	0.252
-6.0	3.365	0.190
-4.4	3.507	0.219
-3.3	3.211	0.162
-2.2	3.349	0.126
-1.1	3.408	0.102
0.0	3.245	0.091
1.1	3.199	0.100
2.2	3.494	0.124
3.3	3.310	0.163
4.4	3.096	0.208
5.9	3.096	0.199
9.3	2.992	0.246
15.3	2.948	0.257

IC1459_Mg1_270

-9.1	0.157	0.009
-8.8	0.151	0.007
-7.7	0.153	0.006

-6.6	0.166	0.005
-6.2	0.169	0.008
-5.5	0.166	0.004
-5.1	0.176	0.009
-4.4	0.168	0.004
-4.0	0.177	0.007
-3.3	0.169	0.003
-2.9	0.182	0.006
-2.2	0.184	0.002
-1.8	0.194	0.005
-1.1	0.192	0.002
-0.7	0.187	0.004
0.0	0.198	0.002
0.4	0.185	0.004
1.1	0.193	0.002
1.5	0.186	0.005
2.2	0.179	0.002
2.6	0.175	0.006
3.3	0.172	0.002
3.7	0.171	0.007
4.4	0.174	0.003
4.8	0.167	0.008
5.5	0.164	0.004
5.9	0.162	0.008
6.6	0.163	0.005
7.0	0.149	0.009
7.7	0.155	0.006
8.8	0.169	0.007
9.9	0.147	0.008
13.2	0.143	0.008

IC1459_Mg1_360

-15.7	0.135	0.010
-6.0	0.153	0.009
-3.8	0.183	0.006
-2.7	0.175	0.005
-1.6	0.191	0.004
-0.5	0.193	0.003
0.6	0.189	0.003
1.7	0.185	0.004
2.8	0.165	0.005
3.9	0.151	0.006
5.0	0.151	0.008
6.1	0.163	0.009
7.2	0.139	0.008
8.3	0.126	0.009
10.5	0.112	0.009
13.8	0.107	0.009

IC1459_Mg2_270

-17.2	0.265	0.010
-14.3	0.305	0.010

-12.8	0.317	0.010
-12.1	0.260	0.008
-11.0	0.284	0.010
-9.9	0.294	0.008
-8.8	0.300	0.008
-7.7	0.306	0.006
-7.5	0.317	0.009
-6.6	0.298	0.006
-5.5	0.313	0.005
-4.6	0.331	0.008
-4.4	0.320	0.004
-3.5	0.351	0.010
-3.3	0.328	0.003
-2.4	0.344	0.008
-2.2	0.336	0.002
-1.3	0.350	0.006
-1.1	0.344	0.002
-0.2	0.351	0.005
0.0	0.352	0.002
0.9	0.349	0.004
1.1	0.348	0.002
2.0	0.348	0.004
2.2	0.334	0.002
3.1	0.343	0.005
3.3	0.329	0.003
4.2	0.328	0.006
4.4	0.322	0.003
5.3	0.336	0.008
5.5	0.322	0.004
6.4	0.320	0.009
6.6	0.311	0.005
7.5	0.329	0.008
7.7	0.297	0.006
8.6	0.321	0.010
8.8	0.285	0.007
9.9	0.288	0.008
10.8	0.297	0.009
11.0	0.285	0.009
12.1	0.301	0.008
13.2	0.303	0.009
14.3	0.289	0.009
15.2	0.281	0.010
16.5	0.268	0.009
19.8	0.272	0.010
28.6	0.253	0.010
32.8	0.258	0.010

IC1459_Mg2_360

-8.5	0.297	0.009
-5.6	0.302	0.008
-4.5	0.312	0.009
-3.4	0.337	0.008
-2.3	0.343	0.007
-0.1	0.356	0.004
1.0	0.347	0.003
2.1	0.337	0.003

3.2	0.332	0.004
4.3	0.311	0.006
5.4	0.311	0.007
6.5	0.315	0.008
7.6	0.301	0.010
8.7	0.297	0.009
9.8	0.285	0.010
12.0	0.272	0.009
16.4	0.258	0.009
29.6	0.240	0.010

IC1459_NaD_270

-14.1	3.862	0.293
-13.9	4.661	0.268
-11.0	4.676	0.241
-9.9	4.715	0.284
-8.8	4.825	0.250
-7.7	5.114	0.214
-6.9	4.493	0.295
-6.6	5.376	0.205
-5.5	5.462	0.170
-4.4	5.951	0.138
-4.0	5.845	0.249
-3.3	6.437	0.109
-2.9	5.857	0.295
-2.2	6.895	0.086
-1.8	6.702	0.209
-1.1	7.170	0.073
0.0	7.291	0.068
0.4	7.375	0.161
1.1	7.234	0.061
1.5	6.837	0.202
2.2	6.592	0.073
2.6	5.867	0.229
3.3	6.129	0.096
3.7	5.644	0.231
4.4	5.620	0.123
4.8	5.298	0.257
5.5	5.311	0.152
6.6	5.201	0.184
7.0	5.033	0.300
7.7	5.079	0.213
8.8	4.422	0.248
9.9	4.511	0.287
11.0	4.562	0.240
12.1	4.374	0.269
14.3	4.212	0.257
14.7	4.554	0.292
18.7	4.155	0.287
29.7	3.243	0.345
31.2	3.104	0.470

IC1459_NaD_360

-27.9	3.821	0.356
-3.8	5.909	0.257
-2.7	6.461	0.203
-1.6	7.194	0.156
0.6	7.483	0.119
1.7	6.733	0.164
2.8	6.582	0.195
3.9	6.204	0.248
5.0	5.594	0.233
7.2	5.255	0.278
13.8	4.536	0.299
47.9	3.356	0.458

IC2006_Mg1_270

-14.4	0.099	0.010
-7.2	0.128	0.010
-6.0	0.105	0.010
-4.3	0.123	0.008
-3.2	0.133	0.009
-2.5	0.119	0.008
-2.1	0.121	0.007
-1.4	0.142	0.008
-1.0	0.162	0.006
-0.3	0.146	0.007
0.1	0.162	0.006
0.8	0.154	0.007
1.2	0.163	0.006
1.9	0.144	0.008
2.3	0.142	0.007
3.0	0.130	0.008
3.4	0.124	0.009
4.1	0.125	0.010
4.5	0.112	0.009
6.7	0.111	0.009
7.4	0.114	0.010
25.0	0.085	0.011

IC2006_Mg2_270

-7.8	0.228	0.009
-6.6	0.230	0.010
-4.3	0.279	0.009
-3.2	0.268	0.010
-2.5	0.253	0.009
-2.1	0.285	0.008
-1.4	0.285	0.009
-1.0	0.301	0.006
-0.3	0.292	0.007
0.1	0.325	0.006
1.2	0.319	0.006
1.9	0.281	0.009
2.3	0.296	0.008
3.0	0.258	0.009
3.4	0.259	0.010
4.5	0.254	0.009
5.2	0.270	0.009

6.7	0.252	0.009
12.2	0.229	0.010
15.1	0.214	0.010
25.0	0.210	0.022

IC2006_NaD_270

-7.7	3.040	0.447
-6.7	2.785	0.291
-3.6	3.822	0.398
-3.2	3.749	0.261
-2.5	3.946	0.412
-2.1	4.801	0.270
-1.4	5.254	0.327
-1.0	4.759	0.237
-0.3	5.460	0.305
0.1	5.170	0.227
0.8	5.047	0.323
1.2	5.337	0.227
1.9	4.730	0.399
2.3	4.617	0.277
3.0	3.772	0.387
3.4	4.137	0.277
5.2	3.411	0.412
5.6	3.279	0.288
10.7	2.906	0.446
12.2	1.602	0.293
25.0	1.567	0.655

IC2035_Fe5270_270

-6.2	2.366	0.397
-4.1	2.648	0.248
-3.1	2.737	0.344
-1.5	2.801	0.284
-0.4	2.488	0.178
0.7	2.339	0.186
1.8	2.262	0.285
3.3	2.456	0.324
7.1	2.159	0.385

IC2035_Mg1_270

-3.3	0.052	0.006
-2.6	0.044	0.007
-2.2	0.042	0.004
-1.5	0.061	0.005
-1.1	0.057	0.003
-0.4	0.063	0.003
0.0	0.072	0.003
0.7	0.057	0.003
1.1	0.051	0.003
1.8	0.067	0.005
2.2	0.052	0.004
2.9	0.056	0.007
3.3	0.057	0.006

IC2035_Mg2_270

-6.6	0.137	0.009
-3.7	0.156	0.008
-3.3	0.160	0.007
-2.6	0.150	0.008
-2.2	0.154	0.006
-1.5	0.166	0.005
-1.1	0.147	0.004
-0.4	0.164	0.004
0.0	0.171	0.003
0.7	0.167	0.004
1.1	0.169	0.003
1.8	0.161	0.005
2.2	0.146	0.005
2.9	0.154	0.007
3.3	0.139	0.007
5.1	0.139	0.009

IC2035_NaD_270

-8.5	2.963	0.288
-6.8	2.854	0.297
-4.4	2.876	0.273
-3.3	2.727	0.259
-2.6	3.083	0.274
-2.2	2.633	0.169
-1.5	2.884	0.213
-1.1	2.786	0.149
-0.4	2.668	0.154
0.0	2.776	0.145
0.7	2.731	0.153
1.1	2.573	0.139
1.8	2.706	0.231
2.2	2.564	0.170
2.9	2.199	0.277
3.3	2.369	0.263
4.4	2.112	0.273
6.2	2.137	0.278
6.6	2.399	0.283
14.3	1.451	0.297
24.9	0.766	0.342
27.5	-5.638	0.949

IC3370_Mg1_270

-4.0	0.115	0.008
-2.9	0.117	0.009
-1.8	0.118	0.007
-0.7	0.130	0.006
-0.7	0.121	0.007
0.4	0.117	0.005
0.4	0.129	0.007
1.5	0.107	0.006
1.5	0.132	0.008
2.6	0.107	0.008

IC3370_Mg1_320

-4.052	0.120	0.008
-2.839	0.120	0.008
-1.852	0.109	0.008
-0.752	0.123	0.006
-0.639	0.137	0.008
0.348	0.126	0.006
0.461	0.136	0.008
1.448	0.109	0.007
1.561	0.129	0.009
2.548	0.121	0.008
3.761	0.122	0.008
7.061	0.124	0.009

IC3370_Mg2_270

-14.3	0.242	0.010
-6.9	0.253	0.010
-5.7	0.239	0.010
-4.0	0.264	0.009
-2.9	0.271	0.010
-2.9	0.261	0.009
-1.8	0.271	0.008
-1.8	0.273	0.010
-0.7	0.280	0.006
-0.7	0.270	0.007
0.4	0.264	0.006
0.4	0.269	0.007
1.5	0.273	0.007
1.5	0.269	0.009
2.6	0.267	0.009
2.6	0.247	0.009
3.7	0.254	0.008
4.8	0.254	0.009
4.8	0.249	0.009
7.0	0.265	0.010
9.2	0.239	0.009
14.7	0.242	0.010

IC3370_Mg2_360

-18.6	0.235	0.010
-6.3	0.239	0.009
-3.0	0.243	0.008
-1.9	0.269	0.009
-1.7	0.271	0.010
-0.8	0.262	0.007
-0.6	0.268	0.009
0.3	0.273	0.006
0.5	0.264	0.009
1.4	0.244	0.007
1.6	0.274	0.009
2.7	0.251	0.008
3.8	0.264	0.009
6.0	0.256	0.009
10.4	0.254	0.010

IC3370_NaD_270

-14.1	4.024	0.311
-5.3	4.127	0.293
-2.4	5.214	0.274
-1.8	5.023	0.255
-0.7	5.434	0.242
-0.7	5.338	0.299
0.4	5.080	0.206
0.4	4.966	0.264
1.5	4.825	0.280
1.5	4.546	0.259
2.6	4.564	0.274
3.7	4.128	0.276
4.8	4.378	0.292
15.8	3.583	0.299

IC3370_NaD_360

-20.2	3.468	0.497
-7.9	3.745	0.422
-4.4	3.944	0.395
-3.3	4.081	0.421
-2.2	4.569	0.339
-1.9	5.441	0.263
-1.1	4.987	0.345
-0.8	5.562	0.288
0.0	5.212	0.411
0.3	5.546	0.245
1.1	4.559	0.381
1.4	4.883	0.224
2.2	4.368	0.433
2.5	4.121	0.254
3.6	3.696	0.250
4.4	3.917	0.414
5.8	3.830	0.264
9.9	3.479	0.438
10.2	3.759	0.297

IC4889_Mg1_270

-6.0	0.113	0.010
-3.8	0.106	0.008
-2.7	0.115	0.008
-1.6	0.128	0.006
-0.5	0.120	0.005
0.6	0.117	0.005
1.7	0.117	0.007
2.8	0.099	0.009
3.9	0.085	0.009
6.1	0.067	0.009
12.7	0.068	0.010

IC4889_Mg1_360

-13.0	0.094	0.010
-8.4	0.101	0.009
-5.6	0.115	0.008
-4.5	0.107	0.009
-3.4	0.122	0.007
-2.3	0.128	0.006
-1.2	0.128	0.005
-0.1	0.109	0.004
1.0	0.099	0.005
2.1	0.114	0.006
3.2	0.112	0.008
4.3	0.084	0.009
5.4	0.102	0.008
6.5	0.097	0.009
8.7	0.083	0.009
12.0	0.083	0.010
19.7	0.065	0.010

IC4889_Mg2_270

-3.8	0.250	0.009
-2.7	0.260	0.009
-1.6	0.269	0.006
-0.5	0.270	0.005
0.6	0.265	0.005
1.7	0.255	0.007
2.8	0.251	0.010
3.9	0.238	0.009
6.1	0.237	0.010
13.8	0.212	0.010

IC4889_Mg2_360

-5.6	0.247	0.009
-4.5	0.255	0.010
-3.4	0.255	0.008
-2.3	0.265	0.006
-1.2	0.260	0.005
-0.1	0.246	0.004
1.0	0.242	0.005
2.1	0.263	0.007
3.2	0.250	0.008
4.3	0.225	0.008
5.4	0.225	0.009
7.6	0.217	0.009
10.9	0.215	0.010
19.7	0.215	0.010

IC4889_NaD_270

-3.3	3.429	0.292
-1.6	4.122	0.292
-0.5	4.587	0.218
0.6	4.258	0.220
1.7	4.244	0.298
3.9	3.616	0.293

IC4889_NaD_360

-7.5	3.282	0.296
-3.4	3.285	0.252
-2.3	3.940	0.249
-1.2	4.344	0.202
-0.1	4.627	0.166
1.0	4.284	0.188
2.1	3.931	0.257
3.2	3.240	0.265
5.4	2.892	0.266
9.8	2.618	0.298

IC4943_Fe5270_270

-5.4	2.465	0.448
-2.3	2.820	0.247
-0.9	2.974	0.206
0.2	3.332	0.181
1.3	3.021	0.203
2.8	2.667	0.255
4.0	2.236	0.393

IC4943_Mg1_270

-4.2	0.093	0.009
-3.3	0.105	0.010
-3.1	0.114	0.008
-2.0	0.121	0.005
-1.6	0.120	0.009
-0.9	0.110	0.004
-0.5	0.115	0.007
0.2	0.131	0.003
0.6	0.122	0.007
1.3	0.133	0.004
1.7	0.095	0.009
2.4	0.114	0.005
3.5	0.114	0.008
4.6	0.102	0.009

IC4943_Mg1_360

-3.4	0.119	0.009
-1.7	0.129	0.008
-0.6	0.145	0.006
0.5	0.108	0.006
1.6	0.098	0.009

IC4943_Mg2_270

-4.2	0.239	0.010
-3.9	0.233	0.010
-3.1	0.236	0.009
-2.0	0.249	0.006
-1.6	0.262	0.009

-0.9	0.259	0.004
-0.5	0.258	0.007
0.2	0.279	0.003
0.6	0.271	0.008
1.3	0.267	0.004
1.7	0.237	0.010
2.4	0.251	0.006
3.5	0.230	0.009
4.6	0.234	0.010

IC4943_Mg2_360

-4.0	0.216	0.010
-1.7	0.254	0.009
-0.6	0.281	0.006
0.5	0.244	0.007
1.6	0.211	0.010
4.9	0.179	0.010

IC4943_NaD_270

-5.4	3.067	0.290
-3.1	3.607	0.270
-2.0	3.966	0.179
-0.9	4.075	0.144
-0.5	4.053	0.282
0.2	4.151	0.135
0.6	3.984	0.282
1.3	4.124	0.151
2.4	3.121	0.227
3.5	3.101	0.291
5.0	3.374	0.294
13.4	2.840	0.295
20.4	2.280	0.732
27.7	1.622	1.068

IC4943_NaD_360

-2.9	3.423	0.296
-0.6	4.126	0.284
0.5	4.027	0.269
3.8	3.192	0.297
24.7	1.637	0.646

N1052_Fe5270_270

-26.5	2.418	0.398
-7.6	2.903	0.248
-5.0	3.047	0.229
-2.3	3.065	0.195
-1.2	3.034	0.161
-0.1	2.835	0.146
1.0	2.935	0.158
2.1	3.022	0.193
3.2	2.864	0.238
4.8	2.898	0.230

8.6	2.872	0.249
10.3	2.831	0.446
14.1	2.793	0.424
21.8	2.519	0.284

N1052_Mg1_270

-16.1	0.116	0.010
-13.3	0.146	0.010
-11.1	0.140	0.008
-10.0	0.149	0.010
-8.9	0.150	0.009
-7.8	0.143	0.008
-6.7	0.166	0.007
-5.6	0.169	0.006
-4.5	0.158	0.005
-3.4	0.176	0.004
-2.3	0.193	0.003
-1.2	0.204	0.003
-0.1	0.222	0.002
1.0	0.217	0.002
2.1	0.203	0.003
3.2	0.181	0.004
4.3	0.177	0.004
5.4	0.175	0.005
6.5	0.171	0.006
7.6	0.149	0.007
8.7	0.146	0.008
9.8	0.141	0.009
10.9	0.155	0.008
12.0	0.144	0.008
13.1	0.146	0.009
19.7	0.140	0.010

N1052_Mg2_270

-20.4	0.241	0.010
-15.0	0.273	0.010
-12.2	0.271	0.009
-10.0	0.269	0.008
-8.9	0.313	0.010
-7.8	0.280	0.009
-6.7	0.291	0.008
-5.6	0.297	0.007
-4.5	0.293	0.006
-3.4	0.322	0.005
-2.3	0.329	0.004
-1.2	0.330	0.003
-0.1	0.344	0.003
1.0	0.335	0.003
2.1	0.326	0.003
3.2	0.314	0.004
4.3	0.312	0.005
5.4	0.304	0.006
6.5	0.301	0.007
7.6	0.284	0.008
8.7	0.296	0.009
9.8	0.264	0.010

10.9	0.284	0.008
12.0	0.278	0.009
13.1	0 263	0.010
15.3	0.258	0.009
18.6	0.278	0.010
27.4	0.240	0.010

N1052_NaD_270

-32.3	1.962	0.318
-14.6	3.424	0.275
-10.6	3.934	0.261
-7.8	4.211	0.250
-6.7	4.572	0.287
-5.6	5.155	0.248
-4.5	5.458	0.207
-3.4	5.944	0.167
-2.3	6.680	0.133
-1.2	7.030	0.114
-0.1	7.256	0.095
1.0	6.893	0.095
2.1	6.383	0.107
3.2	5.487	0.145
4.3	5.246	0.181
5.4	4.479	0.221
6.5	4.187	0.260
7.6	3.677	0.299
8.7	3.366	0.248
9.8	3.584	0.273
12.0	3.522	0.262
15.3	2.699	0.283
24.1	2.430	0.300
45.0	1.817	0.495

N1209_Fe5270_270

-10.2	2.708	0.419
-4.2	3.300	0.233
-2.6	3.214	0.244
-1.5	3.427	0.202
-0.4	3.549	0.199
0.7	3.509	0.173
1.8	3.310	0.196
2.9	3.455	0.222
4.5	3.188	0.216

N1209_Mg1_270

-13.8	0.103	0.009
-10.3	0.134	0.010
-8.1	0.128	0.008
-7.0	0.132	0.009
-5.9	0.130	0.007
-4.8	0.131	0.006
-3.7	0.147	0.005
-2.6	0.136	0.004
-1.5	0.146	0.003

-0.4	0.153	0.003
0.7	0.162	0.003
1.8	0.156	0.003
2.9	0.142	0.004
4.0	0.136	0.005
5.1	0.130	0.006
6.2	0.135	0.007
7.3	0.119	0.009
8.4	0.133	0.008
9.5	0.121	0.009
10.6	0.093	0.010
12.8	0.123	0.010
17.2	0.112	0.010

N1209_Mg2_270

-29.6	0.185	0.014
-16.3	0.232	0.010
-10.9	0.272	0.009
-8.1	0.260	0.008
-7.0	0.259	0.010
-5.9	0.282	0.008
-4.8	0.283	0.007
-3.7	0.280	0.005
-2.6	0.293	0.004
-1.5	0.293	0.004
-0.4	0.306	0.003
0.7	0.319	0.003
1.8	0.310	0.004
2.9	0.289	0.004
4.0	0.279	0.006
5.1	0.259	0.007
6.2	0.258	0.008
7.3	0.274	0.009
8.4	0.256	0.008
9.5	0.247	0.009
11.7	0.233	0.009
16.1	0.227	0.010

N1209_NaD_270

-10.5	3.951	0.277
-7.0	3.912	0.265
-5.9	4.658	0.291
-4.8	4.828	0.243
-3.7	4.780	0.181
-2.6	4.933	0.148
-1.5	5.363	0.143
-0.4	5.292	0.134
0.7	5.410	0.116
1.8	5.262	0.136
2.9	5.159	0.169
4.0	4.737	0.201
5.1	4.528	0.267
6.2	4.660	0.295
7.3	4.790	0.261
9.5	4.793	0.293
13.9	4.519	0.292

N1298_Mg1_270

-4.4	0.067	0.010
-3.3	0.100	0.009
-2.2	0.076	0.007
-1.1	0.088	0.006
0.0	0.095	0.006
1.1	0.088	0.006
2.2	0.072	0.009
3.3	0.077	0.010

N1298_Mg2_270

-5.0	0.206	0.009
-3.3	0.240	0.010
-2.2	0.229	0.007
-1.1	0.238	0.006
0.0	0.242	0.006
1.1	0.234	0.007
2.2	0.225	0.010
4.4	0.219	0.009

N1298_NaD_270

-3.9	3.597	0.288
-2.2	3.410	0.292
-1.1	3.429	0.276
0.0	3.593	0.260
1.1	3.503	0.290
3.3	3.520	0.289

N1947_MNaD_360

2.0	2.629	0.403
4.9	1.608	0.437
10.2	1.298	0.444
21.5	0.530	0.605
0.9	3.444	0.392
-0.2	4.642	0.415
-1.3	5.170	0.445
-2.4	4.942	0.450
-7.9	4.402	0.419
-17.8	3.218	0.450

N1947_Mg1_270

-12.3	0.071	0.010
-7.0	0.086	0.009
-6.6	0.060	0.009
-4.2	0.082	0.008
-3.8	0.075	0.008
-3.1	0.083	0.010
-2.7	0.083	0.010
-2.0	0.095	0.009

-1.6	0.096	0.009
-0.9	0.094	0.008
-0.5	0.112	0.008
0.2	0.102	0.007
0.6	0.108	0.008
1.3	0.103	0.008
1.7	0.111	0.009
2.4	0.106	0.009
2.8	0.116	0.008
3.5	0.090	0.009
5.0	0.108	0.009
6.8	0.104	0.010
10.5	0.088	0.010
15.6	0.071	0.010

N1947_Mg1_360

2.0	0.106	0.008
4.2	0.090	0.010
7.1	0.088	0.010
12.4	0.071	0.009
0.9	0.103	0.009
-0.2	0.104	0.008
-1.3	0.114	0.008
-2.4	0.111	0.008
-4.6	0.113	0.010
-10.1	0.093	0.010
-17.8	0.082	0.010

N1947_Mg2_270

-13.1	0.225	0.010
-10.5	0.207	0.010
-7.7	0.242	0.010
-5.9	0.231	0.009
-4.9	0.242	0.010
-3.1	0.222	0.008
-2.7	0.222	0.008
-2.0	0.229	0.009
-1.6	0.206	0.009
-0.9	0.228	0.008
-0.5	0.251	0.009
0.2	0.243	0.007
0.6	0.263	0.009
1.3	0.245	0.008
1.7	0.275	0.009
2.4	0.231	0.010
2.8	0.249	0.009
3.5	0.220	0.010
5.0	0.221	0.009
7.9	0.222	0.010
11.6	0.264	0.010

N1947_Mg2_360

2.0	0.244	0.008
4.9	0.234	0.009

9.5	0.200	0.009
0.9	0.234	0.010
-0.2	0.251	0.009
-1.3	0.245	0.009
-2.4	0.250	0.009
-6.8	0.242	0.010
-13.4	0.232	0.010

N1947_NaD_270

-15.3	1.613	0.436
-12.7	2.018	0.432
-9.9	1.871	0.433
-8.1	2.181	0.390
-7.1	1.482	0.437
-5.3	2.086	0.377
-4.9	1.560	0.357
-4.2	2.298	0.437
-3.8	2.235	0.433
-3.1	2.412	0.424
-2.7	2.563	0.384
-2.0	3.378	0.346
-1.6	3.421	0.350
-0.9	4.106	0.326
-0.5	3.662	0.314
0.2	4.547	0.303
0.6	4.767	0.315
1.3	4.764	0.303
1.7	4.635	0.325
2.4	4.599	0.396
2.8	5.449	0.375
3.5	4.690	0.442
3.9	5.202	0.350
4.6	4.632	0.426
5.0	5.231	0.421
6.8	4.295	0.431
7.2	4.654	0.416
10.5	3.570	0.444
11.2	4.271	0.439
14.9	3.786	0.441
20.0	3.894	0.439
24.[illegible]	4.565	0.443

N2502_Mg1_270

-7.5	0.085	0.010
-3.4	0.109	0.009
-2.3	0.115	0.009
-1.2	0.116	0.007
-0.1	0.116	0.006
1.0	0.132	0.007
2.1	0.132	0.008
3.2	0.114	0.008
4.3	0.112	0.010
7.6	0.111	0.009

N2502_Mg2_270

-8.2	0.247	0.010
-3.4	0.272	0.009
-2.3	0.267	0.010
-1.2	0.284	0.007
-0.1	0.284	0.007
1.0	0.287	0.007
2.1	0.275	0.009
3.2	0.265	0.009
5.4	0.269	0.009

N2502_NaD 270

-2.3	3.124	0.264
-1.2	3.424	0.274
-0.1	3.558	0.232
1.0	3.730	0.258
2.1	3.010	0.251
4.3	2.502	0.270

N2663_Fe5270_270

-8.3	2.599	0.446
-6.9	2.846	0.301
-3.3	3.088	0.286
-1.8	3.467	0.296
-0.7	3.519	0.234
0.4	3.412	0.226
1.5	3.248	0.269
3.1	3.025	0.264
7.0	2.644	0.286

N2663_Mg1_270

-6.2	0.118	0.008
-5.1	0.115	0.009
-4.0	0.120	0.008
-2.9	0.123	0.006
-1.8	0.135	0.005
-0.7	0.136	0.004
0.4	0.145	0.004
1.5	0.146	0.005
2.6	0.130	0.006
3.7	0.119	0.007
4.8	0.110	0.009
5.9	0.108	0.010
7.0	0.104	0.008
8.1	0.095	0.008
9.2	0.104	0.010

N2663_Mg2_270

-5.1	0.284	0.010
-4.0	0.299	0.008
-2.9	0.300	0.007
-1.8	0.307	0.005
-0.7	0.317	0.004
0.4	0.320	0.004
1.5	0.321	0.005
2.6	0.310	0.006
3.7	0.290	0.008
4.8	0.287	0.009
5.9	0.271	0.008
7.0	0.268	0.008
8.1	0.264	0.009

N2663_NaD_270

-5.1	4.625	0.269
-4.0	4.262	0.298
-2.9	4.901	0.232
-1.8	5.464	0.182
-0.7	5.725	0.146
0.4	5.846	0.140
1.5	5.543	0.177
2.6	5.116	0.214
3.7	4.761	0.277
4.8	4.773	0.235
5.9	4.380	0.266
7.0	3.752	0.277
8.1	3.603	0.298
11.4	3.494	0.286

N2974_Mg1_270

-6.9	0.093	0.008
-5.8	0.090	0.009
-4.7	0.098	0.007
-3.6	0.107	0.006
-2.5	0.109	0.005
-1.4	0.110	0.003
-0.3	0.128	0.003
0.8	0.134	0.003
1.9	0.126	0.004
3.0	0.115	0.005
4.1	0.098	0.007
5.2	0.095	0.008
6.3	0.113	0.010
7.4	0.102	0.009
8.5	0.104	0.010
10.7	0.083	0.009
16.2	0.069	0.010

N2974_Mg2_270

-6.9	0.243	0.008
-5.8	0.264	0.009
-4.7	0.263	0.008
-3.6	0.271	0.006
-2.5	0.272	0.005
-1.4	0.287	0.004
-0.3	0.301	0.003
0.8	0.303	0.003
1.9	0.284	0.005
3.0	0.275	0.006
4.1	0.268	0.007
5.2	0.264	0.009
6.3	0.263	0.008
7.4	0.258	0.009
9.6	0.246	0.009
14.0	0.214	0.010

N2974_NaD_270

-3.6	4.482	0.248
-2.5	4.109	0.210
-1.4	4.730	0.148
-0.3	5.706	0.103
0.8	5.408	0.138
1.9	5.036	0.199
3.0	4.815	0.257
4.1	4.888	0.245
5.2	4.969	0.291
8.5	4.555	0.277

N3078_Fe5270_270

-6.8	2.944	0.310
-3.1	3.486	0.248
-1.6	3.416	0.221
-0.5	3.649	0.164
0.6	3.608	0.167
1.7	3.243	0.234
3.2	3.306	0.261
9.0	2.986	0.309

N3078_Mg1_270

-6.0	0.112	0.008
-4.9	0.129	0.009
-4.1	0.134	0.009
-3.8	0.125	0.007
-3.0	0.136	0.009
-2.7	0.135	0.005
-1.9	0.155	0.007
-1.6	0.146	0.004

-0.8	0.161	0.005
-0.5	0.161	0.003
0.3	0.180	0.004
0.6	0.161	0.003
1.4	0.146	0.006
1.7	0.143	0.004
2.5	0.150	0.008
2.8	0.139	0.005
3.6	0.126	0.008
3.9	0.106	0.007
4.7	0.123	0.010
5.0	0.142	0.009
6.1	0.122	0.008
8.0	0.128	0.010
8.3	0.096	0.009
16.0	0.079	0.010

N3078_Mg1_360

-4.0	0.139	0.008
-2.9	0.150	0.008
-1.8	0.161	0.006
-0.7	0.167	0.005
0.4	0.165	0.005
1.5	0.156	0.006
2.6	0.150	0.007
3.7	0.148	0.009
4.8	0.141	0.009
5.9	0.140	0.010
8.1	0.123	0.010
14.7	0.115	0.010

N3078_Mg2_270

-10.2	0.265	0.010
-10.1	0.241	0.010
-6.0	0.277	0.009
-4.9	0.294	0.009
-4.1	0.278	0.010
-3.8	0.296	0.007
-3.0	0.304	0.010
-2.7	0.307	0.006
-1.9	0.303	0.007
-1.6	0.326	0.004
-0.8	0.317	0.005
-0.5	0.340	0.003
0.3	0.334	0.005
0.6	0.339	0.003
1.4	0.321	0.006
1.7	0.327	0.004
2.5	0.289	0.008
2.8	0.307	0.006
3.6	0.280	0.009
3.9	0.276	0.008

5.0	0.278	0.010
5.8	0.272	0.009
6.1	0.271	0.009
8.3	0.258	0.010
25.6	0.245	0.010
36.9	0.228	0.011

N3078_Mg2_360

-2.9	0.299	0.009
-1.8	0.330	0.007
-0.7	0.336	0.005
0.4	0.338	0.005
1.5	0.330	0.006
2.6	0.312	0.008
3.7	0.304	0.010
4.8	0.295	0.009
7.0	0.287	0.009
12.5	0.271	0.010
41.1	0.261	0.013

N3078_NaD_270

-3.8	4.654	0.250
-2.7	5.209	0.243
-1.9	5.505	0.256
-1.6	5.782	0.171
-0.8	6.539	0.229
-0.5	6.613	0.124
0.3	6.450	0.184
0.6	6.400	0.128
1.4	6.207	0.233
1.7	5.870	0.182
2.5	5.199	0.280
2.8	5.035	0.255
3.9	4.424	0.267
6.1	4.568	0.296
6.9	4.369	0.295

N3078_NaD_360

-1.8	5.842	0.255
-0.7	6.632	0.252
0.4	6.660	0.266
1.5	5.976	0.256
4.8	5.260	0.282

N3100_Mg1_270

-21.1	0.082	0.015

-10.0	0.099	0.010
-6.9	0.105	0.010
-4.0	0.122	0.009
-2.8	0.120	0.008
-1.7	0.146	0.008
-0.7	0.149	0.004
-0.6	0.143	0.006
0.4	0.153	0.004
0.5	0.143	0.006
1.5	0.135	0.005
1.6	0.148	0.007
2.7	0.130	0.008
3.7	0.114	0.009
4.9	0.128	0.009
5.9	0.106	0.009

N3100_Mg1_360

-15.6	0.101	0.010
-11.4	0.101	0.010
-7.0	0.111	0.009
-7.0	0.115	0.010
-4.8	0.120	0.009
-4.2	0.122	0.008
-3.7	0.152	0.010
-3.1	0.150	0.009
-2.6	0.151	0.008
-2.0	0.158	0.007
-1.5	0.155	0.006
-0.9	0.160	0.006
-0.4	0.161	0.005
0.2	0.158	0.005
0.7	0.166	0.005
1.3	0.143	0.006
1.8	0.153	0.007
2.4	0.121	0.008
2.9	0.145	0.010
3.5	0.136	0.010
4.0	0.125	0.009
4.6	0.118	0.008
6.8	0.098	0.009
7.4	0.108	0.010
16.7	0.097	0.010
18.6	0.090	0.010

N3100_Mg2_270

-7.6	0.260	0.010
-4.0	0.269	0.009
-2.9	0.280	0.009
-2.8	0.274	0.009
-1.8	0.273	0.006
-1.7	0.288	0.008
-0.7	0.312	0.004
-0.6	0.298	0.006
0.4	0.320	0.004
0.5	0.301	0.006
1.5	0.297	0.006

1.6	0.291	0.008
2.6	0.289	0.009
2.7	0.271	0.009
3.7	0.252	0.009
4.9	0.245	0.010
7.0	0.257	0.010

N3100_Mg2_360

-11.4	0.235	0.010
-7.0	0.267	0.010
-6.4	0.243	0.010
-4.8	0.267	0.010
-3.7	0.274	0.008
-2.9	0.271	0.009
-2.6	0.291	0.008
-1.8	0.292	0.010
-1.5	0.303	0.007
-0.7	0.300	0.008
-0.4	0.307	0.006
0.4	0.299	0.006
0.7	0.316	0.006
1.5	0.282	0.006
2.6	0.281	0.007
2.9	0.280	0.008
3.7	0.270	0.009
4.8	0.222	0.008
5.7	0.253	0.010
5.9	0.200	0.009
8.1	0.194	0.010
15.0	0.219	0.010

N3100_NaD_270

-2.9	4.160	0.288
-1.8	4.479	0.264
-1.7	5.242	0.258
-0.7	6.052	0.180
-0.6	6.084	0.237
0.4	6.314	0.158
0.5	6.243	0.229
1.5	5.778	0.220
1.6	5.607	0.247
2.6	5.235	0.267
3.8	5.083	0.295

N3100_NaD_360

-8.8	4.161	0.300
-4.8	4.166	0.292
-2.2	4.860	0.258
-1.5	5.122	0.287
-1.1	5.817	0.221
-0.4	5.453	0.234
0.0	6.046	0.206
0.7	6.028	0.268
1.1	6.010	0.234

1.8	5.425	0.266
2.2	5.631	0.234
3.3	4.145	0.284
5.5	3.178	0.296

N3108_Fe5270_270

-14.3	2.498	0.532
-0.8	3.728	0.306
-2.7	3.070	0.302
-0.8	3.728	0.306
0.3	3.860	0.288
1.8	3.327	0.247
12.4	2.794	0.344

N3108_Mg1_270

-8.9	0.099	0.010
-6.0	0.109	0.010
-4.1	0.122	0.010
-3.0	0.138	0.010
-2.6	0.141	0.008
-1.9	0.132	0.007
-1.5	0.141	0.007
-0.8	0.137	0.005
-0.4	0.136	0.006
0.3	0.148	0.005
0.7	0.138	0.007
1.4	0.146	0.006
1.8	0.144	0.009
2.5	0.135	0.007
2.9	0.129	0.008
3.6	0.110	0.009
4.7	0.105	0.009
5.1	0.128	0.009
6.9	0.114	0.009

N3108_Mg1_360

-7.1	0.110	0.010
-6.5	0.118	0.009
-4.3	0.122	0.009
-3.6	0.126	0.008
-3.2	0.129	0.010
-2.5	0.128	0.009
-2.1	0.135	0.007
-1.0	0.151	0.006
-0.3	0.150	0.006
0.1	0.156	0.006
0.8	0.138	0.006
1.2	0.146	0.006
1.9	0.132	0.008
2.3	0.141	0.009
3.0	0.133	0.008
3.4	0.129	0.009
5.2	0.116	0.009
6.9	0.106	0.010

N3108_Mg2_270

-6.7	0.273	0.010
-6.5	0.270	0.010
-3.0	0.302	0.008
-2.6	0.284	0.009
-1.9	0.299	0.008
-1.5	0.306	0.008
-0.8	0.311	0.006
-0.4	0.296	0.006
0.3	0.318	0.005
0.7	0.314	0.007
1.4	0.304	0.006
1.8	0.298	0.009
2.5	0.284	0.008
2.9	0.281	0.009
3.6	0.282	0.010
4.7	0.258	0.009
5.1	0.280	0.010

N3108_Mg2_360

-8.4	0.275	0.010
-7.6	0.270	0.009
-4.3	0.279	0.010
-3.6	0.273	0.009
-3.2	0.274	0.008
-2.5	0.278	0.010
-2.1	0.310	0.008
-1.4	0.314	0.007
-1.0	0.300	0.007
-0.3	0.318	0.006
0.1	0.314	0.006
0.8	0.286	0.007
1.2	0.300	0.007
1.9	0.285	0.008
2.3	0.306	0.010
3.0	0.288	0.009
3.4	0.278	0.010
5.2	0.258	0.010
8.2	0.233	0.010

N3108_NaD_270

-7.5	5.711	0.298
-3.6	5.957	0.274
-1.9	6.451	0.293
-1.5	6.613	0.253
-0.8	6.602	0.202
-0.4	6.764	0.238
0.3	6.670	0.201
0.7	6.367	0.269
1.4	6.156	0.234
1.8	5.675	0.270
2.5	5.197	0.241
3.6	4.926	0.299

4.0	4.855	0.295
6.9	4.689	0.299

N3108_NaD_360

-7.9	4.063	0.297
-3.2	5.537	0.284
-2.5	5.454	0.264
-1.4	6.375	0.245
-1.0	6.147	0.254
-0.3	6.509	0.205
0.1	6.739	0.284
0.8	6.771	0.222
1.2	6.838	0.299
1.9	6.150	0.259
3.6	6.380	0.299
5.2	5.635	0.294

N3136B_Mg1_270

-3.0	0.118	0.010
-1.9	0.134	0.009
-1.9	0.110	0.009
-0.8	0.153	0.008
-0.8	0.143	0.006
0.3	0.142	0.007
0.3	0.146	0.005
1.4	0.154	0.009
1.4	0.141	0.006
2.5	0.119	0.010
4.7	0.107	0.010

N3136B_Mg1_360

-3.5	0.114	0.009
-1.8	0.133	0.009
-0.7	0.148	0.006
0.1	0.151	0.006
1.5	0.135	0.009
2.6	0.124	0.010

N3136B_Mg2_270

-3.6	0.232	0.010
-1.9	0.278	0.010
-1.9	0.251	0.009
-0.8	0.284	0.008
-0.8	0.292	0.006
0.3	0.298	0.008
0.3	0.297	0.005
1.4	0.298	0.010
1.4	0.280	0.007
2.5	0.227	0.009
3.6	0.253	0.010
5.8	0.217	0.010

N3136B_Mg2_360

-3.5	0.247	0.010
-1.8	0.260	0.010
-1.4	0.290	0.009
-0.7	0.298	0.007
-0.3	0.290	0.008
0.4	0.291	0.006
0.8	0.271	0.009
1.5	0.281	0.010
3.7	0.243	0.009

N3136B_NaD_270

-1.9	4.515	0.372
-1.º	3.749	0.287
-0.8	4.381	0.341
-0.8	5.004	0.216
0.3	4.732	0.325
0.3	5.203	0.179
1.4	4.739	0.387
1.4	4.608	0.299
2.5	3.691	0.409
6.9	3.235	0.440

N3136B_NaD_360

-3.6	3.397	0.444
-3.0	2.860	0.294
-0.7	4.858	0.257
-0.3	5.180	0.396
0.4	5.084	0.218
0.8	4.983	0.422
1.5	4.074	0.271
6.2	2.799	0.450
8.1	3.155	0.298

N3136_Mg1_270

-9.3	0.068	0.009
-5.8	0.080	0.008
-4.7	0.094	0.009
-3.6	0.084	0.007
-2.5	0.092	0.005
-1.4	0.107	0.004
-0.3	0.118	0.003
0.8	0.113	0.003
1.9	0.103	0.005
3.0	0.088	0.006
4.1	0.086	0.008
5.2	0.080	0.009
6.3	0.085	0.009
8.5	0.074	0.009
14.0	0.063	0.010

N3136_NaD_270

-7.8	3.666	0.290
-3.6	4.145	0.248
-2.5	5.124	0.241
-1.4	5.953	0.172
-0.3	6.801	0.128
0.8	6.556	0.150
1.9	5.761	0.211
3.0	4.891	0.288
4.1	4.389	0.272
6.3	4.304	0.296

N3226_Mg1_270

-6.3	0.076	0.010
-2.8	0.084	0.008
-1.7	0.106	0.007
-0.6	0.141	0.005
0.5	0.155	0.004
1.6	0.130	0.007
2.7	0.091	0.008
4.9	0.082	0.009
11.5	0.056	0.010

N3226_Mg1_360

-6.2	0.107	0.009
-2.9	0.116	0.009
-1.8	0.130	0.008
-0.7	0.167	0.006
0.4	0.172	0.005
1.5	0.153	0.008
2.6	0.126	0.009
6.8	0.090	0.010

N3226_Mg2_270

-6.9	0.226	0.010
-2.8	0.235	0.008
-1.7	0.268	0.008
-0.6	0.307	0.005
0.5	0.307	0.004
1.6	0.277	0.008
2.7	0.243	0.009
4.9	0.240	0.009
12.6	0.221	0.010

N3226_Mg2_360

-12.8	0.253	0.010
-4.0	0.266	0.009
-1.8	0.278	0.009
-0.7	0.312	0.007
0.4	0.321	0.006
1.5	0.296	0.008

3.3	0.273	0.009
13.2	0.252	0.010

N3226_NaD_270

-7.8	2.727	0.298
-1.7	4.066	0.247
-0.6	5.893	0.186
0.5	6.710	0.159
1.6	5.682	0.253
4.9	4.730	0.293

N3226_NaD_360

-7.3	3.517	0.298
-0.7	5.634	0.295
0.4	6.418	0.254
2.7	4.755	0.288
21.6	1.006	0.475

N3250_Fe5270_270

-8.5	2.902	0.309
-3.2	3.366	0.295
-1.6	3.484	0.295
-0.5	3.459	0.263
0.6	3.748	0.258
2.1	3.514	0.262
7.0	3.260	0.306

N3250_Mg1_270

-4.9	0.132	0.008
-3.8	0.139	0.009
-3.2	0.153	0.008
-2.7	0.127	0.007
-1.6	0.135	0.005
-1.0	0.166	0.008
-0.5	0.146	0.004
0.1	0.153	0.007
0.6	0.149	0.004
1.2	0.155	0.007
1.7	0.140	0.005
2.3	0.155	0.007
2.8	0.140	0.007
3.4	0.136	0.009
3.9	0.107	0.009
4.5	0.136	0.008
5.0	0.125	0.008
7.2	0.124	0.009

N3250_Mg1_360

-5.0	0.144	0.009
-2.8	0.134	0.008

-1.7	0.151	0.006
-0.6	0.158	0.005
0.5	0.156	0.005
1.6	0.147	0.007
2.7	0.137	0.008
4.9	0.137	0.009

N3250_Mg2_270

-8.4	0.287	0.010
-7.3	0.288	0.010
-4.9	0.303	0.009
-3.8	0.308	0.009
-3.2	0.319	0.009
-2.7	0.302	0.007
-2.1	0.320	0.010
-1.6	0.315	0.006
-1.0	0.332	0.008
-0.5	0.328	0.005
0.1	0.322	0.007
0.6	0.328	0.005
1.2	0.310	0.007
1.7	0.318	0.006
2.3	0.307	0.008
2.8	0.312	0.008
3.4	0.292	0.009
3.9	0.289	0.009
4.5	0.296	0.008
5.0	0.302	0.009
6.7	0.288	0.009
7.2	0.295	0.009
12.2	0.265	0.010

N3250_Mg2_360

-7.2	0.298	0.009
-5.0	0.296	0.009
-3.9	0.289	0.008
-2.8	0.308	0.008
-1.7	0.310	0.007
-0.6	0.319	0.006
0.5	0.320	0.006
1.6	0.305	0.007
2.7	0.313	0.009
3.8	0.291	0.008
6.6	0.293	0.010
12.7	0.250	0.010

N3250_NaD_270

-8.0	4.708	0.296
-6.1	4.985	0.284
-3.8	4.788	0.268
-2.7	5.069	0.283
-2.0	5.251	0.244
-1.6	5.555	0.227
-0.9	5.472	0.275

-0.5	6.025	0.177
0.2	6.146	0.262
0.6	5.833	0.175
1.3	5.791	0.292
1.7	5.592	0.224
2.4	5.049	0.298
2.8	5.143	0.286
5.0	4.817	0.273
5.7	4.940	0.294
9.4	4.565	0.299

N3250_NaD_360

-13.8	4.643	0.298
-3.9	4.853	0.292
-1.7	5.224	0.288
-0.6	5.981	0.296
0.5	5.932	0.276
1.6	5.269	0.256
5.7	5.101	0.292
10.1	4.134	0.417

N3260_Mg1_270

-1.7	0.081	0.009
-0.6	0.122	0.008
0.5	0.120	0.008
1.6	0.109	0.009
3.8	0.087	0.010

N3260_Mg2_270

-1.7	0.244	0.009
-0.6	0.299	0.008
0.5	0.293	0.008
1.6	0.268	0.009
4.9	0.239	0.010

N3260_NaD_270

-1.7	3.684	0.386
-0.6	4.963	0.324
0.5	5.207	0.326
1.6	4.110	0.445
2.7	3.841	0.433

N3557_Fe5270_270

-6.9	3.287	0.310
-3.2	3.652	0.254
-1.6	3.638	0.251
-0.5	3.529	0.237
0.6	3.606	0.241
1.7	3.478	0.262
3.2	3.431	0.269

9.2	3.551	0.284

N3557_Mg1_270

-6.0	0.117	0.008
-3.8	0.124	0.007
-2.7	0.127	0.005
-1.6	0.118	0.004
-0.5	0.131	0.004
0.6	0.139	0.004
1.7	0.124	0.004
2.8	0.114	0.006
3.9	0.115	0.007

N3557_Mg1_360

-4.2	0.138	0.008
-3.1	0.132	0.006
-2.0	0.135	0.005
-0.9	0.136	0.005
0.2	0.146	0.004
1.3	0.137	0.005
2.4	0.130	0.006
3.5	0.134	0.007
5.7	0.119	0.008

N3557_Mg2_270

-8.9	0.269	0.010
-6.0	0.281	0.008
-4.9	0.289	0.009
-4.5	0.305	0.009
-3.8	0.305	0.007
-3.4	0.315	0.010
-2.7	0.304	0.006
-1.6	0.313	0.004
-1.2	0.329	0.007
-0.5	0.325	0.004
-0.1	0.320	0.006
0.6	0.324	0.004
1.0	0.325	0.006
1.7	0.316	0.005
2.1	0.308	0.006
2.8	0.310	0.006
3.2	0.295	0.007
3.9	0.286	0.008
4.3	0.292	0.008
5.0	0.291	0.010
5.4	0.288	0.010
6.1	0.291	0.009
6.5	0.285	0.009
8.3	0.284	0.009
8.7	0.283	0.009
13.1	0.285	0.010
13.8	0.268	0.010

N3557_Mg2_360

-13.0	0.277	0.009
-8.6	0.276	0.009
-6.4	0.283	0.009
-5.3	0.279	0.008
-4.2	0.296	0.008
-3.1	0.297	0.007
-2.0	0.306	0.006
-0.9	0.313	0.005
0.2	0.310	0.005
1.3	0.312	0.005
2.4	0.296	0.007
3.5	0.294	0.008
4.6	0.295	0.010
5.7	0.290	0.009
8.6	0.269	0.010
14.6	0.262	0.010
21.6	0.256	0.018

N3557_NaD_270

-9.0	4.164	0.298
-8.4	4.787	0.288
-4.9	4.706	0.291
-3.8	4.965	0.284
-3.6	5.281	0.259
-2.7	5.416	0.228
-2.5	5.634	0.276
-1.6	5.966	0.176
-1.4	6.073	0.234
-0.5	6.337	0.167
-0.3	6.344	0.221
0.6	6.400	0.169
0.8	6.380	0.253
1.7	6.183	0.176
1.9	5.968	0.284
2.8	5.447	0.256
3.0	5.503	0.266
3.9	5.225	0.293
5.2	5.158	0.282
6.1	4.568	0.275
14.0	4.248	0.297
17.1	4.367	0.299

N3557_NaD_360

-13.0	4.647	0.299
-5.3	4.825	0.290
-3.1	5.340	0.286
-2.0	5.982	0.292
-0.9	5.690	0.256
0.2	6.444	0.234
1.3	6.232	0.250
2.4	5.725	0.239
5.9	4.982	0.292
17.6	4.391	0.361

N3706_Fe5270_270

-7.6	2.559	0.444
-5.7	2.976	0.308
-2.3	3.112	0.239
-0.8	3.647	0.231
0.3	3.710	0.208
1.4	3.372	0.257
3.0	3.109	0.286
7.2	3.106	0.309
9.0	2.809	0.442

N3706_Mg1_270

-5.2	0.099	0.010
-4.1	0.124	0.008
-3.5	0.144	0.008
-3.0	0.112	0.007
-2.4	0.160	0.009
-1.9	0.134	0.005
-1.3	0.154	0.007
-0.8	0.154	0.004
-0.2	0.165	0.006
0.3	0.156	0.003
0.9	0.160	0.006
1.4	0.140	0.004
2.0	0.147	0.006
2.5	0.126	0.006
3.1	0.131	0.007
3.6	0.120	0.008
4.2	0.117	0.008
4.7	0.108	0.009
5.3	0.110	0.008
5.8	0.096	0.008
6.4	0.123	0.010
6.9	0.091	0.010
8.6	0.115	0.009
9.1	0.087	0.010
13.1	0.086	0.010
15.8	0.069	0.010

N3706_Mg1_360

-3.4	0.142	0.009
-2.3	0.139	0.007
-1.2	0.166	0.005
-0.1	0.159	0.004
1.0	0.162	0.005
2.1	0.135	0.008
3.2	0.132	0.008
6.6	0.106	0.010
17.6	0.084	0.012

N3706_Mg2_270

-5.2	0.274	0.008
-4.1	0.295	0.009
-3.5	0.309	0.009
-3.0	0.289	0.007
-2.4	0.331	0.010
-1.9	0.312	0.005
-1.3	0.331	0.008
-0.8	0.335	0.004
-0.2	0.333	0.007
0.3	0.339	0.003
0.9	0.329	0.006
1.4	0.322	0.005
2.0	0.327	0.006
2.5	0.307	0.006
3.1	0.309	0.007
3.6	0.273	0.008
4.2	0.287	0.009
4.7	0.296	0.010
5.3	0.272	0.009
5.8	0.266	0.009
7.5	0.282	0.009
8.0	0.268	0.009
11.9	0.247	0.010
13.6	0.242	0.010

N3706_Mg2_360

-3.4	0.287	0.008
-2.3	0.294	0.007
-1.2	0.318	0.005
-0.1	0.329	0.004
1.0	0.321	0.005
2.1	0.294	0.008
3.2	0.285	0.009
7.3	0.245	0.010
18.1	0.200	0.014

N3706_NaD_270

-4.1	3.827	0.264
-3.0	5.155	0.281
-2.5	5.123	0.243
-1.9	5.530	0.235
-1.4	6.251	0.286
-0.8	6.563	0.164
-0.3	6.361	0.258
0.3	6.784	0.142
0.8	6.022	0.265
1.4	6.021	0.171

1.9	5.807	0.214
2.5	5.445	0.256
3.0	5.292	0.265
3.6	5.018	0.259
4.7	4.647	0.290
6.3	4.381	0.281
8.0	4.215	0.295

N3706_NaD_360

-0.1	6.751	0.206
1.0	6.732	0.230
2.7	4.892	0.278
15.6	2.569	0.406

N4374_Fe5270_270

-12.3	3.305	0.308
-7.6	3.260	0.273
-5.0	3.685	0.242
-3.4	3.416	0.277
-2.3	3.447	0.233
-1.2	3.532	0.201
-0.1	3.366	0.206
1.0	3.444	0.196
2.1	3.483	0.228
3.2	3.321	0.269
4.8	3.403	0.269
8.1	3.187	0.281
13.2	3.097	0.302

N4374_Mg1_270

-19.7	0.103	0.009
-15.2	0.146	0.009
-15.0	0.118	0.009
-12.2	0.119	0.009
-10.6	0.133	0.009
-10.0	0.121	0.008
-8.9	0.119	0.009
-7.8	0.128	0.008
-7.7	0.142	0.008
-6.7	0.141	0.007
-6.6	0.151	0.010
-5.6	0.142	0.006
-5.5	0.154	0.009
-4.5	0.139	0.005
-4.4	0.144	0.008
-3.4	0.144	0.005
-3.3	0.154	0.007
-2.3	0.143	0.004
-2.2	0.150	0.006
-1.2	0.152	0.003
-1.1	0.160	0.005
-0.1	0.160	0.003
0.0	0.172	0.005

1993MNRAS.265..553C

1.0	0.157	0.003
1.1	0.155	0.005
2.1	0.151	0.004
2.2	0.149	0.006
3.2	0.143	0.004
3.3	0.159	0.007
4.3	0.154	0.005
4.4	0.145	0.008
5.4	0.147	0.006
5.5	0.134	0.009
6.5	0.144	0.008
6.6	0.138	0.008
7.6	0.146	0.008
7.7	0.120	0.009
8.7	0.135	0.009
8.8	0.118	0.009
9.8	0.128	0.010
10.9	0.125	0.008
11.0	0.117	0.009
12.0	0.117	0.009
14.2	0.106	0.009
14.3	0.119	0.009
17.5	0.125	0.009

N4374_Mg1_360

-14.7	0.134	0.009
-10.3	0.133	0.009
-8.1	0.150	0.010
-7.0	0.153	0.009
-5.9	0.143	0.008
-4.8	0.146	0.009
-3.7	0.152	0.008
-2.6	0.158	0.007
-1.5	0.167	0.006
-0.4	0.162	0.006
0.7	0.167	0.006
1.8	0.156	0.006
2.9	0.152	0.007
4.0	0.159	0.008
5.1	0.135	0.010
6.2	0.140	0.009
9.0	0.138	0.009
13.7	0.139	0.010

N4374_Mg2_270

-19.4	0.252	0.010
-16.8	0.261	0.010
-12.8	0.262	0.009
-12.3	0.273	0.009
-10.0	0.275	0.008
-8.9	0.271	0.009
-8.8	0.278	0.010
-7.8	0.284	0.009
-6.7	0.274	0.008
-6.6	0.284	0.008
-5.6	0.287	0.007

-5.5	0.292	0.009
-4.5	0.293	0.006
-4.4	0.294	0.008
-3.4	0.300	0.005
-3.3	0.293	0.007
-2.3	0.296	0.004
-2.2	0.300	0.006
-1.2	0.304	0.004
-1.1	0.313	0.005
-0.1	0.303	0.003
0.0	0.318	0.005
1.0	0.306	0.003
1.1	0.299	0.005
2.1	0.297	0.004
2.2	0.294	0.006
3.2	0.293	0.005
3.3	0.298	0.007
4.3	0.301	0.006
4.4	0.295	0.009
5.4	0.291	0.007
5.5	0.291	0.010
6.5	0.293	0.008
6.6	0.296	0.008
7.6	0.298	0.009
7.7	0.286	0.009
8.7	0.277	0.007
9.8	0.277	0.008
9.9	0.272	0.009
10.9	0.274	0.009
12.0	0.267	0.010
13.2	0.266	0.009
14.2	0.270	0.009
18.6	0.259	0.009
19.8	0.251	0.009

N4374_Mg2_360

-7.0	0.285	0.010
-5.9	0.295	0.009
-4.8	0.296	0.010
-3.7	0.301	0.009
-2.6	0.308	0.007
-1.5	0.310	0.006
-0.4	0.309	0.006
0.7	0.309	0.006
1.8	0.304	0.007
2.9	0.311	0.008
4.0	0.293	0.009
5.1	0.289	0.008
7.9	0.288	0.009
13.2	0.260	0.010

N4374_NaD_270

-14.8	3.860	0.295
-9.5	4.348	0.270
-9.0	4.360	0.287
-6.7	4.397	0.245

-5.6	4.094	0.280
-5.5	4.226	0.295
-4.5	4.209	0.244
-3.4	4.346	0.213
-3.3	4.686	0.237
-2.3	5.174	0.177
-2.2	5.623	0.259
-1.2	5.279	0.152
-1.1	5.252	0.193
-0.1	5.613	0.141
0.0	5.608	0.208
1.0	5.716	0.148
1.1	5.531	0.198
2.1	5.243	0.169
2.2	5.040	0.251
3.2	4.826	0.202
3.3	4.964	0.299
4.3	4.772	0.238
4.4	3.977	0.265
5.4	4.210	0.285
5.5	4.119	0.275
6.5	4.036	0.250
7.6	4.185	0.283
7.7	4.233	0.268
9.8	4.099	0.272
12.0	4.191	0.300

N4374_NaD_360

-11.4	3.979	0.290
-5.9	4.460	0.269
-3.7	4.270	0.266
-2.6	4.708	0.228
-1.5	3.186	0.221
-0.4	2.727	0.282
0.7	4.935	0.247
1.8	4.930	0.269
2.9	4.075	0.244
5.7	3.931	0.290
13.7	3.386	0.295

N4684_Mg1_270

-4.3	0.034	0.009
-3.2	0.046	0.010
-2.1	0.038	0.007
-1.0	0.063	0.006
0.1	0.062	0.006
1.2	0.066	0.007
2.3	0.058	0.008
3.4	0.044	0.009
4.5	0.045	0.010
7.8	0.042	0.010

N4684_Mg1_360

-7.9	0.019	0.009

-5.7	0.045	0.009
-4.6	0.042	0.008
-3.5	0.042	0.008
-2.4	0.071	0.009
-1.3	0.069	0.007
-0.2	0.090	0.006
0.9	0.088	0.007
2.0	0.057	0.009
3.1	0.054	0.008
5.3	0.058	0.010

N4684_Mg2_270

-7.3	0.150	0.010
-3.2	0.167	0.008
-2.1	0.166	0.008
-1.0	0.165	0.006
0.1	0.139	0.005
1.2	0.157	0.007
2.3	0.169	0.008
3.4	0.158	0.010
5.6	0.161	0.009

N4684_Mg2_360

-6.8	0.162	0.009
-4.6	0.165	0.009
-3.5	0.159	0.008
-2.4	0.168	0.010
-1.3	0.167	0.008
-0.2	0.163	0.007
0.9	0.174	0.007
2.0	0.171	0.010
3.1	0.161	0.009
5.9	0.166	0.009

N4684_NaD_270

-2.1	2.286	0.250
-1.0	3.015	0.288
0.1	3.775	0.263
1.2	3.114	0.239
2.3	2.436	0.285
7.8	2.139	0.297

N4684_NaD_360

-10.1	1.149	0.432
-5.7	1.793	0.400
-3.5	1.916	0.425
-2.4	2.113	0.384
-1.3	2.732	0.340
-0.2	3.445	0.383
0.9	3.586	0.389
2.0	2.887	0.380
4.8	2.474	0.413

9.5	0.640	0.431

N4696_Mg1_225

-1.838	0.140	0.009
0.362	0.138	0.009
1.462	0.142	0.008
3.662	0.121	0.009
8.062	0.127	0.009

N4696_Mg1_270

-2.6	0.135	0.009
-1.5	0.133	0.009
-0.4	0.131	0.008
0.7	0.130	0.008
2.9	0.125	0.009

N4696_Mg1_300

-5.041	0.133	0.009
-1.559	0.130	0.008
1.741	0.140	0.009
3.941	0.122	0.009

N4696_Mg1_330

-1.357	0.129	0.008
-0.257	0.140	0.009
1.943	0.122	0.009
4.143	0.121	0.009

N4696_Mg1_360

-0.7	0.129	0.008
1.5	0.136	0.008
3.7	0.128	0.009

N4696_Mg2_225

-10.868	0.252	0.015
-6.891	0.285	0.015
-4.038	0.286	0.013
-2.938	0.335	0.015
-1.838	0.329	0.012
-0.738	0.308	0.010
0.362	0.322	0.010
1.462	0.323	0.011
2.562	0.306	0.014
3.662	0.290	0.012
4.762	0.304	0.014
6.962	0.308	0.013
10.262	0.280	0.014

N4696_Mg2_270

-6.7	0.307	0.010
-2.6	0.314	0.009
-1.5	0.315	0.009
-0.4	0.319	0.008
0.7	0.322	0.009
1.8	0.321	0.008
2.9	0.314	0.009
5.1	0.311	0.010
10.6	0.322	0.010

N4696_Mg2_300

-10.571	0.321	0.014
-6.604	0.322	0.013
-3.759	0.330	0.013
-2.659	0.299	0.014
-1.559	0.315	0.012
-0.459	0.311	0.010
0.641	0.341	0.011
1.741	0.315	0.012
2.841	0.343	0.014
3.941	0.292	0.013
5.042	0.297	0.015
7.241	0.311	0.014
10.541	0.340	0.015

N4696_Mg2_330

-5.531	0.306	0.009
-1.357	0.319	0.008
-0.257	0.316	0.010
0.843	0.330	0.008
1.943	0.319	0.010
5.243	0.300	0.009

N4696_Mg2_360

-11.5	0.265	0.014
-6.9	0.283	0.014
-1.8	0.309	0.013
-0.7	0.324	0.011
0.4	0.310	0.011
1.5	0.326	0.012
2.6	0.315	0.014
3.7	0.302	0.013
4.8	0.309	0.015
7.0	0.317	0.015
10.3	0.299	0.015
16.9	0.284	0.014

N4696_NaD_225

-15.617	4.231	0.445

1993MNRAS.265..553C

-5.965	5.556	0.426
-1.838	5.394	0.393
-0.738	5.435	0.443
0.362	6.078	0.385
1.462	5.225	0.379
3.662	5.281	0.391
6.962	4.401	0.449
15.762	3.897	0.448

N4696_NaD_270

-7.2	5.094	0.429
-3.7	5.529	0.424
-2.6	5.446	0.437
-1.5	5.472	0.355
-0.4	5.692	0.312
0.7	5.623	0.358
1.8	5.921	0.370
2.9	5.701	0.347
4.0	5.684	0.409
6.2	5.293	0.371
10.6	4.957	0.425

N4696_NaD_300

-25.853	5.100	0.449
-9.709	5.309	0.437
-4.402	5.465	0.410
-1.559	5.640	0.362
-0.459	5.604	0.389
0.641	6.020	0.395
1.741	5.644	0.346
2.841	5.321	0.404
5.041	5.656	0.440
9.441	5.428	0.401
18.241	5.237	0.437
27.042	4.927	0.662

N4696_NaD_330

-13.065	5.262	0.435
-5.968	5.458	0.425
-2.457	5.862	0.397
-1.357	5.416	0.409
-0.257	6.056	0.376
0.843	6.242	0.398
1.943	5.889	0.404
4.143	5.446	0.418
9.642	5.317	0.444

N4696_NaD_360

-8.2	4.646	0.424
-3.6	5.642	0.368
-0.7	5.773	0.344
0.4	5.745	0.440

1.5	5.783	0.434
2.6	5.869	0.390
4.8	5.197	0.437
9.2	4.712	0.441

N4832_Mg1_360

-7.1	0.068	0.010
-3.8	0.071	0.009
-2.7	0.082	0.009
-1.6	0.100	0.007
-0.5	0.111	0.005
0.6	0.099	0.005
1.7	0.095	0.008
2.8	0.086	0.009
7.6	0.081	0.010

N4832_Mg2_360

-4.9	0.200	0.009
-2.7	0.226	0.010
-1.6	0.237	0.007
-0.5	0.253	0.006
0.6	0.244	0.006
1.7	0.224	0.009
2.8	0.216	0.009
8.9	0.193	0.010

N5011_Mg1_270

-9.4	0.107	0.010
-8.7	0.122	0.010
-4.6	0.111	0.009
-4.0	0.122	0.010
-3.5	0.130	0.009
-2.9	0.136	0.010
-2.4	0.114	0.006
-1.8	0.137	0.008
-1.3	0.125	0.005
-0.7	0.139	0.006
-0.2	0.134	0.004
0.4	0.137	0.006
0.9	0.136	0.004
1.5	0.130	0.007
2.0	0.122	0.006
2.6	0.130	0.009
3.1	0.119	0.008
4.2	0.113	0.008
5.9	0.120	0.009
6.4	0.107	0.009
14.7	0.101	0.010

N5011_Mg2_270

-10.7	0.265	0.010
-5.9	0.285	0.010

-4.6	0.271	0.009
-3.5	0.279	0.009
-2.4	0.287	0.007
-1.8	0.307	0.008
-1.3	0.299	0.005
-0.7	0.323	0.008
-0.2	0.309	0.004
0.4	0.312	0.007
0.9	0.306	0.004
1.5	0.310	0.006
2.0	0.291	0.006
2.6	0.311	0.008
3.1	0.298	0.009
3.7	0.298	0.010
4.2	0.249	0.009
4.8	0.280	0.009
6.4	0.263	0.010
8.1	0.252	0.009

N5011_NaD_270

-6.5	4.339	0.295
-3.5	4.486	0.246
-2.4	4.900	0.270
-1.8	4.574	0.264
-1.3	5.022	0.201
-0.7	5.209	0.270
-0.2	5.329	0.146
0.4	5.439	0.259
0.9	5.012	0.174
1.5	4.776	0.242
2.0	5.010	0.252
3.1	4.818	0.274
3.7	4.462	0.256
6.4	4.725	0.285

N5044_Mg1_270

-13.4	0.134	0.010
-7.1	0.156	0.010
-6.1	0.149	0.009
-3.6	0.148	0.010
-3.2	0.153	0.008
-2.1	0.136	0.009
-1.4	0.163	0.008
-1.0	0.153	0.008
-0.3	0.164	0.009
0.1	0.160	0.007
0.8	0.154	0.010
1.2	0.153	0.008
1.9	0.169	0.008
2.3	0.154	0.009
3.0	0.159	0.009
3.4	0.139	0.008
4.5	0.127	0.009
5.2	0.146	0.009
6.7	0.136	0.009
9.6	0.132	0.010

11.1	0.133	0.010

N5044_Mg1_360

-13.0	0.139	0.010
-7.1	0.168	0.010
-4.2	0.162	0.009
-2.0	0.165	0.008
-0.9	0.149	0.009
0.2	0.151	0.009
1.3	0.148	0.010
2.4	0.148	0.008
3.5	0.141	0.009
4.6	0 142	0.010
6.8	0.140	0.010
11.2	0.124	0.010

N5044_Mg2_270

-10.8	0.349	0.010
-6.1	0.303	0.010
-4.2	0.325	0.009
-3.2	0.320	0.008
-2.1	0.319	0.009
-1.4	0.343	0.008
-1.0	0.316	0.008
-0.3	0.312	0.010
0.1	0.313	0.007
0.8	0.315	0.008
1.2	0.317	0.008
1.9	0.322	0.009
2.3	0.334	0.009
3.0	0.331	0.009
3.4	0.299	0.008
4.5	0.296	0.009
5.2	0.321	0.009
6.7	0.304	0.009
10.7	0.303	0.010

N5044_Mg2_360

-10.1	0.328	0.010
-8.3	0.309	0.013
-6.1	0.300	0.014
-5.0	0.325	0.013
-4.9	0.319	0.009
-3.9	0.319	0.012
-2.8	0.318	0.014
-2.0	0.343	0.008
-1.7	0.315	0.013
-0.9	0.321	0.010
-0.6	0.329	0.012
0.2	0.300	0.010
0.5	0.304	0.012
1.3	0.321	0.008
1.6	0.314	0.013
2.4	0.327	0.009

2.7	0.320	0.014
3.5	0.319	0.010
3.8	0.329	0.012
5.7	0.309	0.009
6.0	0.322	0.015
9.5	0.316	0.014
10.1	0.295	0.010

N5044_NaD_270

-13.9	5.303	0.441
-9.8	4.960	0.410
-7.3	5.284	0.412
-6.3	5.101	0.364
-5.2	5.277	0.409
-4.5	5.910	0.392
-4.1	5.214	0.410
-3.4	5.678	0.350
-3.0	5.596	0.353
-2.3	5.975	0.382
-1.9	6.375	0.329
-1.2	6.169	0.450
-0.8	6.320	0.358
-0.1	6.210	0.327
0.3	6.711	0.429
1.0	6.383	0.362
1.4	5.762	0.420
2.5	5.075	0.421
3.2	6.116	0.399
4.7	5.271	0.417
7.6	4.813	0.439
8.0	4.846	0.447

N5044_NaD_360

-7.9	5.732	0.437
-4.4	6.055	0.447
-2.2	6.008	0.359
-1.1	6.360	0.420
0.0	6.006	0.400
1.1	5.815	0.329
2.2	5.741	0.319
3.3	6.678	0.376
4.4	5.397	0.430
5.5	5.417	0.365
6.6	4.949	0.404
8.8	4.861	0.394
12.1	4.849	0.425

N5077_Fe5270_270

-11.6	2.850	0.410
-1.5	3.125	0.259
0.0	3.344	0.261
1.1	3.248	0.297
3.7	3.118	0.301
15.0	2.730	0.558

N5077_Mg1_270

-4.4	0.100	0.009
-3.3	0.119	0.009
-2.2	0.129	0.007
-1.1	0.142	0.005
0.0	0.146	0.004
1.1	0.147	0.004
2.2	0.130	0.006
3.3	0.120	0.009
4.4	0.101	0.009
7.7	0.097	0.009

N5077_Mg1_360

-11.1	0.096	0.010
-6.7	0.113	0.009
-4.5	0.120	0.009
-3.4	0.140	0.010
-2.3	0.156	0.008
-1.2	0.150	0.007
-0.1	0.161	0.006
1.0	0.153	0.006
2.1	0.143	0.008
3.2	0.144	0.010
4.3	0.127	0.009
7.2	0.116	0.010

N5077_Mg2_270

-4.4	0.275	0.010
-3.3	0.297	0.010
-2.2	0.295	0.007
-1.1	0.318	0.005
0.0	0.328	0.004
1.1	0.324	0.005
2.2	0.305	0.007
3.3	0.302	0.009
4.4	0.275	0.009
7.7	0.270	0.010

N5077_Mg2_360

-6.7	0.272	0.010
-4.5	0.283	0.010
-3.4	0.299	0.008
-2.3	0.307	0.008
-1.2	0.320	0.007
-0.1	0.317	0.007
1.0	0.312	0.007
2.1	0.296	0.009
3.2	0.285	0.008
6.1	0.289	0.010

N5077_NaD_270

-3.3	4.856	0.292
-2.2	5.700	0.273
-1.1	6.035	0.192
0.0	6.770	0.181
1.1	6.674	0.214
2.2	6.128	0.299
4.4	5.467	0.290

N5077_NaD_360

-3.4	5.902	0.273
-1.2	6.420	0.244
-0.1	6.242	0.279
1.0	6.005	0.237
4.5	4.663	0.292
17.3	3.823	0.420

N5090_Fe5270_270

-7.9	2.470	0.465
-3.9	3.005	0.445
-2.3	3.417	0.412
-1.2	3.014	0.350
-0.1	3.537	0.360
1.0	3.382	0.373
2.1	2.935	0.424
3.7	3.174	0.407
9.1	3.174	0.464

N5090_Mg1_270

-8.0	0.123	0.010
-5.7	0.160	0.009
-4.5	0.129	0.009
-3.4	0.129	0.009
-2.3	0.142	0.008
-2.3	0.153	0.008
-1.2	0.155	0.006
-1.2	0.141	0.009
-0.1	0.158	0.006
-0.1	0.161	0.009
1.0	0.151	0.006
1.0	0.167	0.009
2.1	0.142	0.007
2.1	0.150	0.008
3.2	0.132	0.009
3.2	0.152	0.010
4.3	0.138	0.008
6.5	0.134	0.009
6.5	0.146	0.009

N5090_Mg1_360

-6.2	0.160	0.010

-5.9	0.149	0.010
-2.4	0.154	0.008
-1.6	0.157	0.009
-1.3	0.153	0.008
-0.2	0.161	0.008
0.6	0.154	0.008
0.9	0.156	0.008
1.7	0.140	0.009
2.0	0.155	0.009
2.8	0.147	0.008
3.1	0.156	0.009
5.0	0.143	0.009
5.3	0.156	0.009

N5090_Mg2_270

-6.9	0.299	0.009
-5.8	0.319	0.010
-3.4	0.314	0.008
-2.3	0.332	0.008
-2.3	0.333	0.009
-1.2	0.338	0.007
-1.2	0.320	0.010
-0.1	0.336	0.006
-0.1	0.326	0.009
1.0	0.345	0.007
1.0	0.328	0.010
2.1	0.336	0.008
2.1	0.316	0.008
3.2	0.316	0.009
4.3	0.319	0.009
4.3	0.319	0.009
6.5	0.321	0.010

N5090_Mg2_360

-6.6	0.313	0.010
-5.3	0.315	0.010
-3.1	0.342	0.009
-2.0	0.314	0.009
-1.2	0.343	0.009
-0.9	0.332	0.008
0.2	0.321	0.008
1.0	0.322	0.009
1.3	0.324	0.009
2.4	0.315	0.009
3.2	0.322	0.010
4.3	0.307	0.009
6.6	0.293	0.010
7.6	0.299	0.010

N5090_NaD_270

-6.9	5.363	0.440
-6.4	5.786	0.299
-3.4	5.368	0.406
-2.3	6.169	0.255

-2.3	5.971	0.410
-1.2	6.065	0.276
-1.2	5.969	0.387
-0.1	6.036	0.261
-0.1	5.995	0.367
1.0	5.834	0.252
1.0	6.353	0.385
2.1	5.882	0.289
2.1	5.754	0.405
3.2	6.054	0.279
3.2	5.619	0.375
5.4	5.542	0.404
7.6	5.089	0.295
10.9	4.139	0.432

N5090_NaD_360

-7.8	4.673	0.449
-2.4	5.806	0.399
-1.6	6.150	0.275
-1.3	6.105	0.428
-0.5	6.148	0.296
0.6	5.908	0.251
0.9	6.141	0.326
0.9	6.127	0.426
1.7	5.689	0.296
2.0	5.991	0.394
4.2	5.543	0.437
7.2	5.072	0.293

N5266_Fe5270_270

-5.0	3.214	0.309
-2.3	3.615	0.265
-0.8	3.435	0.260
0.3	3.667	0.245
1.4	3.298	0.281
2.9	3.159	0.307
9.3	2.826	0.307

N5266_Mg1_270

-6.3	0.074	0.008
-5.2	0.100	0.009
-4.1	0.088	0.008
-3.8	0.103	0.008
-3.0	0.100	0.007
-2.7	0.130	0.009
-1.9	0.114	0.006
-1.6	0.126	0.007
-0.8	0.139	0.004
-0.5	0.135	0.005
0.3	0.139	0.004
0.6	0.147	0.006
1.4	0.121	0.005
1.7	0.119	0.007
2.8	0.128	0.010

3.6	0.113	0.009
4.7	0.091	0.010
6.1	0.113	0.009
6.9	0.090	0.009
9.1	0.071	0.009
9.4	0.085	0.009

N5266_Mg1_360

-8.9	0.087	0.010
-3.5	0.099	0.009
-2.9	0.112	0.009
-2.4	0.112	0.008
-1.8	0.126	0.009
-1.3	0.126	0.006
-0.7	0.136	0.007
-0.2	0.137	0.005
0.4	0.147	0.005
0.9	0.142	0.006
1.5	0.119	0.005
2.0	0.111	0.007
2.6	0.106	0.007
3.1	0.114	0.009
3.7	0.105	0.009
4.2	0.113	0.009
4.8	0.101	0.009
7.0	0.086	0.010

N5266_Mg2_270

-7.4	0.219	0.010
-6.6	0.239	0.009
-5.2	0.228	0.008
-4.1	0.244	0.009
-3.8	0.248	0.008
-3.0	0.259	0.007
-2.7	0.284	0.009
-1.9	0.274	0.006
-1.6	0.289	0.008
-0.8	0.288	0.005
-0.5	0.286	0.006
0.3	0.297	0.004
0.6	0.292	0.006
1.4	0.286	0.005
1.7	0.269	0.008
2.5	0.244	0.007
2.8	0.258	0.009
3.6	0.248	0.010
5.8	0.208	0.009
6.1	0.236	0.009
8.0	0.242	0.009
9.4	0.220	0.010

N5266_Mg2_360

-20.7	0.132	0.025
-10.9	0.198	0.010

-7.4	0.219	0.010
-3.5	0.232	0.009
-2.7	0.255	0.009
-[illegible].4	0.264	0.009
-[illegible].6	0.287	0.010
-1.3	0.269	0.007
-0.5	0.284	0.008
-0.2	0.282	0.005
0.6	0.272	0.006
0.9	0.285	0.006
1.7	0.255	0.006
2.0	0.255	0.008
2.8	0.241	0.007
3.1	0.251	0.010
3.9	0.239	0.010
4.2	0.247	0.010
5.0	0.232	0.010
7.5	0.221	0.010
9.4	0.196	0.010

N5266_NaD_270

-6.9	4.415	0.284
-6.8	4.057	0.285
-4.1	4.795	0.249
-3.0	4.928	0.278
-2.7	5.322	0.284
-1.9	5.814	0.222
-1.6	6.145	0.273
-0.8	6.676	0.172
-0.5	6.942	0.208
0.3	7.458	0.168
0.6	7.214	0.235
1.4	6.679	0.208
1.7	6.896	0.272
2.5	6.338	0.252
2.8	5.797	0.297
4.7	4.570	0.277
7.2	3.653	0.294
9.1	3.826	0.292

N5266_NaD_360

-16.0	2.926	0.458
-9.6	3.552	0.299
-3.1	5.254	0.292
-2.9	4.830	0.292
-1.8	5.375	0.275
-1.3	6.446	0.283
-0.7	7.022	0.198
-0.2	7.256	0.244
0.4	7.007	0.183
0.9	6.272	0.249
1.5	6.018	0.249
2.6	5.035	0.282
3.1	5.164	0.292
7.0	4.103	0.396

N5796_Fe5270_270

-7.0	2.955	0.448
-3.2	3.231	0.389
-1.6	3.454	0.356
-0.5	3.628	0.233
0.6	3.449	0.231
1.7	3.224	0.327
2.8	3.207	0.459
4.3	3.197	0.428
11.9	2.832	0.459

N5796_Mg1_270

-7.6	0.156	0.010
-4.9	0.140	0.010
-3.8	0.140	0.010
-2.8	0.167	0.009
-2.7	0.144	0.007
-1.7	0.166	0.009
-1.6	0.156	0.005
-0.6	0.176	0.007
-0.5	0.156	0.004
0.5	0.170	0.006
0.6	0.163	0.004
1.6	0.171	0.006
1.7	0.145	0.006
2.7	0.150	0.007
2.8	0.143	0.008
3.8	0.148	0.010
3.9	0.135	0.008
4.9	0.155	0.009
5.0	0.140	0.010
8.2	0.129	0.009
8.3	0.133	0.010

N5796_Mg2_270

-9.9	0.284	0.010
-8.6	0.287	0.010
-3.8	0.333	0.010
-3.8	0.317	0.008
-2.7	0.321	0.008
-1.6	0.345	0.007
-1.6	0.336	0.006
-0.5	0.352	0.006
-0.5	0.343	0.004
0.6	0.340	0.006
0.6	0.340	0.004
1.7	0.335	0.008
1.7	0.333	0.006
2.8	0.313	0.008
2.8	0.319	0.008
3.9	0.304	0.008
5.0	0.318	0.009
6.1	0.298	0.009
11.6	0.286	0.010

N5796_NaD_270

-8.2	5.285	0.271
-2.7	5.365	0.273
-1.6	6.044	0.260
-1.6	5.924	0.253
-0.5	6.625	0.253
-0.5	6.558	0.172
0.6	6.755	0.220
0.6	6.568	0.152
1.7	6.149	0.285
1.7	6.340	0.244
2.8	5.585	0.265
3.9	5.476	0.281
5.0	5.125	0.284

N5846_Fe5270_270

-26.3	2.500	0.321
-12.7	2.995	0.252
-8.0	3.135	0.228
-5.3	2.937	0.208
-3.7	3.288	0.241
-2.6	3.100	0.199
-1.5	3.415	0.168
-0.4	3.262	0.151
0.7	3.162	0.146
1.8	3.282	0.159
2.9	3.088	0.201
4.0	3.055	0.242
7.8	3.124	0.258
12.1	2.891	0.238
25.6	2.459	0.308

N5846_Mg1_270

-12.5	0.153	0.008
-14.7	0.146	0.009
-17.5	0.145	0.009
-11.4	0.136	0.009
-10.3	0.168	0.008
-9.2	0.183	0.008
-8.1	0.172	0.007
-7.0	0.172	0.006
-5.9	0.165	0.005
-4.8	0.179	0.005
-3.7	0.181	0.004
-2.6	0.175	0.003
-1.5	0.173	0.003
-0.4	0.179	0.003
0.7	0.180	0.002
1.8	0.172	0.003
2.9	0.168	0.003
4.0	0.173	0.004
5.1	0.166	0.004
6.2	0.169	0.005

7.3	0.163	0.006
8.4	0.178	0.006
9.5	0.169	0.007
10.6	0.168	0.008
11.7	0.173	0.009
12.8	0.177	0.010
13.9	0.185	0.008
15.0	0.179	0.009
16.1	0.153	0.009
18.3	0.171	0.009
20.5	0.150	0.010
24.9	0.135	0.009

N5846_Mg1_360

-17.4	0.156	0.010
-10.8	0.163	0.009
-7.5	0.163	0.009
-7.2	0.177	0.009
-5.3	0.160	0.009
-4.3	0.182	0.008
-4.2	0.154	0.008
-3.2	0.187	0.009
-3.1	0.156	0.009
-2.1	0.158	0.007
-2.0	0.168	0.007
-1.0	0.177	0.006
-0.9	0.171	0.006
0.1	0.175	0.006
0.2	0.173	0.006
1.2	0.159	0.006
1.3	0.173	0.007
2.3	0.175	0.008
2.4	0.168	0.008
3.4	0.166	0.009
3.5	0.146	0.010
4.5	0.170	0.008
4.6	0.155	0.008
5.6	0.172	0.009
7.4	0.159	0.009
7.8	0.154	0.009
12.1	0.149	0.010
19.6	0.168	0.012

N5846_Mg2_270

-12.5	0.319	0.008
-14.7	0.320	0.009
-17.5	0.317	0.009
-22.2	0.319	0.009
-11.4	0.311	0.010
-10.3	0.324	0.009
-9.2	0.306	0.008
-8.1	0.328	0.007
-7.0	0.314	0.006
-5.9	0.324	0.006
-4.8	0.334	0.005
-3.7	0.321	0.004

-2.6	0.331	0.004
-1.5	0.332	0.003
-0.4	0.334	0.003
0.7	0.334	0.003
1.8	0.324	0.003
2.9	0.322	0.003
4.0	0.328	0.004
5.1	0.333	0.005
6.2	0.323	0.005
7.3	0.331	0.006
8.4	0.322	0.007
9.5	0.315	0.008
10.6	0.318	0.009
11.7	0.318	0.009
12.8	0.320	0.008
13.9	0.337	0.009
15.0	0.346	0.009
17.2	0.312	0.008
19.4	0.323	0.010
23.8	0.316	0.009

N5846_Mg2_360

-27.3	0.325	0.010
-11.9	0.316	0.009
-7.5	0.317	0.009
-6.1	0.331	0.009
-5.3	0.306	0.010
-4.2	0.317	0.008
-3.2	0.340	0.008
-3.1	0.321	0.010
-2.1	0.324	0.008
-2.0	0.322	0.008
-1.0	0.317	0.007
-0.9	0.336	0.007
0.1	0.305	0.006
0.2	0.335	0.007
1.2	0.306	0.007
1.3	0.335	0.007
2.3	0.327	0.008
2.4	0.338	0.009
3.4	0.315	0.008
3.5	0.313	0.008
4.5	0.320	0.009
5.6	0.314	0.010
6.3	0.312	0.009
11.0	0.327	0.010
19.2	0.349	0.011

N5846_NaD_270

-10.3	5.346	0.241
-12.5	5.248	0.296
-15.3	5.454	0.297
-20.0	4.899	0.295
-9.2	5.148	0.291
-8.1	5.518	0.258
-7.0	5.641	0.232

1993MNRAS.265..553C

-5.9	5.627	0.205
-4.8	5.670	0.181
-3.7	5.873	0.153
-2.6	5.780	0.128
-1.5	5.848	0.110
-0.4	5.935	0.101
0.7	5.853	0.103
1.8	5.823	0.115
2.9	5.747	0.135
4.0	5.863	0.144
5.1	5.778	0.189
6.2	5.703	0.216
7.3	5.497	0.240
8.4	5.732	0.276
9.5	5.580	0.226
10.6	5.368	0.250
11.7	5.529	0.274
13.9	5.200	0.258
17.2	5.249	0.272
22.7	5.269	0.295

N5846_NaD_360

-3.2	5.684	0.266
-6.7	5.580	0.276
-2.1	6.008	0.278
-1.0	5.728	0.230
0.1	5.772	0.247
1.2	5.891	0.238
3.4	5.639	0.281
5.6	5.558	0.283
10.0	5.506	0.300

N5903_Mg1_270

-3.9	0.107	0.010
-2.9	0.134	0.009
-2.8	0.100	0.009
-1.8	0.133	0.009
-1.7	0.120	0.007
-0.7	0.142	0.007
-0.6	0.141	0.005
0.4	0.146	0.007
0.5	0.140	0.005
1.5	0.126	0.008
1.6	0.118	0.006
2.6	0.110	0.008
2.7	0.117	0.009
3.8	0.106	0.009
4.8	0.113	0.009
7.1	0.104	0.010

N5903_Mg2_270

-4.5	0.253	0.009
-2.8	0.266	0.010
-1.9	0.297	0.010

-1.7	0.282	0.007
-0.8	0.288	0.009
-0.6	0.301	0.005
0.3	0.310	0.008
0.5	0.303	0.005
1.4	0.306	0.008
1.6	0.296	0.007
2.5	0.294	0.009
2.7	0.282	0.010
3.6	0.270	0.009
4.9	0.247	0.009

N5903_NaD_270

-7.1	3.324	0.431
-2.9	4.070	0.379
-1.8	5.059	0.375
-1.7	4.641	0.262
-0.7	4.838	0.331
-0.6	5.323	0.232
0.4	5.241	0.318
0.5	5.207	0.228
1.5	4.699	0.360
1.6	4.713	0.298
2.6	4.295	0.370
4.8	3.843	0.424
4.9	3.523	0.293

N6849_Mg1_270

-8.5	0.100	0.010
-2.0	0.117	0.007
-1.1	0.143	0.009
-0.9	0.122	0.005
0.0	0.123	0.009
0.2	0.137	0.005
1.3	0.125	0.005
2.4	0.094	0.007
3.5	0.084	0.009
5.7	0.069	0.010

N6849_Mg1_360

-3.3	0.111	0.009
-1.6	0.138	0.010
-0.5	0.123	0.008
0.6	0.119	0.008
1.7	0.102	0.009
3.9	0.102	0.009

N6849_Mg2_270

-30.4	0.454	0.025
-18.0	0.200	0.011
-6.6	0.247	0.015
-3.1	0.244	0.009

-2.0	0.273	0.008
-1.8	0.267	0.012
-0.9	0.268	0.006
-0.7	0.284	0.012
0.2	0.281	0.005
0.4	0.265	0.010
1.3	0.282	0.006
1.5	0.258	0.012
2.4	0.255	0.008
2.6	0.259	0.013
3.5	0.233	0.009
6.8	0.213	0.010

N6849_Mg2_360

-8.6	0.234	0.010
-1.2	0.258	0.009
-0.1	0.288	0.009
1.0	0.251	0.009
2.1	0.229	0.009

N6849_NaD_360

-8.3	2.980	0.449
-1.6	4.676	0.387
-0.5	4.985	0.361
0.6	4.843	0.352
1.7	4.180	0.388
3.9	3.266	0.438
6.1	1.757	0.368

N6868_Fe5270_270

-20.9	2.823	0.431
-8.7	2.997	0.247
-5.2	3.356	0.239
-2.5	3.224	0.209
-1.4	3.545	0.178
-0.3	3.503	0.162
0.8	4.094	0.166
1.9	3.615	0.188
3.0	3.146	0.216
4.5	2.952	0.209
8.3	3.078	0.244
20.6	2.890	0.312

N6868_Mg1_270

-8.9	0.150	0.010
-6.9	0.172	0.008
-6.0	0.157	0.009
-5.8	0.163	0.006
-4.9	0.166	0.010
-4.7	0.164	0.005
-3.8	0.156	0.008
-3.6	0.169	0.004

-2.7	0.160	0.007
-2.5	0.153	0.004
-1.6	0.166	0.006
-1.4	0.160	0.003
-0.5	0.173	0.006
-0.3	0.172	0.003
0.6	0.162	0.006
0.8	0.161	0.003
1.7	0.158	0.007
1.9	0.172	0.003
2.8	0.154	0.008
3.0	0.160	0.004
3.9	0.157	0.009
4.1	0.155	0.005
5.0	0.153	0.008
5.2	0.161	0.006
6.1	0.149	0.009
6.3	0.163	0.007
7.4	0.146	0.008
8.3	0.143	0.009
9.6	0.161	0.008

N6868_Mg1_360

-2.3	0.171	0.006
-1.2	0.168	0.005
-0.1	0.158	0.005
1.0	0.161	0.005
2.1	0.152	0.006
3.2	0.161	0.008

N6868_Mg2_270

-14.9	0.275	0.009
-11.3	0.274	0.010
-9.1	0.295	0.008
-8.0	0.301	0.009
-6.9	0.293	0.008
-5.8	0.301	0.007
-4.7	0.303	0.006
-3.6	0.324	0.005
-2.7	0.334	0.008
-2.5	0.319	0.004
-1.6	0.331	0.007
-1.4	0.318	0.003
-0.5	0.325	0.006
-0.3	0.332	0.003
0.6	0.326	0.006
0.8	0.322	0.003
1.7	0.318	0.007
1.9	0.325	0.003
3.0	0.316	0.004
4.1	0.306	0.005
5.2	0.300	0.006
6.3	0.298	0.007

N6868_Mg2_360

-6.3	0.321	0.010
-3.5	0.317	0.008
-2.4	0.331	0.009
-1.3	0.317	0.007
-0.2	0.318	0.006
2.0	0.312	0.006
3.1	0.309	0.007
4.2	0.303	0.009
6.4	0.289	0.010
8.6	0.282	0.010

N6868_NaD_270

-16.9	4.800	0.290
-10.9	4.762	0.266
-8.0	4.781	0.252
-6.9	5.029	0.285
-5.8	5.391	0.230
-5.6	4.714	0.283
-4.7	5.208	0.192
-3.6	5.418	0.172
-2.7	5.183	0.253
-2.5	5.679	0.138
-1.6	5.534	0.276
-1.4	5.945	0.120
-0.5	5.653	0.248
-0.3	6.027	0.110
0.6	5.977	0.249
0.8	6.278	0.112
1.7	5.936	0.277
1.9	6.152	0.126
2.8	5.968	0.297
3.0	5.596	0.151
3.9	5.671	0.296
4.1	5.539	0.182
5.2	5.459	0.224
6.3	5.043	0.270
7.2	5.400	0.281
8.5	5.062	0.274
10.7	4.955	0.272
14.0	5.353	0.291
21.7	4.780	0.231
22.8	5.035	0.275
23.7	4.977	0.298

N6868_NaD_360

-3.4	5.008	0.296
-10.1	5.265	0.296
-2.3	5.134	0.298
-1.2	5 689	0.215
-0.1	5.780	0.195
1.0	6.229	0.232
2.1	6.678	0.252
3.2	5.610	0.261
5.4	5.431	0.287

N7097_Fe5270_270

-13.9	1.653	0.431
-3.9	2.490	0.250
-2.0	3.048	0.248
-0.9	2.969	0.190
0.2	3.199	0.157
1.3	3.057	0.168
2.4	3.160	0.233
5.5	2.558	0.246
12.7	1.667	0.449

N7097_Mg1_270

-10.0	0.110	0.010
-9.9	0.087	0.010
-6.4	0.106	0.009
-5.3	0.118	0.009
-4.2	0.129	0.007
-4.0	0.136	0.010
-3.1	0.135	0.006
-2.9	0.151	0.010
-2.0	0.155	0.004
-1.8	0.163	0.007
-0.9	0.162	0.003
-0.7	0.185	0.005
0.2	0.180	0.003
0.4	0.166	0.006
1.3	0.165	0.003
1.5	0.161	0.007
2.4	0.143	0.004
2.6	0.136	0.010
3.5	0.126	0.006
4.6	0.121	0.008
4.8	0.109	0.009
5.7	0.089	0.010
6.8	0.079	0.009
9.0	0.098	0.010

N7097_Mg1_360

-4.0	0.131	0.008
-6.8	0.129	0.010
-14.1	0.083	0.010
-2.9	0.144	0.009
-1.8	0.170	0.006
-0.7	0.156	0.005
0.4	0.160	0.004
1.5	0.144	0.006
2.6	0.133	0.008
3.7	0.115	0.008
4.8	0.107	0.010
7.0	0.092	0.009
12.5	[illegible]	0.010

N7097_Mg2_270

-25.7	0.148	0.013
-8.1	0.231	0.010
-7.0	0.239	0.010
-5.3	0.230	0.008
-4.2	0.242	0.008
-3.1	0.276	0.006
-2.9	0.283	0.008
-2.0	0.293	0.004
-1.8	0.312	0.008
-0.9	0.303	0.003
-0.7	0.336	0.006
0.2	0.325	0.003
0.4	0.330	0.006
1.3	0.310	0.003
1.5	0.307	0.008
2.4	0.287	0.004
2.6	0.266	0.008
3.5	0.256	0.006
4.6	0.240	0.008
4.8	0.245	0.010
5.7	0.232	0.008
7.9	0.217	0.009
16.7	0.197	0.010

N7097_Mg2_360

-29.7	0.144	0.011
-7.5	0.243	0.009
-4.0	0.256	0.009
-2.9	0.279	0.003
-1.8	0.306	0.007
-0.7	0.301	0.005
0.4	0.302	0.005
1.5	0.295	0.006
2.6	0.266	0.009
3.7	0.235	0.009
5.9	0.233	0.009
10.3	0.204	0.010

N7097_NaD_270

-13.3	3.811	0.300
-5.3	3.757	0.272
-4.2	4.320	0.263
-3.1	5.332	0.192
-2.0	6.364	0.138
-1.8	5.529	0.264
-0.9	6.211	0.112
-0.7	6.723	0.265
0.2	6.213	0.106
0.4	6.221	0.242
1.3	5.793	0.112
1.5	5.079	0.250
2.4	4.345	0.155
3.5	3.899	0.229
4.6	3.741	0.238
4.8	4.088	0.298

5.7	2.884	0.295
10.1	2.729	0.289
17.8	1.602	0.471

N7097_NaD_360

-3.5	4.167	0.292
-12.7	2.705	0.285
-1.8	5.435	0.298
-0.7	6.016	0.212
0.4	6.687	0.189
1.5	6.067	0.243
2.6	5.419	0.250
5.9	4.246	0.299

N7200_Mg1_270

-5.8	0.129	0.010
-4.1	0.132	0.009
-3.0	0.134	0.006
-2.4	0.136	0.009
-1.9	0.151	0.004
-1.3	0.163	0.008
-0.8	0.167	0.003
-0.2	0.157	0.007
0.3	0.168	0.003
0.9	0.154	0.008
1.4	0.160	0.003
2.5	0.145	0.005
3.1	0.138	0.009
3.6	0.117	0.007
4.7	0.098	0.008
8.0	0.091	0.010

N7200_Mg1_360

-4.0	0.116	0.010
-2.3	0.138	0.009
-1.2	0.154	0.007
-0.1	0.160	0.006
1.0	0.139	0.007
2.1	0.137	0.008
6.5	0.106	0.010

N7200_Mg2_270

-18.7	0.082	0.017
-6.4	0.214	0.010
-4.1	0.244	0.010
-3.0	0.275	0.007
-2.4	0.302	0.010
-1.9	0.289	0.004
-1.3	0.324	0.009
-0.8	0.315	0.003
-0.2	0.321	0.007
0.3	0.322	0.003

0.9	0.319	0.009
1.4	0.304	0.003
2.5	0.279	0.005
3.6	0.242	0.008
4.2	0.265	0.010
4.7	0.215	0.009

N7200_Mg2_360

-2.3	0.278	0.008
-1.2	0.309	0.008
-0.1	0.327	0.006
1.0	0.299	0.008
2.1	0.251	0.009

N7200_NaD_270

-4.1	3.887	0.268
-3.1	4.225	0.297
-3.0	4.530	0.209
-1.9	5.194	0.145
-0.8	5.265	0.119
-0.2	5.632	0.286
0.3	5.259	0.112
0.9	5.239	0.265
1.4	5.339	0.128
2.5	4.639	0.190
3.6	4.064	0.262

N7200_NaD_360

-1.2	5.230	0.278
-0.1	5.530	0.270
1.0	5.022	0.276
6.5	4.903	0.296